Chair of Spacecraft Systems
TUM School of Engineering and Design
Technical University of Munich

Adaptive Reconfiguration Framework for Decentralized Optimization in Spacecraft Formation Flight and Collision Avoidance

Sidhant Patra
03758534

Thesis for the attainment of the academic degree

Master of Science (M.Sc.) in Aerospace Engineering

at the TUM School of Engineering and Design of the Technical University of Munich.

Examiner:
Prof. Dr. Alessandro Golkar

Supervisor:
M.Sc. Vincenzo Messina

Submitted:
Munich, 14.03.2024

I hereby declare that this thesis is entirely the result of my own work except where otherwise indicated. I have only used the resources given in the list of references.

Munich, 14.03.2024
03758534

Sidhant Patra

Zusammenfassung

Der Bedarf an fortschrittlicher Betriebsoptimierung ist in der Ära der schnellen Satellitenbereitstellung und der immer komplexeren Weltraummissionen erheblich gestiegen. In dieser Arbeit wird ein dynamischer Rekonfigurationsrahmen vorgestellt, der die betriebliche Effizienz in einem breiten Spektrum von Satellitenoperationen verbessern soll, wobei ein besonderer Schwerpunkt auf der Kollisionsvermeidung als einem wichtigen Anwendungsbereich liegt. Die Studie zielt darauf ab, eine umfassende Bewertungsmethode zu entwickeln und zu validieren, die die Kosteneffizienz von Manöverstrategien innerhalb von Satellitenkonstellationen bewertet und dabei kritische Betriebsparameter wie den Treibstoffverbrauch, den Energiebedarf, zeitliche Beschränkungen sowie die Verfügbarkeit und die Fähigkeiten von Satelliten berücksichtigt.

Die Forschung untersucht, ob Satellitenformationen dynamisch rekonfiguriert werden können, um die Ressourcennutzung und die betriebliche Effizienz zu optimieren. Anschließend wird untersucht, wie die Dezentralisierung zur Anpassungsfähigkeit und Skalierbarkeit des Satellitenbetriebs beiträgt. Und schließlich wird der Rahmen für Möglichkeiten zur Verbesserung von Kollisionsvermeidungsstrategien innerhalb von Satellitenkonstellationen erkundet. Unter Verwendung von MATLAB und Systems Tool Kit (STK) wird eine Optimierungsfunktion formuliert und es werden hochentwickelte Algorithmen eingesetzt, um Raumfahrzeugmanöver effizient zu steuern. Die Methodik betont die Anpassungsfähigkeit zur Unterstützung verschiedener Missionsszenarien und die Skalierbarkeit zur Verwaltung von Formationen, die von kompakten Konstellationen bis hin zu umfangreichen Netzwerken reichen.

Der vorgeschlagene Rahmen verbesserte die Ressourcenoptimierung, die Anpassungsfähigkeit und die Betriebseffizienz über verschiedene Satellitengrößen und -konfigurationen hinweg erheblich. Insbesondere erleichterte es die dynamische Rekonfiguration zur Kollisionsvermeidung und zeigte damit sein Potenzial zur Verbesserung des Missionserfolgs in komplexen und unvorhersehbaren Weltraumumgebungen. Die Arbeit kommt zu dem Schluss, dass der vorgeschlagene dynamische Rekonfigurationsrahmen eine vielseitige und skalierbare Lösung für die Herausforderungen des modernen Satellitenbetriebs bietet. Durch die Einbeziehung von Prinzipien der Dezentralisierung gewährleistet das System eine effektive Verwaltung und Optimierung von Satellitenformationen. Zukünftige Arbeiten werden die Ausweitung dieses Rahmens auf zusätzliche Anwendungen wie Erdbeobachtung, Kommunikationsrelais und Weltraummüllmanagement untersuchen und damit einen weiteren Beitrag zur Effizienz und Widerstandsfähigkeit von Weltraummissionen leisten.

Abstract

The demand for advanced operational optimization has escalated significantly in the era of rapid satellite deployment and increasingly complex space missions. This thesis introduces a dynamic reconfiguration framework designed to enhance operational efficiency across a broad spectrum of satellite operations, with a particular focus on collision avoidance as a key application area. The study aims to develop and validate a comprehensive evaluation methodology that assesses the resource-usage effectiveness of maneuver strategies within satellite constellations, addressing critical operational parameters such as propellant usage, power requirements, time constraints, and satellite availability and capabilities.

The research investigates if satellite formations can be dynamically reconfigured to optimize resource utilization and operational effectiveness. Subsequently, the study investigates how decentralization contributes to the adaptability and scalability of satellite operations. Lastly, it explores the framework for the possibility of improving collision avoidance strategies within satellite constellations. Utilizing MATLAB and Systems Tool Kit (STK), this research formulates an optimization function and employs sophisticated algorithms to direct spacecraft maneuvers efficiently. The methodology emphasizes adaptability to support diverse mission scenarios and scalability to manage formations ranging from compact constellations to extensive networks.

The proposed framework significantly improved resource optimization, adaptability, and operational efficiency across satellite quantities and configurations. Specifically, it facilitated dynamic reconfiguration for collision avoidance, showcasing its potential to enhance mission success in complex and unpredictable space environments. The thesis concludes that the proposed dynamic reconfiguration framework offers a versatile and scalable solution to the challenges of modern satellite operations. By incorporating principles of decentralization, the framework ensures effective management and optimization of satellite formations. Future work will explore extending this framework to additional applications such as Earth observation, communication relays, and space debris management, further contributing to the efficiency and resilience of space missions.

Acknowledgements

I want to acknowledge Prof. Alessandro Golkar, whose expertise in Spacecraft Systems has directed my research path. Having the opportunity to study under his guidance at the Chair of Spacecraft Systems has significantly influenced my academic journey.

Likewise, my supervisor and friend, Vincenzo Messina, has provided steady support and valuable insights that were crucial as I ventured into this research. His bits of advice played a key role in developing this thesis work.

The friendship and guidance of chair members Jaspar Zindermann, Ramón García Alarcia, and Rafael Illiasov enriched this journey. I am also thankful to Sherina and all members of this chair.

I'm grateful to my dear friends who've been both my anchor and my sails, helping me sail through the challenging journey of this thesis. Dibyesh, Lara, Juls, Akki, Vikas, Tanu, Anand, Amit, Paula, and Carlos – your support and belief in me have been the force that's pushed me ahead, especially when things got tough.

Above all, to my two guiding lights, my two stars, Bhai and Maa, who fill my life with constant love and support. Their endless love is a true gift; words alone can never describe my gratitude for them. And Dad, Thank you for being supportive on this journey.

My heart swells with gratitude to each of you who has been a part of my journey. Your belief in me, support, and inspiration have been the essence of my progress.

Ad Astra!

Contents

List of Figures

List of Tables

Acronyms

APFs Artificial Potential Functions. 13

COM Component Object Model. 30

DARF Decentralized Adaptable Reconfigurable Framework. vii, ix, x, xii, xiii, 4, 22, 23, 25, 28, 29, 32, 33, 35–37, 40, 42–61, 63–65, 67–69, 71, 75, 83–85, 87

DOCA Decentralised Optimization Collision Avoidance. 36

DSS Federated satellite systems. ix, 2, 4, 5, 9–12, 14, 23, 25

FAA Federal Aviation Administration. 2

FOM Figure of Merit. 34, 44

FSS Federated Satellite Systems. 12, 13

FSSCat Federated Satellite Systems/3Cat-5. 12

GEO Geostationary Earth Orbit. 1

GGSE-4 Gravity Gradient Stabilization Experiment. 2

GRACE Gravity Recovery and Climate Experiment. 10

GSD Ground Sampling Distance. ix, x, 33, 34, 37–39, 71, 75–77

IRAS Infrared Astronomical Satellite. 2

LEO Low Earth Orbit. 1, 2, 4, 5, 9

LOS Line of Sight. 38

MATLAB Matrix Laboratory. x, 28–31, 55, 67, 69, 74, 75, 83, 85, 86

MDO Multidisciplinary Design Optimization. 9, 23, 25

MEO Middle Earth Orbit. 1

MPC Model Predictive Control. 13

NLP Non-Linear Programming. 23

RAAN Right Accession of Ascending Node. 9, 41–45, 53, 55, 63, 67, 83

SGP4 Simplified Perturbations Models 4. 29

SPICE Spacecraft Planet Instrument C-matrix Events. 29

SSPO Sun-Synchronous Polar Orbit. vii, 54, 64

STK Systems Tool Kit. viii–x, xiii, 28–31, 35, 48, 51, 57, 58, 60, 61, 63–69, 71, 75, 76, 83, 88

TCP/IP Transmission Control Protocol/Internet Protocol. 30

TOF Time of Flight. 19

TWR Thrust-to-Weight Ratio. 44, 45

1 Introduction

In recent years, the space industry has witnessed an unprecedented expansion in satellite deployment, humanity has launched 9,158 spacecraft since 1957 (1), with a significant concentration within about 2,000 kilometers from the Earth's surface, commonly accepted as the region otherwise known as Low Earth Orbit (LEO). The Earth's orbit is densely populated with many satellites, serving many purposes for governmental, military, and civilian applications. These satellites provide essential services such as internet connectivity, television broadcasting, GPS navigation, and more (2). Additionally, they play a crucial role in scientific exploration, facilitating Earth and space observation, and driving advancements in high-level technology.

Despite only about 2,200 of these being operational today, the advent of private ventures and national projects threatens to inflate this number substantially. Forecasts suggest that, by the end of this decade, up to 57,000 (3) (4) new satellites could crowd Earth's orbit, a 25-fold increase from today's active spacecraft. A research team from Dewesoft (5) addressed who controls this orbital space by analyzing data from the UCS Satellite Database (6), ESRI, and the Space Foundation. This analysis culminated in identifying the top 50 entities that own the most satellites. As of 5 May 2023, SpaceX emerges as a front-runner in this domain, with plans under its Starlink satellite program to deploy over a thousand new satellites annually. A more recent study accounts for the total number of operational satellites to 9,494 as of 7 March 2024, among which 84 percent of satellites are in LEO, and Middle Earth Orbit (MEO) and Geostationary Earth Orbit (GEO) accounting for the rest 3 percent and 12 percent of total satellites respectively. (7). A significant portion of these satellites, over half of the 4,550 currently in orbit, are dedicated to communication, a sector expected to expand as initiatives to offer high-speed internet access globally gain momentum.

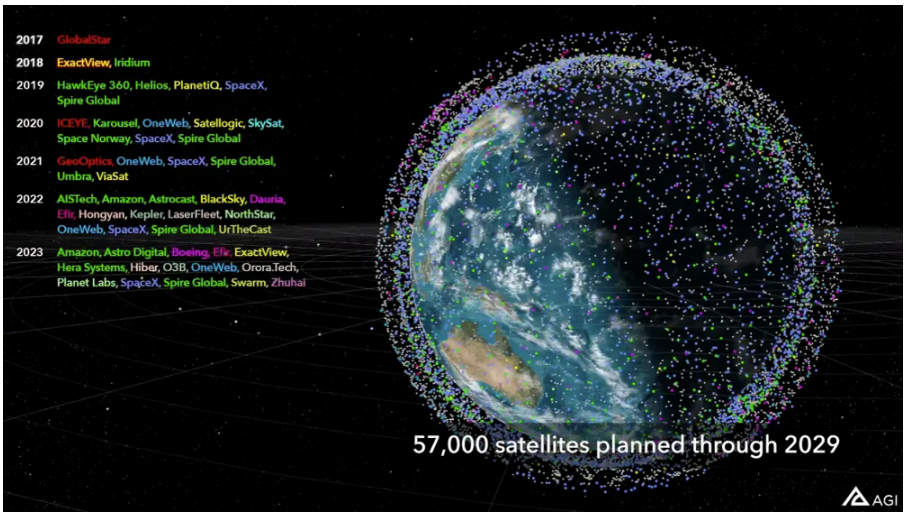

Figure 1.1 57,000 planned satellites being deployed around Earth through 2029 (3)

1.1 Thesis Motivation

This research study articulates a novel methodology for the dynamic reconfiguration of federations of satellites to mitigate collision risks, employing a dynamic framework that prioritizes decentralized optimization. This methodological innovation is critical as it challenges the limitations of traditional centralized optimization strategies amidst the escalating complexities and growth of satellite constellations. The study introduces and develops a simulation model framework for a federation of *n* satellites undergoing reconfiguration, incorporating models for orbital dynamics, space-borne object detection, collision avoidance algorithms, and resource management strategies. Central to this study is a comprehensive examination of centralized and decentralized management models for satellite reconfiguration. This research assesses their effectiveness in operational performance enhancement by methodically simulating various reconfiguration scenarios, including satellite numbers and maneuver strategy changes. This analysis lays the groundwork for understanding how decentralized optimization can improve satellite operations' scalability, adaptability, and cooperative behaviors. The study posits decentralization as a critical mechanism for augmenting decision-making processes and system adaptability across satellite constellations. This decentralized approach is pivotal for optimizing satellite constellation reconfigurations—ensuring efficient resource utilization and improved data transmission—and has broader implications for enhancing cyber security, managing big data, and supporting the development of emergent communication technologies. (8)

Through a meticulous structural narrative, this research transitions from a theoretical framework to a detailed exposition of the reconfiguration model, including its design considerations, operational parameters, and the integration of simulation modules. This comprehensive exploration culminates in critically analyzing the results, offering insights into the limitations and potential future directions. By advancing decentralized coordination strategies for reconfiguring satellite federation, this research aims to contribute to space systems research, ensuring the sustainability and safety of space operations in an increasingly congested orbital environment.

1.1.1 Problem Description

While pivotal for technological advancement and global connectivity, this rapid growth introduces significant challenges in space traffic management, notably the escalating risk of collisions and the resultant space debris - a concern particularly pressing for the European Union (EU) audience. Such challenges underscore the critical need for innovative collision avoidance models tailored for DSS architectures.

The research work by Alfano et al., 2020 (9) presented at the Federal Aviation Administration (FAA)'s Commercial Space Transportation Conference vividly illustrated this escalating density of orbital objects. The importance of their (9) illustration highlighted an incident in which two inactive satellites, namely the Gravity Gradient Stabilization Experiment (GGSE-4), a gravity-measuring satellite from 1967, and Infrared Astronomical Satellite (IRAS), an infrared space telescope, narrowly avoided collision above Pittsburgh. Had such a collision occurred, it would have been observable from Earth and resulted in significant space debris, worsening the already serious orbital congestion. Once rare, the frequency of these near-misses has markedly increased, indicating a shift towards a more congested and complex orbital environment. This shift occurs before the projected exponential rise in satellite launches, indicating an urgent need for improved space traffic management and collision avoidance mechanisms. The thesis addresses this need by proposing a dynamic reconfiguration framework for DSS, which prioritizes adaptability and decentralization to mitigate collision risks effectively. While new satellites are being designed with avoidance systems, the sheer volume of orbital objects necessitates more sophisticated solutions (10).

In an increasingly crowded LEO with projections estimating up to 58,000 satellites by 2030, the shift towards decentralized, distributed satellite systems presents unique operational challenges, particularly in

collision avoidance (11) and implies a need to explore efficient path management. While fostering operational agility and responsiveness, the paradigm of local information parsing and autonomous decision-making inherently carries the risk of decisional overlap or misalignment due to identical reward functions or inadequate information dissemination among satellites. This scenario mirrors the complexities of human decision-making, equipped with the same set of objectives and limited communication, where if each individual human is treated as an agent of a decentralized system, there are possibilities that two or more such agents may inadvertently converge on identical decisions or actions. In the context of our research study, this could manifest as two or more satellites in a federation locally determining they are best positioned to execute a particular maneuver based on their local assessments.

In such cases in space, without a well-developed system for satellites in a federation to manage where they go or how they effectively coordinate in a decentralized system, they might end up too close together or even on a crash course with each other. A federation satellite acting on outdated or incomplete information might initiate a maneuver unaware of concurrent actions taken by others in its vicinity, leading to potential conflict trajectories. Such occurrences underscore the critical need for advanced collision countermeasures within decentralized systems, enabling efficient, conflict-free orbital transfers and incorporating mechanisms for robust, real-time communication and coordination. These countermeasures should ensure that while satellites operate autonomously, they do so within a framework that maximizes collective situational awareness and operational harmony, thereby safeguarding the sustainability and safety of space operations.

Fairly organized, this thesis addresses the theoretical preparation needed to design and develop a framework for resource optimization to demonstrate autonomous collision avoidance for satellites in federation by delivering a simulable, scalable, and adaptable platform to simulate various reconfiguration scenarios for addressing the thesis research questions outlined in *Section 1.4*. The thesis presents an extensive and detailed description of the developed decentralized framework, from design principles to all simulation models used to cater to various important framework aspects, outlined in *Section 3.1.4* and discussed in detail in *Chapter 3*. The thesis provides a detailed analysis of all the research findings and the effect of selecting particular research metrics such as design variables, parameters, and objective functions for our reward-based model optimization strategy. The thesis also introduces and implements a collision avoidance strategy into the framework, successfully identifying collision risks and deploying countermeasure maneuvers to avoid them. It also discusses its capability and practical usability, showcasing a use-case of spacecraft formation flight reconfiguration for a group of satellites in a federation, conforming to a reconfiguration request to arrange some of the satellites into a particular formation, while ensuring that resource-wise, only the best-required number of satellites perform the reconfiguration with collision avoidance capability for ensuring operational safety. The research closes with a discussion of the developed framework's performance, key research findings, imitations, and potential for further research.

1.2 Highlights

- Satellites in federations, and operating in a decentralized pattern create elevated collision risks due to a largely predicted growth in satellite deployments and increasingly LEO.
- This expansion necessitates understanding such means of decentralized coordination and resource optimization for spacecraft formation flights that sustain vital satellite services.
- The Thesis introduces a dynamic framework, DARF, focusing on decentralized coordination and resource optimization for adaptable reconfiguration of satellite federations.
- DARF integrates models for orbital dynamics, object detection, collision avoidance, and resource management to gain insights into the performance metrics.
- By simulating various scenarios, the research highlights the scalability and adaptability of decentralized approaches to improve satellite operations.
- This contribution aims to ensure the sustainability and safety of space operations amidst growing orbital congestion and the increasing number of satellites.

1.3 Research Statement

This study proposes a dynamic reconfiguration framework for DSS, designed to optimize resource utilization and operational effectiveness while ensuring robust collision avoidance capabilities. The framework leverages decentralized decision-making to facilitate rapid and efficient adjustments to satellite formations, thereby accommodating the evolving demands of space missions and the challenges posed by the crowded orbital landscape.

1.4 Research Questions

Guided by the overarching goal of enhancing satellite formation management, this research delves into the following specific questions:

1. Which figure of merit, constraints, and design variables should be considered to formulate the problem of achieving a specific spacecraft formation architecture while optimizing resource utilization?
2. What are the advantages and disadvantages of a decentralized approach in optimizing spacecraft cooperation to achieve a specific formation?
3. How does the developed optimization algorithm demonstrate scalability and adaptability?

1.5 Thesis Outline

The thesis is organized as follows:

1. **Chapter 1: Introduction**
   Provides an overview of the current state of space systems, the challenges posed by the increasing satellite population in LEO, and the motivation behind this study. It introduces the research questions, tasks, problem definition, and the need to explore a dynamic reconfiguration and decentralized decision-making for safer and more resource-efficient satellite operations in DSS.

2. **Chapter 2: Literature Review**
   Examines existing methodologies and technologies in spacecraft formation flying, reconfiguration, and collision avoidance, identifying gaps and innovation opportunities. This review lays the foundation for the development of our novel framework.

3. **Chapter 3: Methodology**
   The DARF framework leverages a combination of simulation models to efficiently manage and optimize satellites in federation. DARF aims to ensure safe and effective satellite operations by incorporating elements from astrodynamics for precise orbit propagation, optics for collision detection, and resource optimization algorithms. Key to its approach is the decentralized management of constellations, which enhances operational flexibility and scalability.

4. **Chapter 4: Results**
   Highlights findings from simulations and theoretical models, focusing on improvements in resource optimization, scalability, adaptability, and collision avoidance compared to other simulated scenarios.

5. **Chapter 5: Discussion**
   Analyze the implications of the findings, discussing the study's significance, strengths, and limitations associated with this framework and the decentralized approach. It explores potential future research directions to further enhance the framework.

6. **Chapter 6: Conclusion**
   The study's contributions to DSS and space operations management are summarized. Reflects on the importance of dynamic reconfiguration and decentralized decision-making for the future of space exploration and utilization.

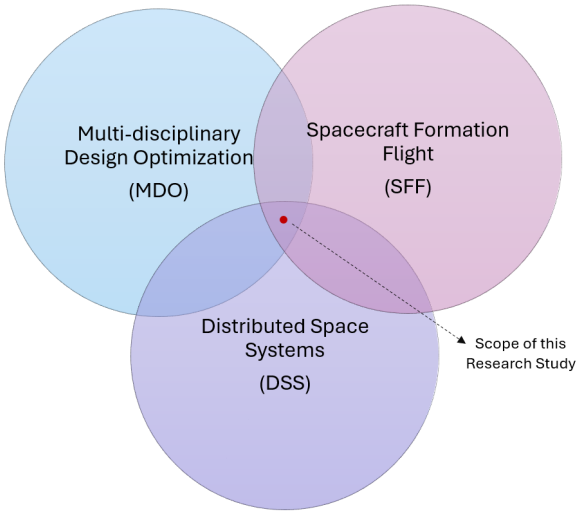

Figure 1.2 Venn-Diagram depicting the scope of this research study

1.6 Thesis Objectives

Table 1.1 Objectives for this Thesis

ID	Objectives
TO-1	Identify which figures of merit, design variables, and parameters should be considered to formulate the problem of achieving a specific spacecraft formation architecture while optimizing resource utilization. Addressed in *Section 3.1*
TO-2	Develop a dynamic reconfiguration framework to simulate the behavior and interaction of *n* satellites within various mission architectures. Addressed in*Sections 3.1 - 3.7.*
TO-3	Implement a quantitative reward function model using the identified figures of merit to evaluate space resource optimization for reconfiguration. Addressed in *Section 3.9.*
TO-4	Develop collision avoidance strategies compatible with the framework's decentralized approach. Addressed in *Section 3.8.*
TO-5	Incorporate strategies into the framework to improve the coordination flexibility of spacecraft formation flight. Addressed in *Section 3.7*
TO-6	Assess and optimize the use of space resources, individually and collectively, through the framework to enhance efficiency. Addressed in *Section 3.9.*
TO-7	Assess and validate the framework's working and scalability by evaluating performance under configuration size changes. Addressed in *Section 4.1.*
TO-8	Validate the adaptability of the framework through simulations involving multiple operational scenarios and configurations. Addressed in *Section 4.2.*
TO-9	Simulate one use case scenario to provide practical implications for the framework. Addressed in *Section 4.3.*
TO-10	Validate the created decentralized decision-making algorithms to enable autonomous satellite responses within the framework. Addressed in *Section 4.4.*
TO-11	Validate coordination protocols within the framework to prevent conflicts during maneuver execution. Addressed in *Section 4.5.*
TO-12	Analyze and discuss the simulation results to validate the framework's effectiveness in optimizing satellite formation configurations. Addressed in *Chapter 5*

1.7 Definitions

Table 1.3 Important Definitions within the Thesis

Def. No.	Definition
D1	**Autonomy:** The capability of a satellite or spacecraft to perform tasks and make decisions without external control or intervention.
D2	**Bielliptical Transfer:** A type of orbital maneuver involving three impulsive burns and an intermediate elliptical orbit extending beyond the altitude of the final orbit.
D3	**Centralized:** An approach to satellite control where decisions and commands are issued from a single control center or entity.
D4	**Circular Orbit:** An orbit with a path that forms a circle around the central body, characterized by an eccentricity of 0.
D5	**Collision Risk:** The probability that two or more orbiting objects, such as satellites, might collide, potentially causing damage or creating space debris.
D6	**Continuous Burns:** A propulsion method that applies continuous, low-thrust over long durations, typical of electric propulsion systems like ion thrusters.
D7	**Decentralized:** An approach to satellite control where decision-making processes are distributed across multiple satellites within the constellation.
D8	**Elliptical Orbit:** An orbit with an elliptical shape, characterized by an eccentricity greater than 0 but less than 1.
D9	**Exclusion Spheres:** Imaginary spheres around satellites within which other satellites or objects are not allowed to enter, to prevent collisions.
D10	**Genuine Transfers:** The most efficient orbital transfers that minimize fuel consumption and time.
D11	**Ground Sample Distance (GSD):** The distance between two consecutive pixel centers measured on the ground, related to the resolution of satellite imagery.
D12	**High-Order Splines:** Mathematical functions used to model the trajectory of satellites in orbit collision avoidance algorithms.
D13	**Hyperbolic Orbit:** An open orbit with an eccentricity greater than 1, indicating an unbounded trajectory where a satellite escapes the central body's gravitational pull.
D14	**Nadir:** The direction pointing directly "down" from a satellite towards the center of the Earth, opposite to zenith.
D15	**Nodal Transfer:** Orbital maneuvers aimed at changing the ascending or descending nodes, thus affecting the orbit's inclination.

Continued on next page

Table 1.3 continued from previous page

Def. No.	Definition
D16	**Non-Hohmann Transfer:** Orbital transfers that do not adhere to the criteria of Hohmann transfers, possibly involving multiple burns or transfers between non-circular orbits.
D17	**Parabolic Orbit:** An orbit with an eccentricity of exactly 1, represents the threshold between bound elliptical and unbound hyperbolic orbits.
D18	**Phasing Maneuver:** A maneuver to adjust the timing of a satellite's orbit, changing its position along the orbit without altering the orbit's shape.
D19	**Reconfiguration:** Adjusting the formation or configuration of a satellite constellation to meet changing mission requirements or to respond to operational conditions.
D20	**Specific Impulse (I_{sp}):** A measure of propulsion system efficiency, representing the impulse (change in momentum) per unit of propellant.
D21	**Tangent Plane Maneuver:** Orbital maneuvers where the thrust is applied tangent to the spacecraft's orbit, typically to change the orbit's shape or altitude.
D22	**Vis-viva Equation:** An equation relating the speed of an object in orbit to its distance from the central body and the semi-major axis of its orbit.

2 Literature Review

Chapter 2 of this thesis comprehensively examines the extensive knowledge and technological advancements pertinent to DSS and the dynamic reconfiguration of satellite constellations. This literature review is meticulously crafted to encapsulate the fundamental principles of orbital mechanics, delving into the intricacies of various maneuvers essential for delta-v calculations—ranging from plane changes, Right Accession of Ascending Node (RAAN) adjustments, altitude modifications, to complex combinations thereof, alongside tangent burns, and both Hohmann and non-Hohmann transfer orbits. The exploration extends to cover the nuanced strategies and applications of spacecraft formation flying, underpinning the operational dynamics of DSS. Furthermore, this section illuminates the interdisciplinary approach of Multidisciplinary Design Optimization (MDO) in enhancing the efficiency and efficacy of satellite constellations. it facilitates optimizing satellite systems (12) (13) to meet multifaceted mission requirements by integrating considerations from diverse fields.

2.1 Increasing Congestion in Earth's Orbital Space

Data analysis reveals that SpaceX accounts for 56 percent of all active satellites orbiting Earth, with about 5,289 mass-produced small satellites in LEO as of January 2024 (14). The company has demonstrated its capability to launch significant numbers of satellites simultaneously, notably setting a record by deploying 143 satellites on a single rocket at the start of 2021 (6). Under Elon Musk's leadership, SpaceX has set ambitious goals to provide high-speed broadband internet globally through the Starlink venture. In 2021 alone, SpaceX aimed to add 1,500 Starlink satellites to its fleet and add about 12,000 with a possible extension to 42,000 satellites for Starlink (14), further solidifying its status as the largest satellite operator. Furthermore, the company has opened the door for other entities to launch their satellites, offering a 1 million dollar service fee per satellite, thus facilitating the growth of commercial satellite launches. This exponential increase, driven by governmental ambitions and private sector ventures, underscores a looming challenge of orbital congestion, with a significant focus on the LEO. The implications of this rapid expansion are multifaceted, impacting global connectivity and technological advancement and raising substantial concerns regarding space traffic management and the heightened risk of collisions. This number is projected to soar to approximately 58,000 (15) by 2030, largely due to ambitious constellation models planned by major corporations like Amazon, SpaceX, Multinational Corporations, and Government Agencies worldwide.

2.2 Distributed Space Systems

The roots of satellite technology can be traced back to the mid-20th century, with the launch of Sputnik 1 (12) by the Soviet Union in 1957, marking the dawn of the space age. This historic event spurred a flurry of space exploration efforts, culminating in significant milestones such as the Apollo Moon landings and the deployment of communication satellites in geostationary orbit. Over time, advancements in technology and engineering paved the way for developing increasingly sophisticated satellite systems. Since then, satellite technology has evolved remarkably since its inception, transforming from rudimentary devices launched during the Space Race era to sophisticated ones deployed in the modern era. DSS (16)

Distributed Space Systems, sometimes referred to as Distributed Satellite Systems, have showcased their significance across various domains in space missions, from demonstrating advancements in com-

munication technology to enabling high-resolution Earth observation capabilities. The emergence of the DSS architecture represents a paradigm shift in satellite architecture, moving away from traditional monolithic satellites towards a distributed network of smaller spacecraft. (17) *Figure 2.1* briefly classifies Earth orbit satellite systems that further classify monolithic and distributed systems, while giving an overview of the state-of-the-art satellite architectures under DSS. These satellites communicate and collaborate using advanced networking protocols, enabling them to perform tasks traditionally assigned to larger, singular satellites (18).

Table 2.1 Multifaceted Advantages of Distributed Satellite Systems (DSS) against Monolithic Systems: Decentralized vs Centralised

Advantage	Description
A1	**Better Failure Mechanisms:** Distributed satellite constellations are designed to fail gracefully, ensuring that the loss of a single satellite does not critically impair the entire system's functionality.
A2	**Simultaneous Multi-point Data Collection:** Enables data gathering from multiple points concurrently, enhancing the system's observational capabilities.
A3	**Diverse Observational Capacity:** DSS can monitor various phenomena simultaneously, making it highly versatile in its application.
A4	**Distributed Coordination:** Facilitates dynamic data sharing and priority adjustments among satellites, enhancing adaptability to changing conditions.
A5	**Autonomous Re-tasking:** Allows satellites to autonomously respond to environmental changes without direct control from ground operators, improving responsiveness.
A6	**Autonomy:** Elements of glsdss can learn and generate their unique laws and norms.
A7	**Relay Command Capability:** Ensures system availability by allowing individual spacecraft to relay commands to other components, maintaining operational continuity.
A8	**Augmented System Availability:** Increases the overall availability of the system, facilitating continuous operation and data acquisition.
A9	**Workload Balancing:** Employs strategic re-tasking based on current computational, power, and communication resources to optimize system performance.
A10	**Minimal Downtime with Lower Degradation:** Minimizes operational downtime and maintains functionality gracefully, even under partial failure conditions.

A comparative analysis between monolithic and distributed satellite systems, as seen in *Table 2.1* and *Table 2.3* underscores the strategic advantages of scalability, resilience, and adaptability offered by DSS. Some well-known satellites such as PRISMA, Gravity Recovery and Climate Experiment (GRACE), and TerraSAR-X–TanDEM-X are examples of distributed satellite architectures. This decentralization means that each satellite within a DSS can operate independently or in a coordinated manner with others without relying on a central control unit. This structure improves the constellation's robustness against individual satellite failures and enhances the system's overall adaptability and responsiveness to dynamic operational environments. The architecture of the DSS emphasizes modularity‘, resiliency, and adaptability, allowing for efficient deployment and reconfiguration as mission requirements evolve. These networks of satellites, by their nature, eliminate the single point of failure.

Table 2.3 Key Disadvantages of Distributed Satellite Systems (DSS)

Disadvantage	Description
D1	**Complex Coordination:** The need for dynamic and autonomous satellite coordination increases system complexity and the risk of communication failures and effective information parsing with respect to time.
D2	**Collision Risk:** Increases with the number of satellites in orbit without a centralized monitoring system for checking collision paths, the risk of collision and the generation of space debris becomes significant.
D3	**Regulatory and Frequency Allocation Challenges:** DSS would involve complex regulatory environments and frequency allocations.
D4	**Resource Allocation Challenges:** Effectively distributing resources like propellant, power, and bandwidth across the constellation requires advanced management algorithms.
D5	**Software and Algorithm Complexity:** The software for managing autonomous operations and data processing must be highly reliable and complex, requiring extensive validation.

They also offer several key advantages over traditional monolithic satellite systems. Firstly, DSS provide enhanced system redundancy, mitigating the risk of mission failure due to the loss of individual satellites (19). Thus, DSS inherently eliminates the single point of failure, a critical vulnerability in traditional satellite systems where the malfunction or loss of a single satellite can compromise the entire system's functionality. (20) Moreover, eliminating a single point of failure through DSS architecture significantly mitigates the risk of systemic breakdowns. This approach ensures that the failure of one or even several satellites does not hinder the entire constellation. Instead, the remaining operational satellites can reconfigure themselves to maintain coverage, service continuity, and mission objectives. While monolithic systems excel in certain applications requiring high payload capacity and specialized instrumentation, they are inherently limited in scalability and fault tolerance. Secondly, DSS offer greater operational flexibility, allowing for dynamic task allocation and real-time adaptation to changing mission objectives (21). Additionally, DSS are inherently cost-effective, leveraging economies of scale associated with the mass production of smaller satellites (22). Furthermore, DSS enable enhanced mission capabilities, such as distributed sensing and monitoring, by leveraging the collective intelligence of the satellite network.

2.2.1 Federated Satellite Systems

Federated Satellite Systems are a class of DSS. In satellites involved in decentralized operations, the advent of the concept of Federated Satellite Systems (FSS) marks a significant stride towards autonomy (23) and collaboration in space. These satellites form opportunistically, with their mission goals centered, but can cooperate in data relay and parsing. The past decade has seen a surge in interest in FSS, fueled by advancements in small satellite technologies, such as Nanosatellites, Cubesats, and Picosats, making satellite federations technically and economically viable (23). These federations embody the principle of satellites working in concert, opportunistically (23) sharing resources and capabilities to achieve collective objectives, albeit presenting technological hurdles in in-orbit implementation.FSS represents a cutting-edge approach in satellite technology, where multiple satellites operate in synergy, leveraging the power of federated learning to enhance their capabilities. (24) This innovative method involves the satellites collaboratively refining their machine-learning models by exchanging model updates rather than transferring potentially sensitive raw data. Such an approach significantly minimizes the need for extensive communication bandwidth, a valuable resource in space operations (13) (16). By exchanging model updates, satellites can collectively harness a broader spectrum of knowledge, enabling them to make more informed decisions and predictions about their environment and the tasks at hand.

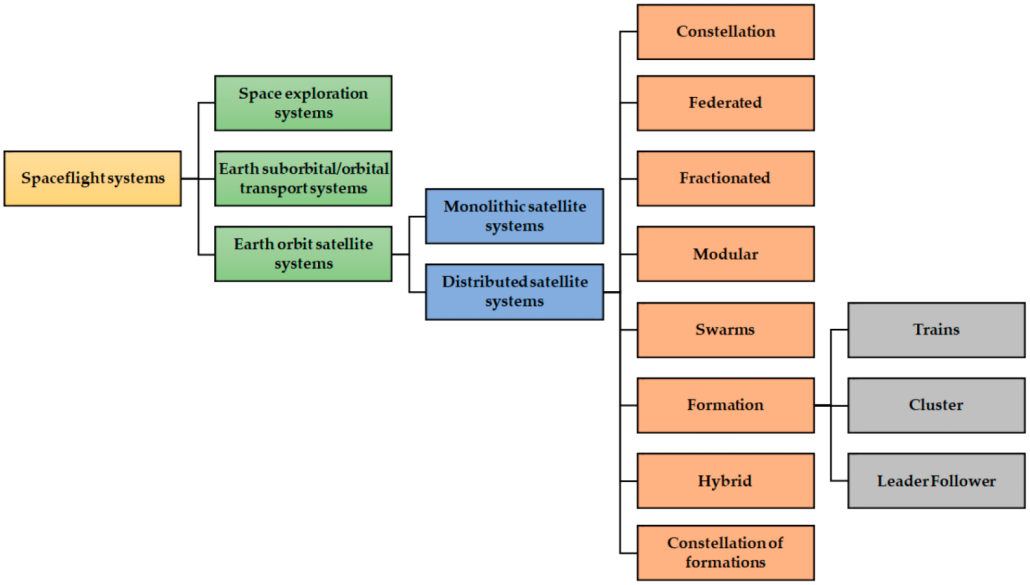

Figure 2.1 Classifications of Spaceflight Systems and a look at possible satellite architectures under DSS (12)

This method not only ensures the privacy and security of the data but also facilitates a distributed learning process across the network of satellites. (16) This distributed knowledge accumulation empowers the satellite systems to become more intelligent and efficient, optimizing their functions for various applications ranging from Earth observation to deep space exploration. The concept of federated learning within satellite systems underscores a shift towards more autonomous, secure, and collaborative space assets, enhancing their utility and effectiveness in scientific and commercial endeavors (24) (25).

The Federated Satellite Systems/3Cat-5 (FSSCat) (26) mission exemplifies the practical application and benefits of federated satellite systems. Launched as a part of this mission, two CubeSats equipped with Earth observation instruments have successfully demonstrated the ability to generate valuable scientific data through federated operations. This mission showcases how federated learning can be applied in real-world satellite operations to achieve remarkable scientific outcomes. By operating federated, these CubeSats could efficiently manage and process data, contributing significantly to our understanding of Earth's systems without requiring direct raw data exchange. This achievement validates the concept of federated satellite systems and opens new avenues for future space missions to leverage federated learn-

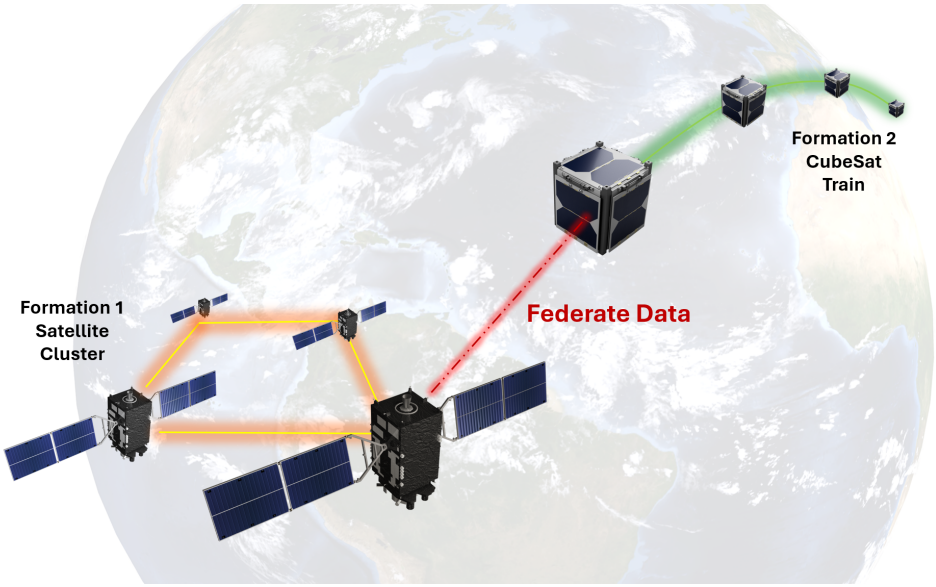

Figure 2.2 An illustration of data federation among different architectures of Spacecraft Formation Flight in Distributed Space Systems

ing for enhanced data acquisition and processing capabilities (27). FSS heralds a novel paradigm in space missions, enabling clusters of satellites to collectively perform functions traditionally reserved for larger monolithic satellites. Through intra-cluster communication, these satellites distribute processing, communication, and payload tasks among themselves, exemplifying distributed satellite operations as shown in the work of Jordan L et al., 2022 (28). However, optimizing and automating these complex, decentralized systems pose significant research challenges, necessitating further exploration into effective models and techniques.

2.3 Spacecraft Formation Flying

Formation flying is a fundamental concept (29) within the satellite systems, enabling coordinated movement and task execution among individual satellites. In formation flying, satellites maintain precise spatial relationships with each other, allowing them to perform complex maneuvers and achieve mission objectives with high precision. (30) Advanced control algorithms facilitate this capability (31) and communication protocols, which enable seamless coordination and collaboration among the satellite constellation. The advantages of spacecraft formation flying according to analyses conducted by Alzubairi et al., 2022 (32) and Riccardo et al., 2022 (33) reveal this kind of systems have enhanced adaptability, increased feasibility, reduced mission cost, increased probability of success, and wider operating area. Dawei et al., 2022 (34) describe a strategy for cooperative formation reconfiguring multiple spacecraft, considering collision avoidance and controller saturation constraints, using sequential convex optimization. Another study by Menegatti et al., 2022 (35) demonstrates a collision-free formation control strategy for spacecraft flying in formation. It uses Model Predictive Control (MPC) and Artificial Potential Functions (APFs) to avoid collision by maintaining a safe distance from obstacles. Figure 2.4 depicts a typical formation flying incorporated by SpaceX's Starlink constellation with the first orbital shell: 72 orbits with 22 each, therefore 1584 satellites at 550 km altitude. (36)

2.4 Spacecraft Reconfiguration Manuevers

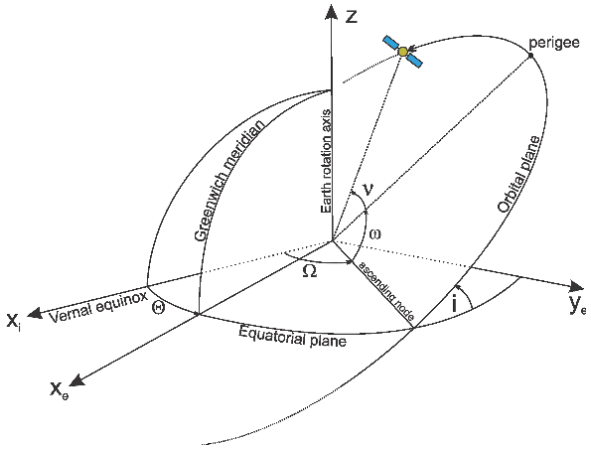

Figure 2.3 Keplerian Elements that represent and define an Orbit fully
(36)

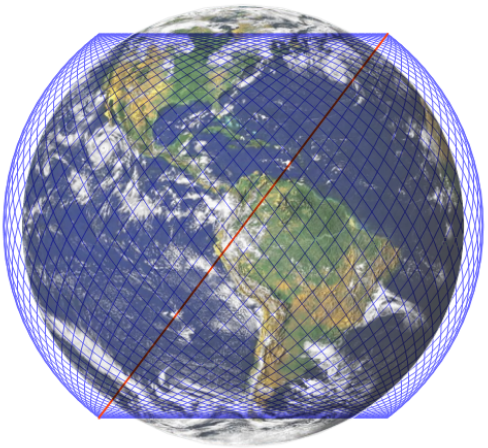

Figure 2.4 The Starlink constellation, phase 1, first orbital shell: 72 orbits with 22 each, therefore 1584 satellites at 550 km altitude
(37)

Figure 2.3 shows the six keplerian elements needed to define an orbit fully (36), which makes reconfigurations very challege due the large amount of variables that comes with, as it will be discussed in Chapter 3. The dynamic nature of space missions necessitates the ability to reconfigure DSS to meet evolving objectives and challenges. Reconfiguration involves adjusting the satellite constellation's spatial arrangement, task allocation, and operational parameters in response to changing mission requirements. This adaptability allows DSS to adapt to unforeseen events, optimize resource utilization, and extend mission life by leveraging the collective intelligence and capabilities of the satellite network. (37) Orbital mechanics forms the cornerstone of spacecraft maneuvering and constellation management, essential for the dynamic reconfiguration of satellite systems. This discipline encompasses the fundamental laws and techniques required to alter spacecraft orbits, facilitated by gravitational forces from celestial bodies. The thesis explores the principal maneuver scenarios of orbital transfer which are pivotal for shifting a spacecraft between different trajectories and are crucial for enhancing the system's operational flexibility and responsiveness.

2.4.1 Elliptical Orbits

Elliptical orbits are characterized by an eccentricity e between 0 and 1, indicating a varying radius dependent on the true anomaly. The orbit maintains an elliptical shape since the denominator of the orbit equation never reaches zero. The distances to periapsis (r_p) and apoapsis (r_a) represent the minimum and maximum values of the radius, respectively.

Vis Viva Equation

(36)

$$v = \sqrt{\mu \left(\frac{2}{r} - \frac{1}{a} \right)} \tag{2.1}$$

Given the total distance d from periapsis to apoapsis along the apse line, the semi-major axis a and semi-minor axis b define the orbit's dimensions (38):

$$a = \frac{h^2}{\mu} \frac{1}{1 - e^2} \tag{2.2}$$

Here, a is the semi-major axis. The orbit equation in terms of a becomes (39):

$$r = a \frac{1 - e^2}{1 + e \cos \nu} \tag{2.3}$$

With the orbit's parameter p defined as (39):

$$p = a(1 - e^2) \tag{2.4}$$

The distance to periapsis and the offset c from the ellipse's center are (39):

$$r_p = a(1 - e), \quad c = ae = a - r_p \tag{2.5}$$

For b, the semi-minor axis, in terms of a and e (39):

$$b = a\sqrt{1 - e^2} \tag{2.6}$$

Finally, the orbital period T is given by *Equation 2.14:* (40), (39):

$$T = \frac{2\pi a^{3/2}}{\sqrt{\mu}} \tag{2.7}$$

2.4.2 Impulsive Maneuvers

Impulsive maneuvers alter a spacecraft's orbit by applying a sudden force, typically from an on-board propulsion system. Such maneuvers are characterized by an instantaneous change in the spacecraft's velocity vector, denoted as $\Delta \mathbf{v}$, with no change in position during the impulse. (13) These maneuvers allow us to ignore the force term in the motion equations, simplifying calculations.

Change of Velocity

The change in velocity, $\Delta \mathbf{v}$, for impulsive maneuvers, is crucial, representing either a change in speed (Δv) or direction. The relationship between the velocity change and propellant consumption is derived by using the Tsiolkovsky rocket equation (41) as *Equation 2.1*:

$$\frac{\Delta m}{m} = 1 - e^{\left(-\frac{\Delta v}{I_{\text{sp}} g_0} \right)} \tag{2.8}$$

where Δm is the propellant mass, m is the spacecraft mass, I_{sp} is the specific impulse, and g_0 is standard gravitational acceleration.

Specific Impulse

The specific impulse I_{sp} is a measure of propulsion efficiency (41) as *Equation 2.2*:

$$I_{\text{sp}} = \frac{\text{Thrust}}{\text{propellant mass-flow rate x g}} \tag{2.9}$$

High I_{sp} engines are fuel-efficient but often produce low thrust, making them unsuitable for situations requiring large accelerations, like Earth lift-off.

Total Velocity Change

For maneuvers involving multiple impulses, the total Δv is the vector sum of individual velocity changes:

$$\Delta \mathbf{v} = \mathbf{v}_2 - \mathbf{v}_1 \tag{2.10}$$

The total propellant demand is exponentially related to the cumulative Δv, with maneuvers often evaluated based on their Δv requirements. In a single impulse burn, a spacecraft's trajectory is altered instantaneously, with the resulting eccentricity e of the new orbit described by *Equation 2.4* (40):

$$e = \frac{h_0}{R_E\,(1 + \cos\nu) + h_0}, \tag{2.11}$$

where h_0 is the initial altitude above Earth's surface, R_e is Earth's radius, and ν is the true anomaly at the burn point.

The transitions between orbits are classified based on their interception points (40):

- For *intercepting orbits*, maneuvers employing single impulsive thrusts suffice to achieve direct transfer to the target orbit, exemplifying the efficiency of one-impulse maneuvers.
- *Non-intercepting orbits* demand more complex strategies, including two-impulse transfers for classical trajectory adjustments and continuous thrust transfers for gradual orbital changes. As an optimal case, the Hohmann transfer and Lambert transfer as a more general approach are usually implemented to achieve efficient orbital insertions.

2.4.3 One Impulse Maneuvers and Genuine Plane Change

Maneuvers, based on the number of kick-burns, can be classified into one-impulse maneuvers or multi-impulse maneuvers that are integral to spaceflight dynamics, characterized by an instantaneous application of thrust resulting in a change in velocity, denoted as Δv. These maneuvers, typically short in duration and high in thrust, induce alterations in the spacecraft's velocity vector, consequently modifying its orbit. The subsequent analysis aims to correlate the Δv applied during these maneuvers with changes in specific orbital elements.

The analysis is structured around elementary maneuvers, which include tangent burns aligning with the orbital motion, outbound burns within the orbital plane, and normal burns orthogonal to this plane. These maneuvers selectively influence orbital elements and do not affect orbital energy if applied perpendicularly to the velocity vector, as they do not alter the spacecraft's speed. For the orbital elements semimajor axis (a), eccentricity (e), inclination (i), argument of periapsis (ω), and right ascension of ascending node (Ω), we observe the following:

- The semimajor axis is altered by tangent maneuvers at periapsis or apoapsis, with its change being a function of the maneuver's Δv and the orbit's eccentricity.
- The eccentricity is exclusively modified by burns at specific points where the alteration does not impact other elements like the semimajor axis or argument of periapsis.
- Inclination changes occur solely with normal burns that adjust the orbital plane's orientation without influencing the semimajor axis or eccentricity.

These dependencies are quantified at specific orbital positions for optimal impulse utilization, ensuring minimal propulsion mass is expended for the desired orbital element change. The table represents normalized kick-burns' effects on the various orbital elements at specific orbital positions. Symbols in the *Table 2.5* represent the effects of impulse on orbital elements: empty entries signal no impact, dashes show unchanged elements for specific orbital positions, and circles denote complex or impractical relationships and finally greyed cells represent dependencies.

Table 2.5 Effects of Normalized Kick-Burns on Orbital Elements

(32)

Orbital Element	$\Delta v_{\parallel}/v_h$	$\Delta v_{\perp O}/v_h$	$\Delta v_{\perp\perp}/v_h$	Special Orbit Positions
$\delta a/a$	$2/(1 \pm c)$			Peri/Apoapsis
δe	± 2	$-$		
$\delta \omega$	$-$	$\pm 1/e$	o	
δi			$\pm c$	Nodes
$\delta \Omega$			$-$	
$\delta \omega$	o	o	$-$	
δi			$-$	Orthogonal to nodes
$\delta \Omega$			$\pm s/\sin i$	
$\delta \omega$	o	o	$\pm s \cot i$	

2.4.4 Elementary Maneuvers in Circular Orbits

Circular orbits, characterized by zero eccentricity (e = 0), are prevalent around planets as they minimize atmospheric drag and offer stable conditions. Due to the absence of a periapsis, changes in orbital elements for circular orbits are not determined by usual equations that require a defined true anomaly. Instead, they can be derived from fundamental orbital mechanics principles. For a circular orbit, the semi-major axis (a) change is usually (40) understood as:

$$\frac{\delta a}{a} = 2\sqrt{\frac{a}{\mu}}\delta v_{\parallel} \tag{2.12}$$

For other orbital elements such as eccentricity (e), inclination (i), and right ascension of ascending node (Ω)—with the argument of periapsis (ω) being irrelevant for circular orbits—a different analytical approach is required, which can be summarized as (40);

$$\begin{bmatrix} \delta a/a \\ \delta e \\ \delta i \\ \delta \Omega \end{bmatrix} = \sqrt{\frac{a}{\mu}} \begin{bmatrix} 2 & 0 & 0 \\ 2 & 1 & 0 \\ 0 & 0 & 1 \\ 0 & 0 & 0 \end{bmatrix} \begin{bmatrix} \delta v_{\parallel} \\ \delta v_{\perp O} \\ \delta v_{\perp\perp} \end{bmatrix} \tag{2.13}$$

2.4.5 General Maneuvers

General maneuvers involve finite one-impulse maneuvers transitioning a spacecraft from an initial state vector $\mathbf{r}, \mathbf{v}_1$ to a final state vector $\mathbf{r}, \mathbf{v}_2$ at any point in space. The change in velocity (Δv) for such a maneuver is given by (40)

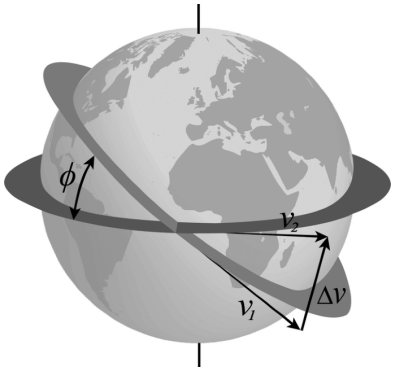

(41)

Figure 2.5 Tangent Plane Maneuver for genuine plane change

$$\Delta v = \sqrt{v_1^2 + v_2^2 - 2v_1 v_2 \cos\phi} \tag{2.14}$$

$$= \sqrt{(v_1 - v_2)^2 + 4v_1 v_2 \sin^2(\phi/2)} \tag{2.15}$$

where ϕ is the angle between $\mathbf{v}_1$ and $\mathbf{v}_2$. This equation is the most general way to calculate the delta-v for any single-burn maneuver.

2.4.6 Tangent Plane Maneuvers

Tangent plane maneuvers critically influence the geometry and orientation of a spacecraft's orbit. These maneuvers have the capability to alter the orbit's shape, characterized by the semi-major axis (a) and eccentricity (e), as well as the orientation of the orbital plane, denoted by inclination (i) and the right ascension of the ascending node (Ω). Notably, the argument of periapsis (ω) is typically of less concern, as many spacecraft operate in circular orbits where ω is undefined. For transitions between orbits, maneuvers such as the Hohmann transfer are employed, modifying both a and e, alongside a concurrent plane change affecting i and Ω. It is determined that only the components of the velocity change in the direction of motion ($\Delta v_{\parallel}$) and normal to the orbital plane ($\Delta v_{\perp\perp}$) are necessary for exclusively altering a, e, and the plane's orientation. This indicates that the initial and final velocity vectors, v_1 and v_2, lie within a plane tangential to the orbit at the maneuver point, thus defining the maneuver as a tangent plane maneuver.

Flight Path Angle

The flight path angle is between the orbiting body's velocity vector (equal to the vector tangent to the instantaneous orbit) and the local horizontal. Under standard assumptions of the conservation of angular momentum, the flight path angle ϕ satisfies the equation 2.15 (38):

$$h = rv\cos\phi \tag{2.16}$$

where:

- h is the specific relative angular momentum of the orbit,
- v is the orbital speed of the orbiting body,
- r is the radial distance of the orbiting body from the central body,
- ϕ is the flight path angle.

- ψ is the angle between the orbital velocity vector and the semi-major axis.
- ν is the local true anomaly.

So, $\phi = \nu + \frac{\pi}{2} - \psi$, therefore (40), (38),

$$\cos\phi = \sin(\psi - \nu) = \sin\psi\cos\nu - \cos\psi\sin\nu \tag{2.17}$$

$$\cos\phi = \frac{1 + e\cos\nu}{\sqrt{1 + e^2 + 2e\cos\nu}} \tag{2.18}$$

$$\tan\phi = \frac{e\sin\nu}{1 + e\cos\nu} \tag{2.19}$$

These equations describe the fundamental characteristics of elliptical orbits, from their shape and dimensions to the period of revolution around the central body.

2.4.7 Hohmann Transfers

The Hohmann transfer between two circular orbits involves a two-impulse maneuver, transitioning via an elliptical transfer orbit. The semi-major axis a_t of this transfer orbit is the average of the radii R_1 and R_2 from the central body to the initial and final orbits, respectively (38):

$$a_t = \frac{R_1 + R_2}{2} \tag{2.20}$$

For circular orbits, the velocity V at any point is (38):

$$V = \sqrt{\frac{\mu}{R}} \tag{2.21}$$

where μ is the standard gravitational parameter of the central body. Using the specific mechanical energy ϵ for the transfer orbit with the semi-major axis a_t, we have (38):

$$\epsilon_t = -\frac{\mu}{2a_t} \tag{2.22}$$

The velocity V_{t1} at the perigee of the transfer orbit, which coincides with the radius R_1 of the initial orbit, can be determined from:

$$V_{t1} = \sqrt{2\left(\frac{\mu}{R_1} - \frac{\mu}{2a_t}\right)} \tag{2.23}$$

The required ΔV to initiate the transfer from the initial orbit to the perigee of the transfer orbit is (38):

$$\Delta V_1 = |V_{t1} - V_1| \tag{2.24}$$

In the Hohmann transfer, the ΔV required at the apogee to insert the spacecraft into the final orbit, and the total ΔV for the entire maneuver are (38):

$$\Delta V_2 = |V_{t2} - V_2|, \quad \Delta V_{total} = \Delta V_1 + \Delta V_2 \tag{2.25}$$

where V_{t2} is the velocity at the apogee of the transfer orbit, and V_2 is the velocity in the final orbit. The Time of Flight (TOF) for the transfer is half the orbital period T of the transfer orbit (38):

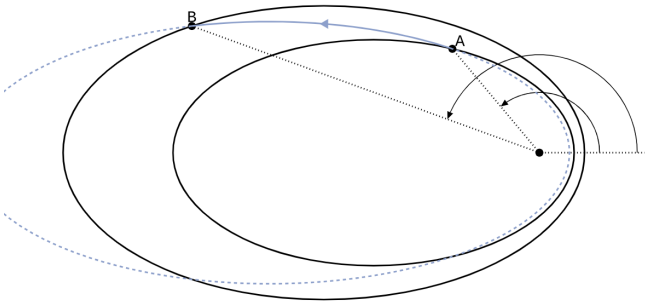

Figure 2.6 Non-Hohmann Transfer with a common apse line, the transfer orbit is shown in blue
(35)

$$TOF = \frac{T}{2} = \pi\sqrt{\frac{a_t^3}{\mu}} \tag{2.26}$$

2.4.8 Non-Hohmann Transfers with a Common Apse Line

Non-Hohmann transfers allow for more flexible maneuver timings than Hohmann transfers' strict periapsis and apoapsis impulse requirements. They require that the transfer orbit intersects the initial and final orbits, sharing a common focus and apse line.
Assuming we depart from the initial orbit at true anomaly ν_A and arrive at the target orbit at true anomaly ν_B, the radii at these points are related by the orbit equation (42):

$$r_A = \frac{p_t}{1 + e_t \cos\nu_A}, \quad r_B = \frac{p_t}{1 + e_t \cos\nu_B} \tag{2.27}$$

The Δv required for a transfer not occurring on the apse line must account for speed and direction changes. The magnitude of Δv is given by (42):

$$\Delta v = \sqrt{v_A^2 + v_{A_t}^2 - 2v_A v_{A_t}\cos\Delta\phi} \tag{2.28}$$

This equation determines the necessary velocity change at the departure point, with a similar calculation at the arrival point to find the total Δv for the maneuver.

Thrust Direction

The thrust must be aligned with the direction of Δv. The angle γ, relative to the local horizon, is determined by (42):

$$\tan\gamma = \frac{\Delta v_r}{\Delta v_\perp} \tag{2.29}$$

Here, Δv_r is the radial component change, and $\Delta v_\perp$ is the perpendicular component change in velocity. These calculations are essential for planning the propellant usage and maneuver strategy for space missions requiring non-Hohmann transfer orbits where the reconfiguration request requires the fastest transfer times, in such cases, waiting for the periapsis to execute the maneuver would be costly.

2.4.9 Phasing maneuvers

Phasing maneuvers are critical in orbital rendezvous missions, where two spacecraft align their positions and velocities. The phasing maneuver typically involves a two-impulse transfer, characterized by minimal propellant consumption but a longer duration. The orbital periods are dictated by their respective semi-major axes (42):

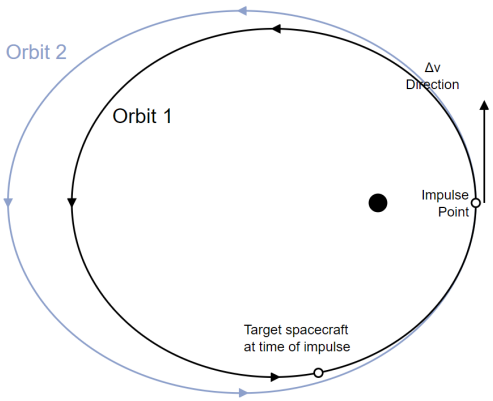

Figure 2.7 Phasing Maneuver where the transfer orbit is shown in blue

(35)

$$T_2 = \frac{2\pi a_2^{3/2}}{\sqrt{\mu}} \tag{2.30}$$

$$T_1 = \frac{2\pi a_1^{3/2}}{\sqrt{\mu}} \tag{2.31}$$

The longer period of the transfer orbit allows the interceptor spacecraft to match timing with the target, facilitating rendezvous at the original impulse point (42), in the context of our research exploration, this provides itself as a good candidate for implementing collision avoidance models. The unique time considerations allow the phasing maneuver to enter a particular true anomaly in the orbit.

2.5 Space Propulsion Systems

The selection of propulsion systems is suspected to play a pivotal role in the satellite constellation's fitness evaluation. Specifically, chemical and electric propulsion systems present unique characteristics that influence the overall fitness due to their divergent propellant mass consumption profiles. Chemical propulsion systems are known for their high-thrust, impulsive burns, allowing rapid orbital maneuvers. The instantaneous nature of these burns results in a discrete change in velocity, typically requiring significant amounts of propellant. This propellant consumption is critical to the satellite's fitness, impacting the mission's mass and cost. On the other hand, electric propulsion systems, such as ion thrusters, utilize continuous low-

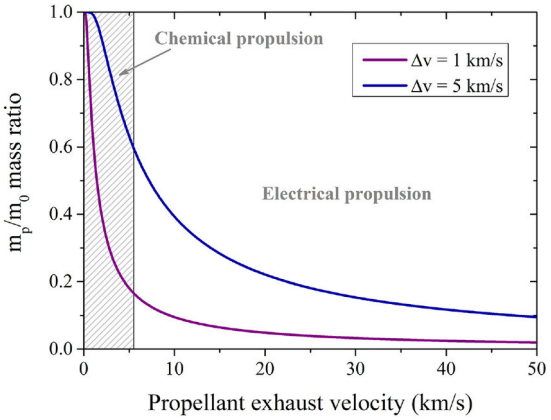

Figure 2.8 Chemical vs Electric Propulsion - Mass Ratio v/s Exhaust Velocity
(36)

thrust burns to gradually modify the satellite's trajectory (43). While these systems are highly fuel-efficient and can significantly reduce the propellant mass required over time, they necessitate prolonged periods to achieve the same orbital changes as chemical systems. (43) The contrasting propellant mass requirements between chemical and electric propulsion systems introduce a complex dynamic into the fitness evaluation process. Electric propulsion may be favored for missions where minimizing propellant mass is paramount despite the longer maneuver times. (39). Conversely, missions that prioritize rapid deployment or reconfiguration may lean towards chemical propulsion despite its heavier propellant demands. This dualistic nature of propulsion systems presents an intriguing aspect of the study, as the fitness evaluation must balance the immediate propellant mass and maneuver time against long-term operational efficiency and cost-effectiveness. Therefore, carefully considering propulsion types is essential in strategically planning satellite constellations to optimize their fitness within the DARF framework.

3 Methodology

Chapter 3 delves into a methodology specifically designed to address research questions *RQ-1* and thesis objectives *TO-1* through *TO-6*, as detailed in *Chapter 1* and summarized in *Table 1.1.* This part of the thesis is dedicated to pinpointing essential metrics, constraints, and design variables critical for optimizing spacecraft formation within federations and enhancing resource utilization. The chapter introduces robust mathematical modeling and develops a novel framework tailored to the specific objectives of this research. It incorporates a range of simulation models and sub-models, thoroughly addressing the framework aspects highlighted in *Section 3.2.4*, to methodically achieve the research goals. It presents mathematical formulations for diverse reconfiguration scenarios, providing insights into the orbital dynamics involved in such intricate mission scenarios. A framework for simulating adaptable and scalable reconfiguration processes for resource-efficient spacecraft formation adjustments is proposed. This framework integrates optical models for detection, astrodynamics, and reconfiguration models to efficiently manage and reconfigure spacecraft formation flights. A reward function model is introduced to further optimize the use of space resources. Additionally, a collision avoidance model with coordination strategies and countermeasures is proposed. The chapter concludes by outlining various mission scenarios and configurations to test the effectiveness of the developed algorithms and framework.

3.1 Mathematical Problem Definition for DARF

The modeling of our reconfiguration framework, focused on optimizing space resources for adaptable and scalable mission scenarios for satellites in federation is rooted in the principles of MDO from systems engineering. The framework shall be called Decentralized Adaptable Reconfiguration Framework (DARF), enhancing the satellite constellation's management and operational efficiency by optimizing critical factors that will be investigated and coined as the figure of merits. In spacecraft formation flight, adjusting the orbits of individual satellites to form a predefined configuration, DARF aims to offer a unique solution to the challenges of satellites in federation, focusing specifically on decentralized coordination. A strong emphasis on local computations and collective intelligence within DSS marks a strategic departure from traditional considerations discussed in previous chapters.

The core of DARF's mathematical approach treats it as a Non-Linear Programming (NLP) problem, reflecting the nonlinear dynamics between satellite resources and the overarching objectives of reconfiguration. Formulating a non-linear fitness function, $\boldsymbol{f}$, within a general NLP framework, is pivotal to capturing the complexities of satellite formation adjustments and setting a foundational strategy for decentralized constellation management. This strategy employs adaptive and reconfigurable techniques to improve satellite operations efficiency, encapsulating *Equation 3.1* as a key minimization function. In principle, each approach consists of a mathematical formulation of the minimization optimization problem and some techniques to solve the problem. Each model is structured so that all criteria relevant to achieving greater contributions toward mission success are rewarded accordingly.

3.1.1 Generalized Minimization Problem

Given a function $f : \mathbb{R}^n \times \mathbb{R}^m \to \mathbb{R}$, where $f(x, p)$ is the objective function to be minimized over design variables $x = (x_1, x_2, \ldots, x_n) \in \mathbb{R}^n$ and parameters $p = (p_1, p_2, \ldots, p_m) \in \mathbb{R}^m$, the goal is to find the optimal set of design variables x^* that minimizes $f(x, p)$.

Problem Definition

Objective:

$$\text{Minimize} \quad f(x, p) = \sum_{i=1}^{n} f(x_i, p_i) \tag{3.1}$$

Subject to constraints (if applicable):

- Equality constraints: $g(x) = 0$, where $g : \mathbb{R}^n \to \mathbb{R}^k$.
- Inequality constraints: $h(x) \leq 0$, where $h : \mathbb{R}^n \to \mathbb{R}^l$.

Formulation:

$$\begin{aligned} &\text{Minimize} && f(x, p) \\ &\text{subject to} && g(x) = 0, \\ &&& h(x) \leq 0, \end{aligned}$$

where $f(x, p)$ represents the composite objective function, $g(x)$ and $h(x)$ represent the constraints to be satisfied by the solution. The solution to this problem, x^*, represents the optimal set of design variables that minimizes the objective function $f(x, p)$ while satisfying all constraints, providing a balanced and efficient design or operational strategy.

Fitness Parameter Calculation

The fitness parameter for each satellite can be formulated for us by:

$$F(x) = \min \sum \{A \cdot F_i(x, p) + B \cdot F_i(x, p) + C \cdot F_i(x, p) + D \cdot F_i(x, p) + E \cdot F_i(x, p)\} \tag{3.2}$$

where *A, B, C, D, and E* are some weights given to it to normalize the data.

3.1.2 Decentralized Coordination and Resource Optimization Strategy

Through sorting and combinatorial analysis, the model identifies the subset of satellites that minimizes the overall fitness parameter sum, facilitating strategic reconfiguration decisions. This approach underscores the nuanced consideration of maneuver dynamics, propellant efficiency, and satellite health in orchestrating constellation reconfigurations, promoting operational longevity and performance. This methodological approach extends to a decentralized optimization model, focusing on collaborative problem-solving across a network of nodes without centralized oversight. Each node aims to minimize a collective function, F(x), independently assessing its local cost and contributing to a broader optimization goal without direct data sharing, see *Figure 3.1*. However, this framework will not deal with communication or optimizing and parsing data among satellites. This framework assumes the information has been parsed fully among the satellites in the federation. This simplifies the complexities of decentralized communication and enables us to focus more on decentralized coordination to find the minimum resource paths for reconfigurations.

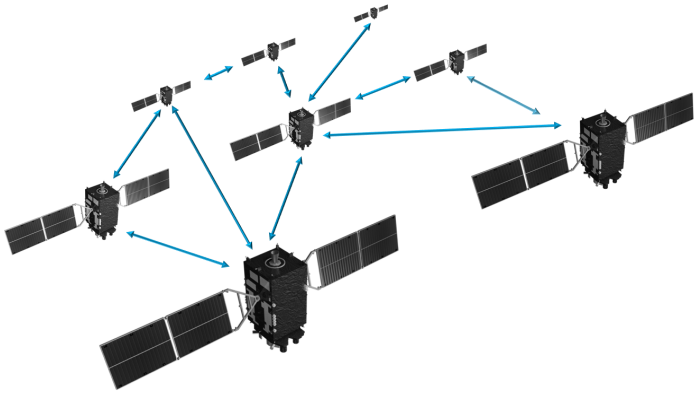

Figure 3.1 Information flow in DSS network

By integrating these principles, the optimization methodology for satellite reconfiguration within DSS utilizes MDO to target the reduction of certain figures of merits, steering individual satellite orbits towards a specified formation. This approach diverges from conventional satellite operation concerns, focusing on exploiting local computational capabilities and the collective intelligence inherent in DSS for decentralized optimization.

3.1.3 Performance Metrics

Establishing performance metrics involves defining operating or design parameters, design variables, internal variables, penalization factors, and weights that collectively inform the optimization process. These metrics are crucial for evaluating the performance of satellite configurations in terms of collision risk, operational efficiency, and mission fulfillment.

3.1.4 DARF Simulation Design Variables

Simultaneously designing satellite subsystems and configuring orbital arrangements necessitates a judicious selection of design variables. An overly constrained set of variables might overlook important objectives, whereas an extensive set could surpass our computational limits, impeding the optimization effort. Finding an equilibrium facilitates swift prototyping while maintaining the model's detail. A comprehensive suite of design variables is indispensable for DARF. These variables are essential for accurately modeling and endowing the framework with the versatility for effective spacecraft reconfiguration. This approach ensures that the developed framework remains adept at addressing the complexities of satellite operations, aligning with our research goals of adaptability and efficiency.

3.1.5 DARF Simulation Internal Variables:

Internal variables are derived during the simulation or computational processes, often resulting from arithmetic operations, logic conditions, or outputs of functions and algorithms. In the context of DARF, internal variables are dynamically generated based on the current state of the system, interactions between components, and external inputs. They might include values such as Delta-V calculations for maneuvers, propellant mass required for a maneuver, or time required for satellite reconfiguration. These variables are essential for understanding the evolving state of the satellite constellation, enabling the framework to adapt and reconfigure based on mission objectives and constraints. Internal variables provide insights into the system's performance, efficiency, and overall capabilities, serving as indicators for adjustments and improvements in real time or during subsequent analysis phases.

Table 3.1 Design Variables for used for thesis objectives in DARF Framework

Design Variable	Description	Range	Unit
numSats	Tot. number of satellites	[15, 25, 500, 50000]	-
numTimeSteps	Tot. number of time steps	[7, 86400]	-
numPlanes	Tot. number of planes	[3, 5, 20, 200]	-
numSatsPerPlane	Satellites per plane	[5, 25,]	-
numSatsAvPer	Tot. Percentage of Satellites Available	[0:100]	%
numSatsCapPer	Tot. Percentage of Satellites Capable	[0:100]	%
i2	Final Inclination	[56, 98.2]	degrees
e2	Final Eccentricity	[0, 0.1]	degrees
h2	Final Altitude	[500, 950]	km
Omega2	Final RAAN	[10, 20, 30, 40, 50]	degrees
omega2	Final Argument of Perigee	[0, 180]	degrees
nu2	Final True Anamoly	[0, 180]	degrees

Table 3.2 Internal Variables and DeltaV Calculations in the DARF Simulation

Internal Variable	Definition
a1	Initial semi-major axis
a2	Final semi-major axis
availability	Binary values for satellite availability
capability	Binary values for satellite capability
Delta_V1	DeltaV for increasing altitude
Delta_V2	DeltaV for decreasing altitude
Delta h	Reconfiguration Delta Height
Delta h_elec	DeltaV for Altitude Change (Electric)
Delta h	DeltaV for Altitude Change (Chemical)
Delta i	Reconfiguration Delta Inclination
Delta i_elec	DeltaV for Inclination Change (Electric)
Delta i	DeltaV for Inclination Change (Chemical)
Delta V_Omega	DeltaV for RAAN Change (Chemical)
Delta V_Omega_elec	DeltaV for RAAN Change (Electric)
Delta r	Reconfiguration Delta RAAN
Delta V_t	Reconfiguration Total DeltaV (Chemical)
Delta V_t_elec	Reconfiguration Total DeltaV (Electric)
fitnessparams	Fitness parameter
GSD	Ground Sampling Distance
m_dot	Fuel Flow Rate
Omega 1	RAAN Walker
omega 1	AOP Walker
omega 2	AOP Target
propellantMass_t	Total Fuel Mass Consumption
propellantMass_h	Fuel Mass required for Altitude change
propellantMass_i	Fuel Mass required for Inclination change
propellantMass_o	Fuel Mass required for RAAN change
R 1	RAAN Walker
timeForBurn	Time for Burn (Chemical)
timeForBurn_elec	Time for Burn (Electric)

Continued on next page

Table 3.2 continued from previous page

Internal Variable	Definition
timeForManeuver	Time for the Maneuver (Chemical)
timeForManeuver_elec	Time for the Maneuver (Electric)
totalSats	Total number of satellites
TWR	Thrust to Weight Ratio
t_h	Time for Altitude Change (Chemical)
t_h_elec	Time for Altitude Change (Electric)
t_i	Time for Inclination Change (Chemical)
t_i_elec	Time for Inclination Change (Electric)
t_o	Time for RAAN Maneuver (Chemical)
t_o_elec	Time for RAAN Maneuver (Electric)
v1	Initial orbital velocity
v2	Final orbital velocity

3.1.6 DARF Simulation Design Parameters:

Unlike internal variables, design parameters are predefined constants that describe the system's characteristics, constraints, and operating conditions. They are not subject to change during the simulation or operational phase. These parameters set the initial conditions and boundaries within which the system operates, including satellite mass, orbital heights, operational lifetime, and propulsion system mass. In DARF, these parameters are crucial for defining the baseline architecture of the satellite constellation, propulsion requirements, and optical sensing capabilities. By establishing these constants, researchers and engineers can simplify the simulation environment to focus on key areas of interest, compare different design architectures under consistent conditions, and ensure that the system meets its objectives within the specified constraints.

Table 3.3 Design Parameters in the DARF Simulation

Design Parameter	Description	Value	Unit
Diameter	Aperture Diameter	0.09	m
i1_walker	Walker Initial inclination	[54, 56, 98.2]	degrees
I_sp	Specific Thrust	[220, 7500]	s
FocalLength	Focal Length	0.07	m
h1_walker	walker Initial altitude	[550, 950]	km
m_p	Propulsion System Mass	1	kg
m	Satellite Mass	10	kg
Min_sep	Minimum Sep. Distance	[4e4, 6e4]	m
POSValuesX2, Y2, Z2	Collision target position	[2423.2606, 6508.9620, -11.35404]	km
propulsionType	Type of Propulsion	[chem "0", elec "1"]	-
start_time	Simulation Start Time	[DD MM YYYY 00:00:00:000]	-
stop_time	Simulation Stop Time	[DD MM YYYY 00:00:00:000]	-
StepSize	Simulation Step Size	[1, 10, 30, 60, 120, 240]	s
Thrust	Chemical or Electric	[1, 220e6]	N
ObjectSize	Target Size	[0.3, 3, 5, 10, 25]	m
F	Walker Phasing Parameter	1	-
Wavelength	Wavelength	7e-7	m
perigee1_walker	Initial perigee altitude	[500, 550, 950]	km
apogee1_walker	Initial apogee altitude	[500, 550, 950]	km

3.2 DARF System Architecture

This section represents the structural blueprint of a highly dynamic and modular framework for optimizing spacecraft formation flights in a federation. This architecture is pivotal in addressing the intricate challenges posed by the framework's management and operation of the data handling required to initiate, propagate, compute, evaluate, and visualize the reconfigurations. It leverages advanced computational models and integrated simulation environments, ensuring optimal performance, and increased resilience against external perturbations and mission-specific requirements. Its decentralized approach is central to the architecture, allowing individual satellites in the federation to make autonomous decisions. This is facilitated by incorporating state-of-the-art algorithms such as collision avoidance algorithms, detection algorithms, maneuvering algorithms, and optimization algorithms and protocols that enable satellites to communicate, coordinate, and execute reconfiguration maneuvers in a distributed manner. Moreover, the architecture's modularity and scalability support various satellite architecture sizes and configurations, making it adaptable to diverse mission objectives and operational scenarios. Integrating with external simulation and analysis tools such as STK and MATLAB, DARF provides a comprehensive environment for mission planning, simulation, and analysis, allowing for visualization, performance assessment, and optimization of satellite constellations.

3.2.1 Simulation Environment Decision Process & Decision Rationale

Table 3.4 Comparison of Simulation Approaches for this research study

Approach	Accuracy	Complexity	Dev. Time	Exec. Time	Total Points
Python SGP4 / Spice (44)	Low (-1)	High (-1)	Long (-1)	Slow (-1)	-4
Simulink / STK (45)	High (1)	High (-1)	Long (-1)	Very Slow (-2)	-3
MATLAB / PoliAstro (46)	Medium (0)	Medium (0)	Medium (0)	Slow (-1)	-1
C++ Simulator (47) / Python	Medium (0)	High (-1)	Long (-1)	Very Fast (2)	0
Simulink / STK / C++	High (1)	High (-1)	Long (-1)	Fast (1)	0
Basilisk (48) / Python / C++	Medium (0)	Medium (0)	Medium (0)	Fast (1)	1
MATLAB / STK (49)	High (1)	Medium (0)	Medium (0)	Medium (0)	1

Langtangen et. al, 2009 (50) research on "Numerical Computing in Python" acknowledges the computational speed of Python with NumPy as being quite close to MATLAB. However, MATLAB's built-in functions and optimization tools, specifically designed for numerical computing and modeling, often produce more efficient code with less development time. (50) MATLAB's extensive library of predefined functions directly supports a wide range of engineering and scientific calculations, reducing the need to develop complex functions from scratch as might be required in Python or C++. As illustrated in *Table 3.4*, a systematic comparison of various simulation approaches is presented in the field of satellite systems modeling. Each approach is evaluated based on several critical parameters: accuracy, complexity, development time, execution time, and an aggregate score reflecting its overall suitability for satellite simulation projects. The points assigned to each parameter are as follows: "High" accuracy and complexity contribute positively, indicating a method's robustness and thoroughness, each awarded 1 point. Conversely, "Low" scores in these categories denote potential shortcomings in simulation fidelity or simplicity, receiving -1 point. Execution time preferences are skewed towards swiftness, with "Fast" and "Very Fast" conditions considered ideal, scored at 1 and 2 points, respectively, to emphasize the benefit of rapid simulation results.

"Slow" and "Very Slow" execution times detract from an approach's appeal, scored at -1 and -2 points, respectively. Development time is critically assessed based on the urgency and fluidity of project timelines: "Short" development periods (less than 3 months) are highly prized for their agility, earning 1 point. "Medium" spans (4-5 months) represent a balanced compromise, scored neutrally at 0 points, while "Long" duration (6 months and beyond), marked by uncertainty, are seen as a drawback, receiving -1 point. The first approach to be explored was a Simplified Perturbations Models 4 (SGP4) Python-based model (51) incorporating SGP4 for orbital mechanics and Spacecraft Planet Instrument C-matrix Events (SPICE) (44) for planetary and spacecraft trajectory computations. This route promised a tailored solution, finely attuned to the specific requisites of our exploratory research study. However, concerns regarding the protracted development time frame, potentially extending beyond the thesis deadline, alongside the risk of significant deviations in accuracy when juxtaposed with established simulators, steered the decision away from this option. The anticipated low fidelity of this model, coupled with the specter of substantial refinement efforts, underscored the impracticality of this route, especially given the uncertainties surrounding telemetry link simulations.

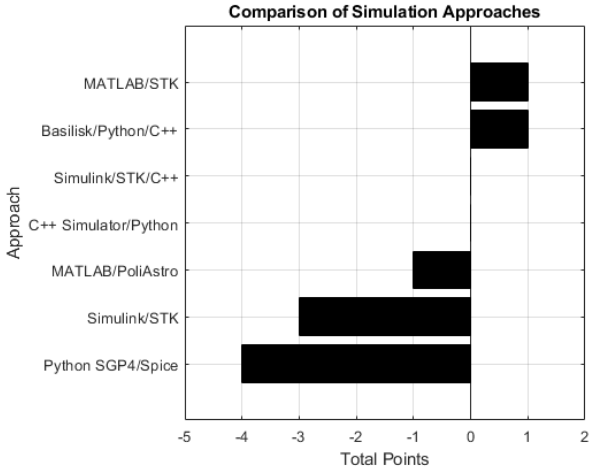

Figure 3.2 Comparison of Simulation Approaches

Integrating a MATLAB Simulink model (52) with STK Connect offered a promising approach to utilizing an existing framework for simulating individual satellites. The potential to harness AGI Server's reliable data was attractive. However, the computational demands of simulating a large group of satellites with STK posed significant challenges. This method mirrored the development time of the initial approach but offered improved accuracy if scalability and decentralization issues could be addressed. At our TUM Chair of Spacecraft Systems, a newly developed C++ simulator presented a quicker alternative with the capability of independent subsystem operation. Though this method provided moderate accuracy and allowed for subsequent visualization in Python, its basic nature fell short compared to the comprehensive data available from STK. A hybrid model, combining Simulink/STK with the C++ simulator (47), seemed to offer a balanced solution, true to the thesis's objectives. It proposed separating tasks, with the C++ simulator generating initial outputs for satellites that would then be processed through a high-accuracy collision avoidance framework in Simulink/STK. Despite its potential, the hybrid approach's complexity and required development effort led us to consider other options. Figure 3.3 shows STK's various levels of integration when seen against ease of use. Since DARF manages the computations for maneuvers within MATLAB as illustrated in *Figure 3.7*, file interoperability was given precedence and mostly needed, and STK connect through COM was primarily desired.

Integrating with STK and MATLAB

After meticulously evaluating, integrating MATLAB with STK was identified as the optimal simulation environment for our dynamic reconfiguration framework as also identified in the *Table 3.4* and *Figure 3.2*. This

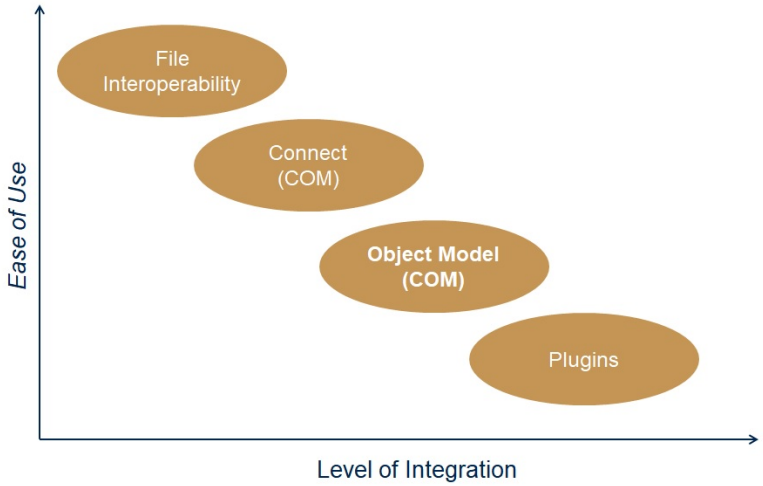

Figure 3.3 Ease of integration vs level of integration

hybrid model facilitates the generation of simulated outputs for an adaptable number of satellites, subsequently refining these through a dynamic reconfiguration framework devised in MATLAB. This setup promised an efficacious amalgamation of low and high-fidelity models, culminating in a robust, high-accuracy final model. The balance between development duration, computational efficiency, and the overarching accuracy imperative of our research underpinned this choice. A culmination of multiple factors propelled the decision to harness MATLAB and STK for our simulation environment: the nuanced balance between development time and model accuracy, the computational efficiency and ease of user experience afforded by MATLAB, and the fidelity of STK's environmental modeling. MATLAB's extensive analytical tools and STK's comprehensive environmental data provide a formidable foundation for simulating complex satellite constellation behaviors and reconfiguration maneuvers. This environment offers a rigorous platform for our analyses and aligns seamlessly with the research's aim to pioneer advancements in satellite operational strategies. *Figure 3.4* illustrates the intricacies of the data exchange processes between MATLAB and STK, focusing on the two primary communication protocols: Component Object Model (COM) and Transmission Control Protocol/Internet Protocol (TCP/IP). This comparison delineates how each protocol facilitates the interoperability between MATLAB and STK, underscoring their respective advantages and operational contexts within the simulation framework which will be further discussed in detail in *Section 3.5.1.*

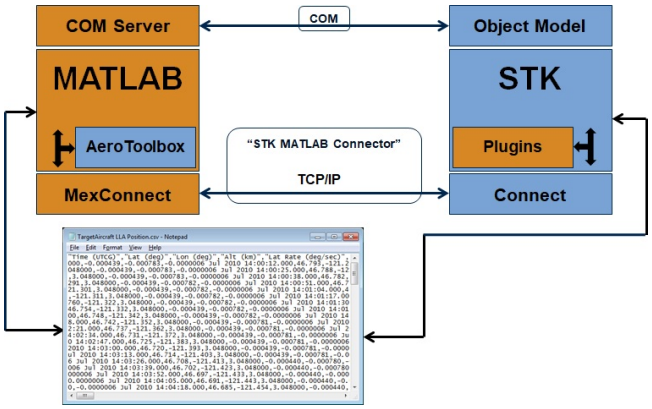

Figure 3.4 Integrating STK and MATLAB

3.3 Integration with STK

A significant component of our methodology is the integration of MATLAB with STK, enabling a seamless transition from theoretical modeling to practical, high-fidelity simulation. This integration facilitates the visualization and simulation of satellite constellations and procurement of vital data such as positional and keplerian elements for each timestep, leveraging STK's robust capabilities for space scenario analysis. Integrating the MATLAB with STK was the design decision and a pivotal step for aligning computational intelligence with spatial visualization. This hybrid approach enriches satellite constellations' strategic planning and operational management by offering an intuitive visual representation of complex maneuvers and configurations in a dynamic space environment.

Communication Establishment

Communication between MATLAB and STK is facilitated via two primary methods: TCP/IP connections for transmitting Connect commands through a specified port (default is 5001), and the COM interface for direct command relay to STK. This dual-method approach ensures robust and flexible integration, accommodating various system configurations and user preferences.

Utilization of STK Connect

The Connect feature within STK provides a streamlined mechanism for DARF to engage with STK, enabling command execution, data retrieval, and scenario control directly from MATLAB. This capability allows for the automation of scenario setups, execution of reconfiguration strategies, and real-time visualization of satellite operations.

Astrogator Connect Integration

DARF employs Astrogator Connect commands to precisely manipulate mission control sequences and satellite mission parameters and can effectively and accurately simulate and visualize satellite maneuvers, trajectory adjustments, and mission outcomes through the Astrogator's specialized command structure, enhancing decision-making processes and mission planning.

3.3.1 Framework Aspects

The table presented in *Table 3.5* delineates a brief overview of the foundational elements critical to developing our simulation framework from scratch. This structure is necessary for guiding the systematic construction of the simulator from the ground up, ensuring that each aspect of the framework aligns precisely with the predefined requirements and objectives of the thesis. The detailed categorization into aspects such as *Propagation, Detection, Resource Optimization, Maneuver,* and *Risk of Collision* offers a methodical approach to addressing the complex dynamics of satellite systems optimization strategies. Each category is meticulously defined to encapsulate essential functions and operational strategies, providing a clear foundational blueprint for simulator development. This organization not only streamlines the simulation framework's construction but also ensures that all critical parameters and operational conditions are accounted for, thereby minimizing the risk of deviation from the intended research path. By establishing a clear outline of framework aspects, we are afforded a strategic starting point for simulator development. This enables a targeted focus on achieving the thesis's objectives, such as optimizing satellite constellation configurations, enhancing collision avoidance techniques, and improving resource management strategies. This approach aims to ensure that the final product is robust comprehensive and tailored to meet the specific challenges and inquiries posed by our research.

Table 3.5 Aspects Table for the DARF

Aspect	Requirements / Approach
Propagation	**Astrodynamics Model** Geometry engine for determining the time-dynamic position and attitude of objects
Detection	**Optics Resolution Model** Updating GSD & Detecting GSD < Object Size
Resource Optimization	**Reward Function Model** Minimization Function with fitness parameters
Maneuver	**Reconfiguration Model** DeltaV Budgets, burn and reconfiguration times
Risk of Collision	**Tolerance & Probability Model** Distance < Min Allowable Distance Exclusion Spheres

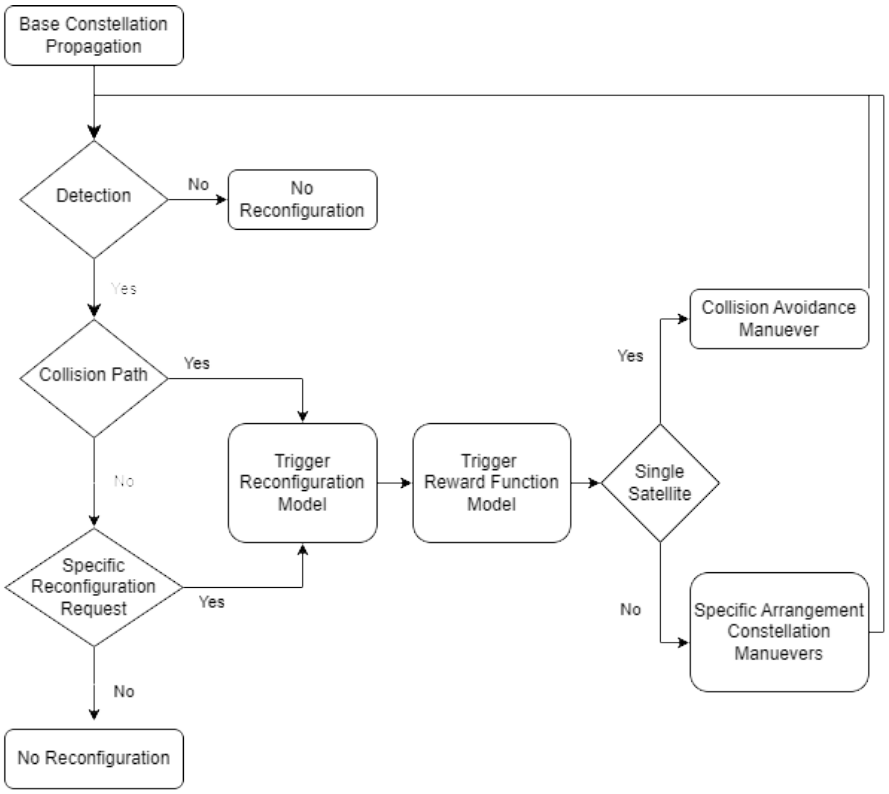

Figure 3.5 Prospected Flow Diagram of Simulator's Detection and Collision Avoidance Aspects

3.4 Simulation Models within DARF and its Subsystems

DARF employs a multi-faceted approach to tackle reconfiguration requests, which are a set of required parameters by a user detailing the desired state of the requested arrangement of satellites. The framework integrates sophisticated simulation models across various subsystems. These models are meticulously designed to address the operational challenges of maintaining and optimizing a dynamic constellation architecture. Through the synergy of astrodynamics, optics resolution, resource optimization, maneuver planning, and risk assessment models, the framework ensures satellites in federations are safe, efficient, and responsive operation. Table 3.5 encapsulates the critical aspects and the corresponding methodologies adopted within DARF to tackle these challenges. From the precise propagation of satellite orbits to the nuanced detection of potential collisions and the strategic optimization of resources, each model plays a pivotal role in the framework's ecosystem. This structured approach allows DARF to anticipate and mitigate risks and leverage opportunities for enhancing constellation performance. Figure 3.6 further illustrates the interconnectedness of these subsystems, while Figure 3.7 showcases a more detailed data flow and processing hierarchy within DARF. This integration is fundamental to the framework's ability to deliver a comprehensive solution for satellite constellation management, balancing the dual mandates of operational efficiency and mission success.

3.4.1 Data Flow in DARF

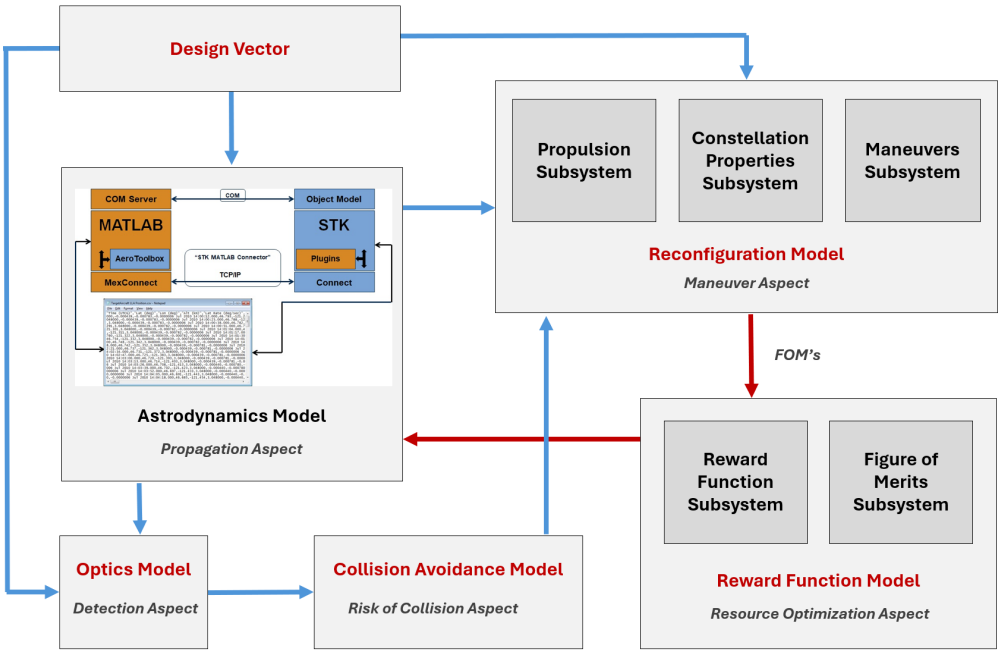

Figure 3.6 Simpe Data Flow Diagram of DARF

3.4.2 Detailed Diagram for Data Flow in DARF

Figure 3.7 illustrates a very detailed description of the overall architecture of DARF. These inputs and outputs will be discussed in detail in the subsequent sections. In a nutshell, the Design Vector puts design variables into the astrodynamics model, which propagates as the initial data provider. It utilizes inputs from the design vector to propagate orbital scenarios, thereby generating positional data and Keplerian elements. This output feeds into the optics model, which calculates the GSD, essential for detecting potential collision objects. In parallel, the constellation properties subsystem utilizes design variables to refine orbital parameters, which informs the propulsion subsystem alongside the astrodynamics model's output.

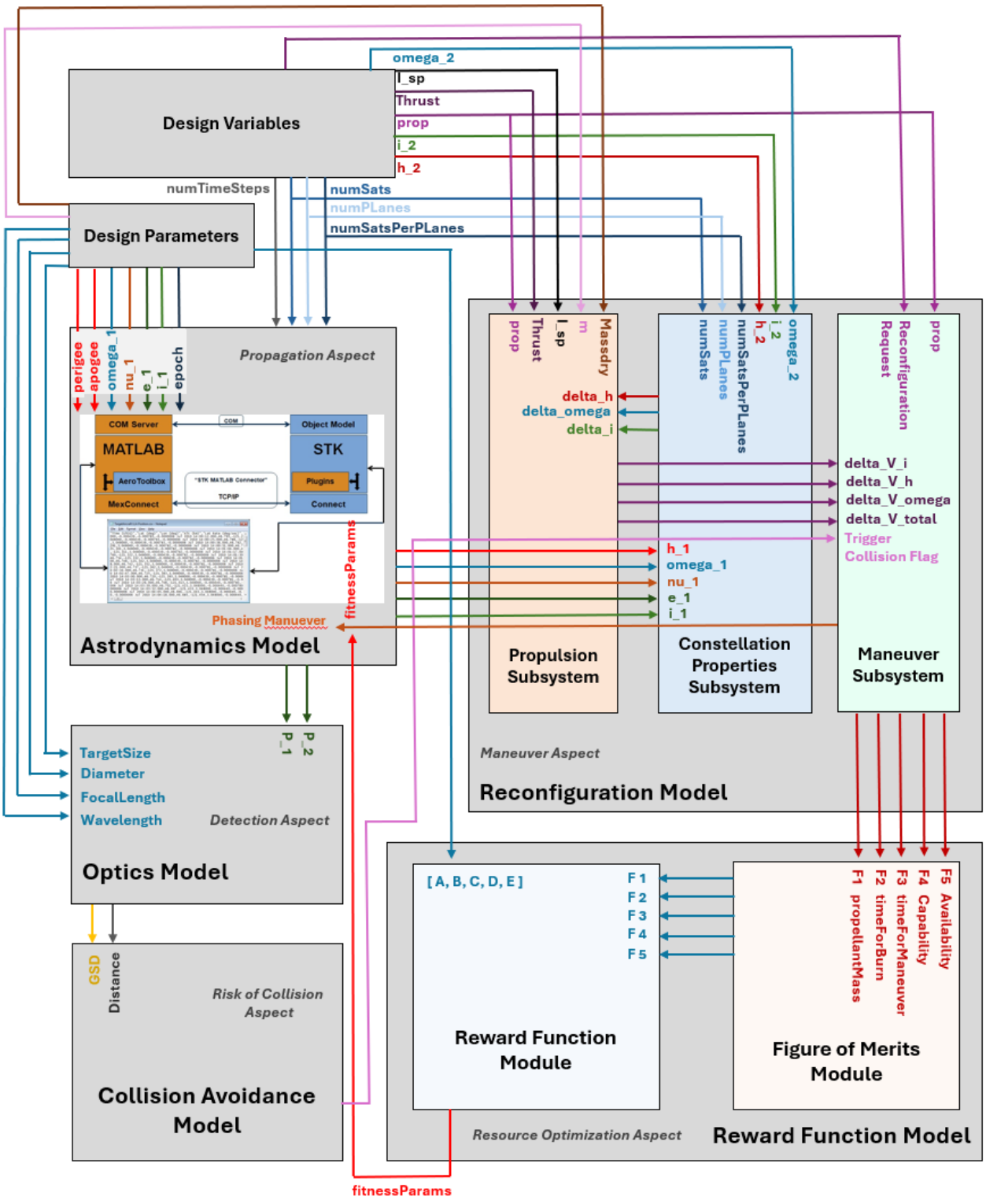

Figure 3.7 Detailed Data Flow Diagram of DARF

This subsystem calculates the necessary delta-Vs for maneuvers, laying the groundwork for the maneuver subsystem to execute reconfigurations and generate specific Figure of Merit (FOM). These FOMs, alongside capability and availability metrics from other subsystems, are input to the reward function model, which optimizes and outputs fitness parameters guiding the final reconfiguration decisions. Additionally, leveraging GSD data, the collision avoidance model triggers phasing maneuvers within the reconfiguration model, ensuring the constellation's safe and efficient operation.

3.5 Astrodynamics Model

This section outlines the function of the integrated STK engine, being connected to MATLAB's initialization design vector for propagating our scenarios. The two subsystems within this model, as illustrated in detail in *Figure 3.7* within the proposed framework, STK and MATLAB's connected environment are a set of interdependent subsystems, each specialized in performing critical functions necessary for importing mission-critical data such as Keplerian orbital elements and positional data over time for each satellite. This subsystem can be seen as the data provider for our simulations. This subsystem is therefore responsible for the *' Propagation Aspect '* as defined in *Table 3.5* of the DARF, which is the given name for this framework. However, this model is also responsible for receiving propagation requests, a set of defined orbital parameters pushed as a final output from the Reward Function Model. Therefore, within MATLAB an Orbit Simulator Model is implemented within this subsystem that considers the number of satellites, the number of planes in the federated formation, the number of satellites per plane, and the target altitude of some or all Keplerian elements to provide inputs to the integrated STK.

3.5.1 Data Flow in DARF

Table 3.7 Inputs and Outputs of the Astrodynamics Model

Type	Description	Details
Input	Design Vector	Design variables including total number of satellites, planes, etc.
Input	Keplerian Elements	Orbital parameters for each satellite
Input	Constellation Configuration	Information from the Reward Function Model
Output	Positional Data	Data provided to the Optics Model for further processing

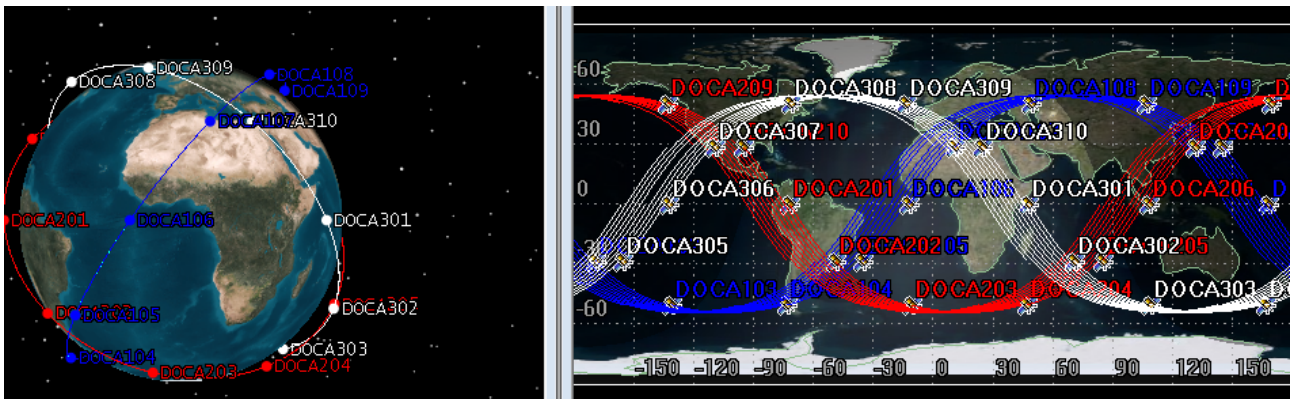

Figure 3.8 Walker Delta Constellation 54: 30/10/0 visualized on STK

It ensures that the desired constellation configuration and the relative satellite positions are maintained over time. The astrodynamics subsystem's initialization critically underpins the definition of essential orbit parameters, which are crucial for the computation of Earth-orbiting satellite trajectories. These trajectories hinge upon six orbital elements: (a), (e), (i), (Ω), (ω), (ν). This module draws the computational capabilities of the high fidelity orbit propagator engine of STK and loops in these six kelplerian elements over all timesteps back into the framework. The selection of the Walker Delta constellation as the base model for our simulations stems from its widespread adoption within the satellite community for circular orbit constellations (53). This preference is largely due to the constellation's inherent symmetry, which significantly simplifies the design and management of satellite formations. Such symmetry ensures uniform perturbation effects across the constellation, streamlining operational management tasks. The choice of Walker Delta as the foundational configuration is made to leverage these benefits, providing a robust and well-understood starting point for our analysis. However, it is essential to highlight that DARF's flexibility and

adaptability extend beyond the confines of the Walker Delta configuration. The framework is designed to accommodate a variety of constellation designs, ranging from Walker Star and Pendulum configurations to custom arrangements tailored to specific mission requirements. This versatility is a testament to DARF's capability to cater to a broad spectrum of operational scenarios, making it a comprehensive tool for constellation management. Described by $i : t/P/F$, this configuration evenly distributes t satellites across P planes, inclined at i degrees, with a separation of $360/t \times F$ degrees. (30) The Iridium constellation (54), utilizing an 86.4: 66/6/2 Walker pattern, serves as a notable example. The phasing parameter F, varying from 0 to $P - 1$, finely tunes the satellites' relative positions, optimizing the constellation layout. For this research study, a walker configuration of 54: 25/5/1 is selected as a base configuration. *Figure 3.8 (left)* illustrates a three-dimensional Earth-centered view of a Walker delta constellation 54: 30/10/0 at a 500 Km circular orbit where each satellite is represented by the nomenclature format DOCAXXX, where 'XXX' represents the index of the satellite. At the first set of simulations and numerical iterations, the framework was called Decentralised Optimization Collision Avoidance (DOCA) Framework and later named DARF. The inclination range of 54 to 56 degrees, often chosen for constellations, an example like the Galileo navigation system 56: 24/3/1 (55), offers us a practical baseline for our simulations, reflecting conditions of numerous existing large formations. This range is not arbitrarily selected but represents a commonly utilized orbital region that effectively balances coverage, communication latency, and environmental perturbations (53). However, DARF's architecture is inherently designed to transcend this default, enabling the exploration and optimization of satellite formations across various inclinations, altitudes, and configurations.

3.6 Optics Model

The optics subsystem is focused on the payload capabilities related to imaging and observations. This subsystem is therefore responsible for the *' Detection Aspect '* as defined in *Table 3.5* of the DARF. GSD, traditionally used to denote the ground resolution capability of satellite imagery, measures the distance between pixel centers recorded by a satellite sensor. This parameter is necessary for determining the level of detail captured in satellite images. It is directly influenced by factors such as the satellite's altitude, the sensor's optical properties, and the imaging system's configuration. Within the context of our study, the GSD concept is adapted to assess the satellite's ability to resolve and detect other satellites as objects within the space segment. By employing an *' Optics Resolution Model '*, the research meticulously evaluates the optical requirements necessary for such detection tasks. This model considers the *aperture size* (diameter of the lens), *focal length*, and *wavelength* perceived by the optical instrument, which is critical in calculating the GSD and by extension, the imaging system's resolution capabilities. As seen in *Equation 3.7,* the model only takes the input of the optic's wavelength of the upper limit of the visible spectrum of light, the diameter of the optics onboard the observing satellite, and the distance between the satellite and the target object. *Equation 3.9* calculates distance, the formulation for the distance between two points in space. *Note:* Focal Length of optics is not used.

Table 3.8 Inputs and Outputs of the Optics Model

Type	Description	Details
Input	Positional Data	Data received from the Astrodynamics Model
Input	Design Vector	Design Parameters on Optics
Output	GSD (Ground Sampling Distance)	GSD values provided to the Collision Avoidance Model

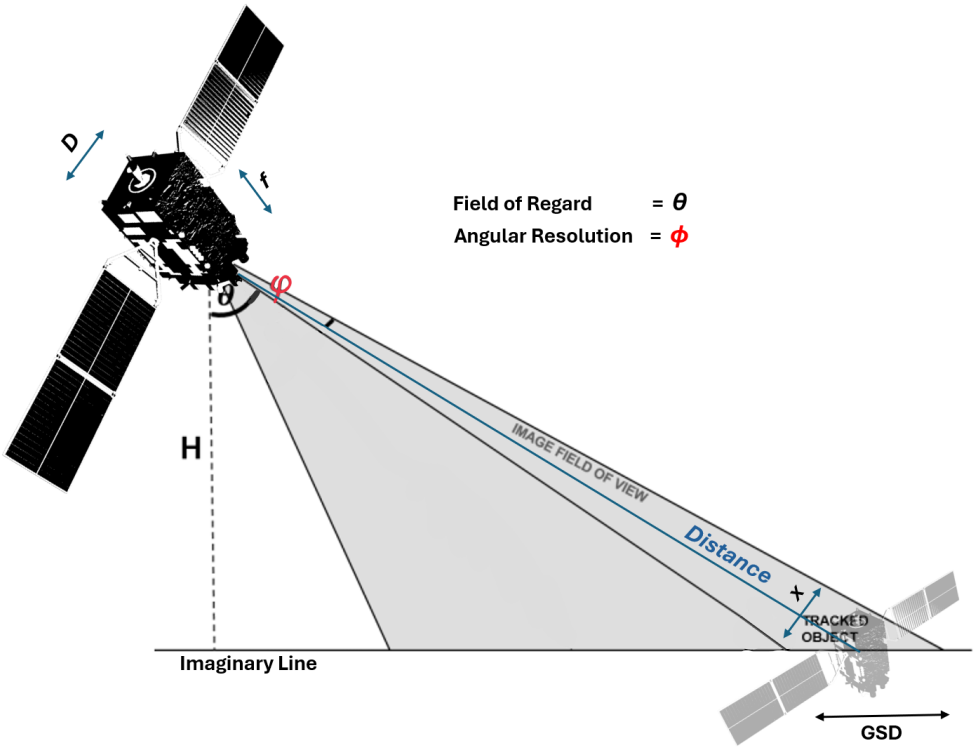

Figure 3.9 Ground Sampling Distance (GSD) visualized in the context of satellite tracking and detection by image resolution.

In satellite-based imagery, particularly concerning inter-satellite observations, the traditional concept of GSD is reinterpreted to address the unique dynamics of space, serving as a strategic metric for evaluating the imaging systems' efficacy in identifying and tracking orbital objects. If the computed GSD is lesser than the target object's size, it implies the observing satellite's generalized resolution sufficiency for *'detection,'* as depicted in *Figure 3.9*. This detection threshold highlights the applicability of GSD in space, offering a methodological foundation for assessing the effectiveness of satellite imaging systems in object identification and tracking. Incorporating this metric into our analysis ensures the simulator accurately reflects satellite constellations' detection capabilities, providing a realistic portrayal of their surveillance and reconnaissance potential. The enlargement of GSD with increasing satellite distance from Earth and pixel size results in less detailed imagery. Extending the optical instrument's focal length can mitigate heightened GSD effects, albeit at the expense of enlarging the payload size. The optical system's angular resolution (θ), constrained by the Rayleigh criterion, delineates the diffraction limit as d', illustrated by:

$$\theta = 1.22\frac{\lambda}{D} = \frac{d'}{2f}, \tag{3.3}$$

where λ denotes the wavelength, D represents the aperture diameter and f represents the focal length. This equation underscores the system's resolving capacity, assuming it is not limited by lens imperfections or pixel size. Observations aimed at terrestrial imaging necessitate larger apertures for resolution maintenance when the satellite's Line of Sight (LOS) deviates from the perpendicular to Earth's surface (deviates from Nadir), as shown:

$$D = 2.44\frac{\lambda \cdot h}{x \cdot \cos\theta}, \tag{3.4}$$

where h represents the satellite's altitude. The pixel's ground projection into the GSD, for an off-nadir angle with an angular resolution θ, is given by:

$$D = 2.44\frac{\lambda \cdot h}{\mathrm{GSD} \cdot \cos^2\theta}, \tag{3.5}$$

The ground projection of a pixel into the GSD, given an on-nadir angle, ϕ is *0 degrees* is described by:

$$\mathrm{GSD} = 2.44\frac{\lambda \cdot h}{D}, \tag{3.6}$$

In the context of our research, which primarily focuses on space imagery and satellite detection, we adopt this LOS approach for simplifying our observational model. This decision streamlines the computational process, enabling faster and more efficient analysis. By concentrating solely on LOS perspectives, we intentionally bypass the complexities associated with a skewed field of regard and terrestrial imaging scenarios. This methodological choice markedly diminishes the equation's complexity, particularly concerning angular resolution ϕ as seen in *Equation 3.3*. This approach inherently negates the need to account for angular deviations. It reduces the number of variables and assumptions involved or adjustments that would otherwise be necessary for terrestrial observational models.

Focusing on inter-satellite observations, the traditional GSD concept is redefined to suit the specific dynamics of space. Here, GSD's role expands to quantify spatial resolution in the context of satellite-to-satellite detection, necessitating considerations beyond the conventional terrestrial imaging parameters. This further allows us to discern other satellites as distinct entities within the spatial confines of outer space. Herein, parameters such as the optical system's angular resolution, diffraction limits, and specifications (notably *aperture size* and observation *wavelength*) assume critical importance. The inclusion of the LOS distance between satellites, as illustrated in *Figure 3.10*, emphasizes the optical system's resolving power in space. This approach simplifies our observational model, focusing on direct, unobstructed paths between satellites, enhancing the efficiency and precision of space-based observations. The inter-satellite

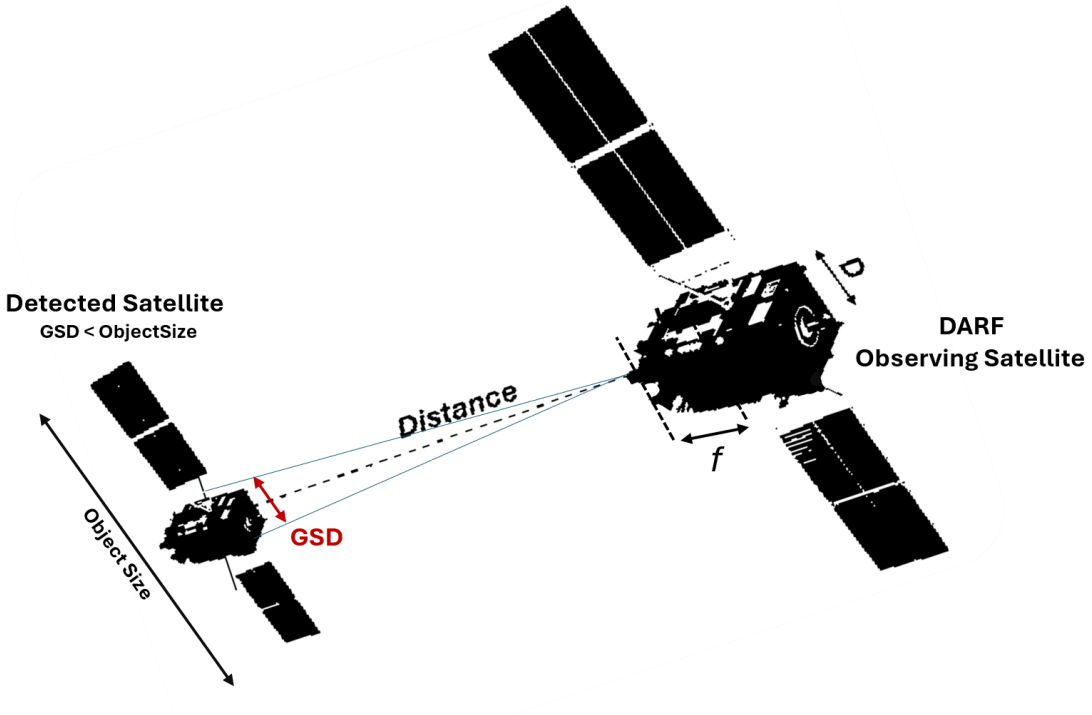

Figure 3.10 Line of Sight (LOS) GSD resolution of the detected satellite by the observing satellite in space. Note: Distance is NOT according to scale.

distance crucially influences the optical system's ability to resolve a satellite as a separate object against the spatial backdrop of space. The *Equation 3.5*:

$$\text{GSD} = 2.44 \frac{\lambda \cdot \text{Distance}}{D}, \tag{3.7}$$

although unconventional for GSD calculations, it aligns with the logic of detecting satellites in space. It integrates inter-satellite distance into the analysis, acknowledging its significance in determining space-based detection capabilities. This approach also offers a direct and unobstructed path from the observing satellite to the target, which is paramount for space-based observations where accuracy and simplicity are valued. In optics modeling, a critical function is a computation of the distance d between two satellites, which is determined based on their Cartesian coordinates, $p_1 = [x_1, y_1, z_1]$ and $p_2 = [x_2, y_2, z_2]$. The formula for calculating this distance is:

$$d = \sqrt{(x_2 - x_1)^2 + (y_2 - y_1)^2 + (z_2 - z_1)^2} \tag{3.8}$$

This distance measurement is vital for the subsequent Collision Avoidance Model, elaborated in *Section 3.7*. Furthermore, the satellite's size is an essential design parameter in this subsystem. As illustrated in *Figure 3.10*, detection of the target satellite by the observing satellite is contingent upon the conditions:

$$\text{GSD} < \text{ObjectSize} \tag{3.9}$$

where the GSD must be less than the target's size for detection to occur. This subsystem simplifies the model by not accounting for space losses, optical diffraction, or radiation interference, focusing on the core parameters for satellite detection.

3.7 Reconfiguration Model

This section talks about the Reconfiguration Model, with its internal components: *Propulsion Subsystem*, *Maneuver Subsystem*, and *Constellation Properties Subsystem* which plays a crucial role in satellite operation within the DARF simulation. This subsystem, responsible for the *' Maneuver Aspect '*, integrates inputs from the Astrodynamics subsystem and simulation design variables and parameters to effectively manage and execute satellite maneuvers. It focuses on calculating the *total delta-v* required for trajectory or orientation adjustments based on propulsion type, chemical or electric, and its characteristics to determine maneuver parameters, including propellant mass and burn times.

Table 3.9 Inputs and Outputs of the Reconfiguration Model

Type	Description	Details
Input	Keplerian Data	Data received from the Astrodynamics Model
Input	Positional Data	Data received from the Astrodynamics Model
Input	Design Variables	Data from the Design Vector
Input	Collision Avoidance Trigger	Trigger for Phasing Maneuver
Input	Reconfiguration Request	User
Output	DeltaV Budgets and Times	Maneuver specific FOM provided to the Reward Function Model

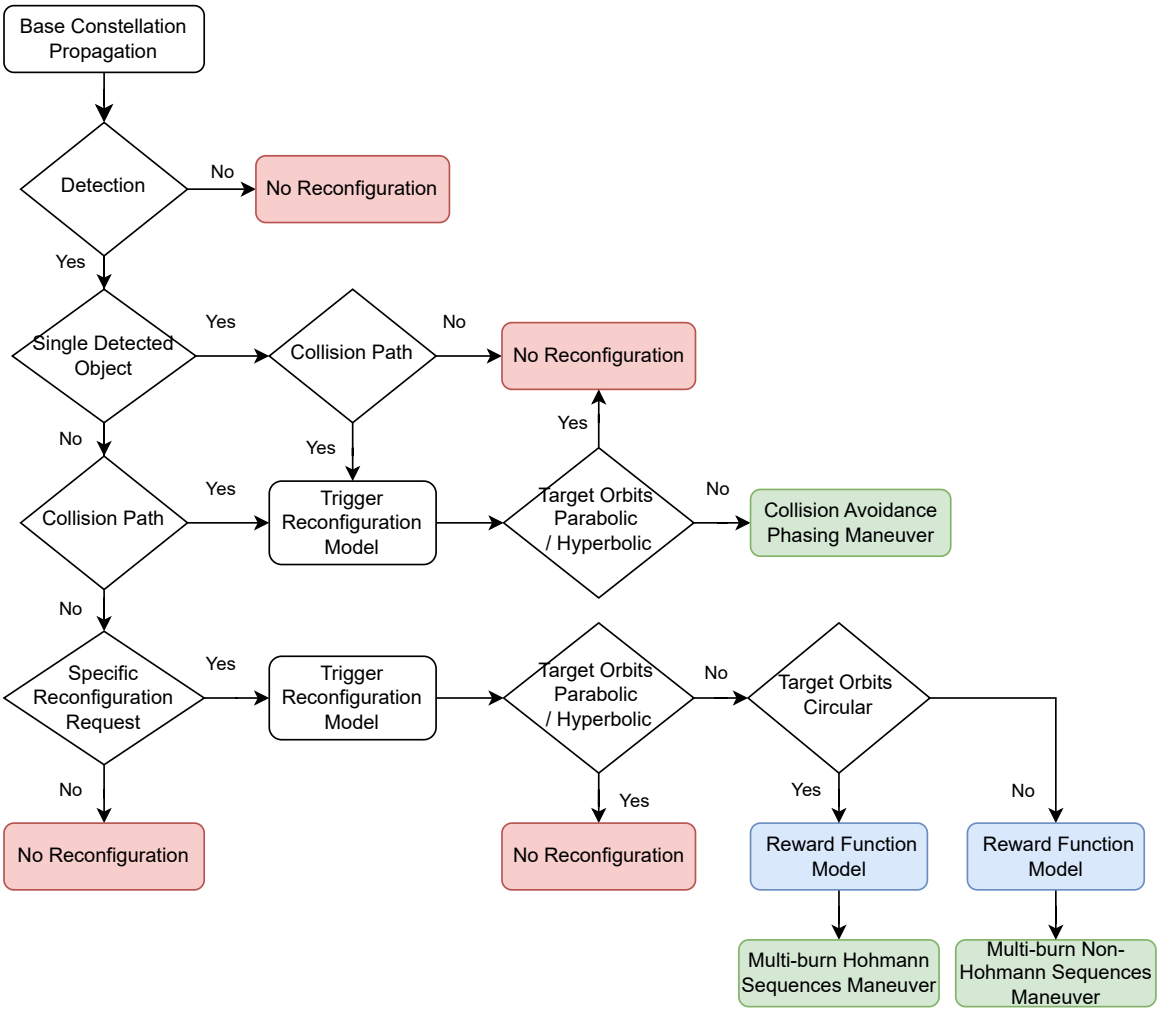

Figure 3.11 Updated Flow Diagram of Simulator's Detection and Collision Avoidance Aspects

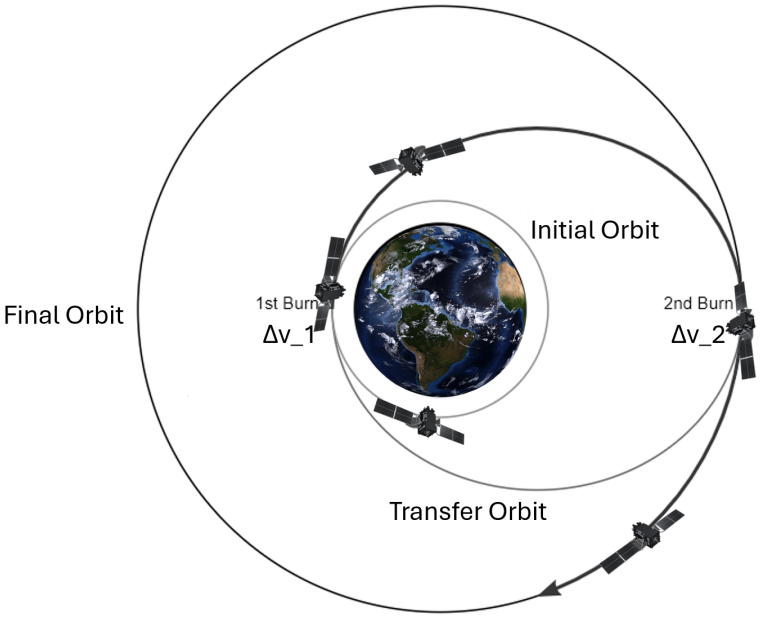

Figure 3.12 Hohmann Transfer Orbit

The Maneuver Subsystem collaborates with propulsion and astrodynamics subsystems to calculate necessary maneuvers for maintaining or altering constellation configurations, directly influencing propellant usage and maneuver and burn times. The Constellation Properties Module maintains data on the constellation's characteristics, such as satellite mass and fuel capacity, which are essential for operational planning and execution. This structured approach ensures precise maneuver execution within mission constraints, optimizing satellite constellation management.

3.7.1 Constellation Properties Subsystem

The Constellation Properties Subsystem functions as a comprehensive database, encapsulating vital data on the base constellation's current attributes and the desired characteristics post-reconfiguration. This subsystem meticulously records each satellite's mass, onboard propellant volume, and the constellation's typology, among other parameters. It is instrumental in shaping the constellation's operational methodologies. It seamlessly conveys crucial reconfiguration parameters—such as inclination adjustments, Right Ascension of the Ascending Node (RAAN) values at each timestep, and altitude modifications to the Propulsion subsystem. This integration ensures the reconfiguration aligns with strategic goals, enhancing the constellation's efficacy and adaptability within the designated architectural framework.

Table 3.10 Inputs and Outputs of the Constellation Properties Subsystem

Type	Description	Source/Destination
Input	Design Variables (Altitude, Keplerian Elements)	Design Vector
Input	Orbital and Positional Data	Astrodynamics Model
Input	Read Files for Predefined Configurations	External Data Files
Output	Delta Inclination, Delta RAAN, Delta Altitude	Propulsion Subsystem

3.7.2 Propulsion Subsystem

The propulsion subsystem is crucial in the satellite's ability to execute maneuvers that modify its trajectory or orientation in space. This capability is in direct service to the *Maneuver Aspect* as outlined in *Table*

3.5 within the DARF framework. A Reconfiguration Model facilitates these adjustments, calculating the requisite total delta-v (Δv_t), predicated on the propulsion characteristics and maneuver parameters.

Table 3.11 Inputs and Outputs of the Propulsion Subsystem

Type	Description	Details
Input	Base Propagation Data	Position and Keplerian inputs from the Astrodynamics Model
Input	Design Variables	Specific variables influencing propulsion requirements
Input	Base Configuration Properties	From Constellation Properties Subsystem
Output	DeltaV's	Outputs DeltaV requirements to the Maneuver Subsystem

Data from the Constellation Properties Subsystem, alongside simulation design variables and parameters, feed into this subsystem, enabling a comprehensive approach to satellite reconfiguration. The maneuvers primarily involve changes in inclination, RAAN, and altitude, necessitating a three-stage burn process for most scenarios that require total reconfigurability without prioritizing the satellite's location in orbit. The velocity of a satellite in an orbit around the Earth is given by the formula:

$$v = \sqrt{\frac{\mu}{r_1}} \tag{3.10}$$

where, μ is the standard gravitational parameter and r_1 is the initial orbit radius.
These maneuvers are computed as follows:

Inclination Change (Δv_i)

The change in inclination requires a Δv applied normally to the orbital plane. The required Δv for an inclination change is given by (41):

$$\Delta v_i = 2 \cdot v_1 \cdot \sin\left(\frac{\delta_i}{2}\right) \tag{3.11}$$

where v_1 is the initial orbital velocity, and δ_i is the change in inclination.

RAAN Change (Δv_Ω)

Changing the RAAN involves a Δv applied in the orbital plane perpendicular to the direction of motion. The required Δv for RAAN change is calculated as (41):

$$\Delta v_\Omega = 2 \cdot v_1 \cdot \sin(i_1) \cdot \sin\left(\frac{\delta_\Omega}{2}\right) \tag{3.12}$$

where i_1 is the initial inclination, and δ_Ω is the change in RAAN.

Altitude Change (Δv_h)

For altitude change, especially when transitioning between different circular orbits through an elliptical transfer orbit, the Δv is determined by Hohmann transfer equations (41):

$$\Delta v_{h1} = \sqrt{\frac{\mu}{a_1}} \cdot \left(\sqrt{\frac{2 \cdot a_2}{a_1 + a_2}} - 1\right) \tag{3.13}$$

$$\Delta v_{h2} = \sqrt{\frac{\mu}{a_2}} \cdot \left(1 - \sqrt{\frac{2a_1}{a_1 + a_2}}\right) \tag{3.14}$$

where a_1 and a_2 are the semi-major axes of the initial and final orbits, respectively. The total Δv for altitude change is the sum of $|\Delta v_{h1}|$ and $|\Delta v_{h2}|$.

Combinations of Inclination, RAAN and Altitude: Formulations

For the scenario where $a_{\text{initial}} = a_{\text{final}}$, the Δv for inclination and RAAN changes are given by (40):

$$\Delta v_{\text{i},\Omega} = 2 \cdot v \sin\left(\frac{\delta}{2}\right) \tag{3.15}$$

where v is the orbital velocity and Ω is the angle between the initial and final orbit planes, calculated as:

$$\cos(\delta) = \cos(\text{i}_{\text{initial}}) \cdot \cos(\text{i}_{\text{final}}) + \sin(\text{i}_{\text{initial}}) \cdot \sin(\text{i}_{\text{final}}) \cdot \cos(\Delta\Omega) \tag{3.16}$$

The Δv for RAAN change is given by (40):

$$\Delta v_{\Omega} = 2 \cdot v \sin(\text{i}) \cdot \sin\left(\frac{\Delta\Omega}{2}\right) \tag{3.17}$$

The Δv for inclination change is (40):

$$\Delta v_{\text{i}} = 2 \cdot v \sin\left(\frac{\Delta\text{i}}{2}\right) \tag{3.18}$$

For the case where $a_{\text{initial}} \neq a_{\text{final}}$, we consider whether a_{intial} is greater than or less than a_{final}. The general form for Δv when $a_{\text{initial}} > a_{\text{final}}$ is:

$$\Delta v_1 = \sqrt{(v_{\text{parking}})^2 + (v_{\text{H}_{\text{parking}}})^2 - 2 v_{\text{initial}} \cdot v_{\text{H}_{\text{initial}}} \cdot \cos(\Delta\text{i})} \tag{3.19}$$

where v_{initial} and $v_{\text{H}_{\text{initial}}}$ are the orbital and Hohmann velocities at the initial orbit, respectively.
For altitude changes where $a_{\text{initial}} < a_{\text{final}}$ and RAAN changes, the Δv is calculated as:

$$\Delta v_1 = \sqrt{(v_{\text{final}})^2 + (v_{\text{H}_{\text{final}}})^2 - 2 \cdot v_{\text{final}} \cdot v_{\text{H}_{\text{final}}} \cdot \cos(\Delta\text{i})} \tag{3.20}$$

where v_{final} and $v_{\text{H}_{\text{final}}}$ are the orbital and Hohmann velocities at the final orbit, respectively.
In the special case where the inclination remains unchanged but the RAAN changes, the Δv is given by:

$$\Delta v_1 = \sqrt{(v_{\text{final}} - v_{\text{H}_{\text{final}}})^2 + 4 \cdot v_{\text{final}} \cdot v_{\text{H}_{\text{final}}} \cdot \sin^2\left(\frac{\Delta\Omega}{2}\right)} \tag{3.21}$$

These equations (40) provide a comprehensive method for calculating the necessary Δv for various orbital maneuvers based on the changes in the orbital parameters. However, there are different cases, and for each case, DARF chooses a trajectory based on its maneuvering algorithms that differentiate the maneuvers based on the initial and final orbit's Keplerian elements.

All-in-One Rule

(40) *"If possible combine all orbital changes that need to be done into one kick-burn at one orbital position rather than making single burns at successive positions."*, as such DARF considers a single point combined burn for all combinations of altitude, inclination, and RAAN changes.

Total Δv for Reconfiguration

The total Δv required for the reconfiguration is the sum of the Δv components for inclination, RAAN, and altitude changes:

$$\Delta v_{\text{total}} = \Delta v_i + \Delta v_{\Omega} + \Delta v_h \tag{3.22}$$

3.7.3 Maneuver Subsystem

This module interfaces closely with the propulsion and propulsion subsystem. It receives input on different deltasVs from the propulsion subsystem. Then, it calculates the necessary maneuver parameters to determine the FOM that decide to maintain or alter the constellation configuration. It directly affects the propellant usage and the time required for reconfiguration. The subsystem tracks the propellant mass of the satellite, burn, and maneuver times to calculate the achievable maneuvers within the mission constraints and exports the figure of merits as shown in the table FOM into the reward function model. The DARF Maneuver Sub-Model outlines the procedural steps for computing the propellant mass, burn time, and total maneuver time for each satellite within a constellation. This subsystem is essential for reconfiguration maneuvers, ensuring that each satellite efficiently achieves the desired orbital adjustments.

Table 3.12 Inputs and Outputs of the Maneuver Subsystem

Type	Description	Source/Destination
Input	Design Vector	Design Parameters on Propulsion
Input	Delta-V's	Propulsion Subsystem within the Reconfiguration Model
Input	Collision Phasing Maneuver Trigger	Collision Avoidance Model
Output	Propagation Request	Astrodynamics Model
Output	Maneuver Specific FOMs	Reward Function Model

3.7.4 Propellant Mass Calculation

The rocket equation determines the propellant mass for each maneuver:

$$m_{\text{propellant}} = m\left(1 - \exp\left(-\frac{\Delta V_t}{I_{\text{sp}} g}\right)\right) \tag{3.23}$$

where m is the spacecraft mass, I_{sp} is the specific impulse, g is the acceleration due to gravity, and ΔV_t is the total delta-v required for the maneuver.

Burn Time Calculation

The burn time (t_{burn}) depends on the mass flow rate ($\dot{m}$) and the thrust (T) generated by the propulsion system:

$$t_{\text{burn}} = \frac{\dot{m}}{m}, \quad \text{where} \quad \dot{m} = \frac{T}{I_{\text{sp}} g} \tag{3.24}$$

3.7.5 Total Maneuver Time

Orbital Maneuver Time Estimation in the DARF Framework

In satellite constellation management within the DARF, a critical challenge arises when estimating the time required for orbital maneuvers, specifically changes in the RAAN and inclination. The literature offers limited generalized formulations for these times, as such calculations are highly dependent on the specifics of the orbital transfer and the characteristics of the spacecraft.

Chemical Propulsion and Impulsive Burns

For systems utilizing chemical propulsion, which are capable of delivering impulsive burns, the maneuver time can be estimated by a simplified equation that relates the delta-v component for the maneuver and the Thrust-to-Weight Ratio (TWR):

$$\Delta t_{chem,h} = \pi \sqrt{\frac{((R_e + h_{1_{\text{val}}}) + (R_e + h_{2_{\text{val}}}))^3}{8 \cdot G \cdot M_e}} \tag{3.25}$$

Here, ΔV_{comp} denotes the delta-v component necessary for inclination or RAAN change, and g is the acceleration due to Earth's gravity. For chemical propulsion that utilizes impulsive burns, the time of maneuver for RAAN (Δt_Ω) and inclination change (Δt_i) can be estimated as:

$$\Delta t_{comp,i,omega} = \frac{\Delta V_{comp}}{TWR \cdot g} \tag{3.26}$$

Here, Δt_{comp} denotes the computation time for the respective maneuver component, (h for altitiude, i for inclination, omega for RAAN), assuming direct proportionality with the corresponding delta-v component and inversely with the spacecraft's TWR. The total time for maneuver can be computed as;

$$\Delta t_{\text{total}} = \Delta t_i + \Delta t_\Omega + \Delta t_h \tag{3.27}$$

Electric Propulsion and Continuous Thrust

In contrast, electric propulsion systems such as ion thrusters, which provide continuous but low thrust, require a fundamentally different approach to calculate the transfer orbit and delta-v (41):

$$\int_{v_0}^{v} dv' = \int_0^t \frac{\dot{m} v_*}{m_0 + \dot{m} t'} dt' \tag{3.28}$$

We can solve to obtain:

$$v - v_0 = v_* \ln\left(\frac{m_0}{m_0 + \dot{m} t}\right) = v_* \ln\left(1 - \frac{\dot{m} t}{m_0}\right) \tag{3.29}$$

As velocity v is a function of the orbit radius r, this leads to the spiral trajectory equation (41):

$$r(t) = \mu \left(v_0 + v_* \ln\left(1 - \frac{\dot{m} t}{m_0}\right)\right)^{-2} \quad \text{at} \quad \dot{m} = \text{const} \tag{3.30}$$

For the transfer time equation derived from the velocity change equation, we have:

$$\Delta t_{elec,h} = \frac{m_0 v_*}{F_*} \left[1 - \exp\left(-\sqrt{\frac{\mu}{r}} \left(\frac{1}{\sqrt{r_f}} - \frac{1}{\sqrt{r_0}}\right)\right)\right] \tag{3.31}$$

Given the substantial variation in potential orbit scenarios and maneuvers, our framework does not encompass hyperbolic and parabolic reconfigurations, which present significant computational complexities due to their unbounded trajectories. The DARF framework's maneuver subsystem must thus reconcile the theoretical underpinnings of orbital mechanics with practical limitations and propulsion system realities. This necessitates a bifurcated approach where chemical propulsion favors rapid, impulsive changes, and electric propulsion requires gradual, continuous modifications.

3.7.6 Capability and Adaptability Sub-models and Penalty Assignments

Penalties for reduced capability and availability are assessed based on operational needs and reconfiguration outcomes, with a predetermined number of satellites receiving penalties to simulate real-world constraints on constellation performance. This comprehensive approach to maneuver planning and execution ensures that the DARF framework can efficiently manage satellite constellations, optimizing orbital configurations for enhanced operational effectiveness. The Penalties in this model raise the fitness parameter by a multiplication factor of *10e7* when unavailable or incapable when reads "1" within the framework, wherein if it reads "0" state, determining it to be capable and available has no penalizations. This is done to ensure the fitness parameter is so large that they never get selected for maneuvers if they are either unavailable or incapable.

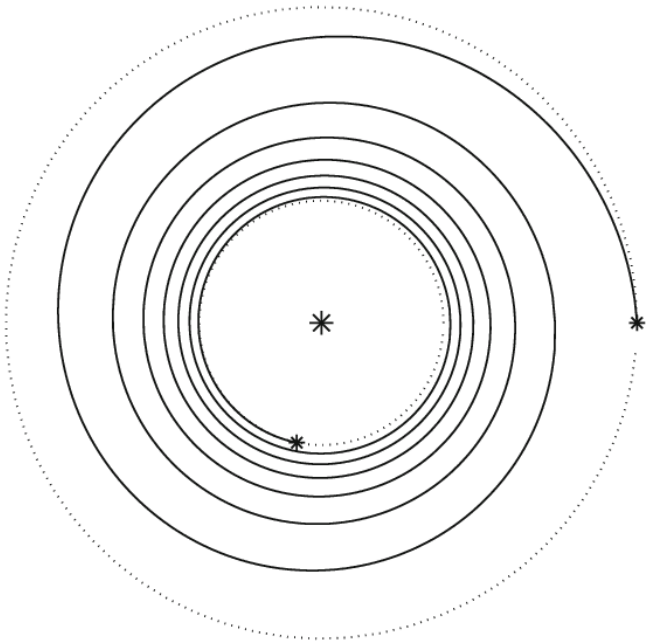

Figure 3.13 Spiral Orbit Maneuver from a Continuous Thrust Burn
(32) (56)

3.8 Collision Avoidance Model

This section delineates the Collision Avoidance Model, an integral component of the DARF simulation, pivotal for ensuring the safety and longevity of satellite constellations. The Collision Avoidance Model (CAM) synergizes with the *Propulsion Subsystem* and the *Maneuver Subsystem*, drawing upon inputs from the Astrodynamics subsystem to preemptively identify and mitigate potential collision threats. The CAM is designed to continuously monitor satellite trajectories and to flag proximities that may lead to potential collisions. Upon detecting a potential collision, the model activates Collision Avoidance Maneuvers (CAMs), bespoke to each scenario, encompassing a range of maneuvers from non-Hohmann transfers to intricate phasing shifts, sculpting spline-like trajectories for evasion.

Table 3.13 Inputs and Outputs of the Collision Avoidance Model

Type	Description	Source/Destination
Input	GSD (Ground Sampling Distance)	Optics Model
Output	Collision Trigger	Reconfiguration Model

3.8.1 Collision Prediction and Flagging

The CAM employs predictive algorithms to calculate the relative positions of all satellites within the constellation at given time steps. Utilizing a threshold distance, termed the *collision risk distance*, the model flags any pair of satellites breaching this proximity.

3.8.2 Collision Avoidance Maneuvers

Upon a flag initiation, CAMs are triggered to reconfigure satellite orbits and avoid collisions. These maneuvers are calculated based on current satellite positions, velocities, and the required delta-v for orbital adjustments. The maneuvers may involve impulsive thrusts for rapid repositioning or continuous thrusts for gradual trajectory alterations.

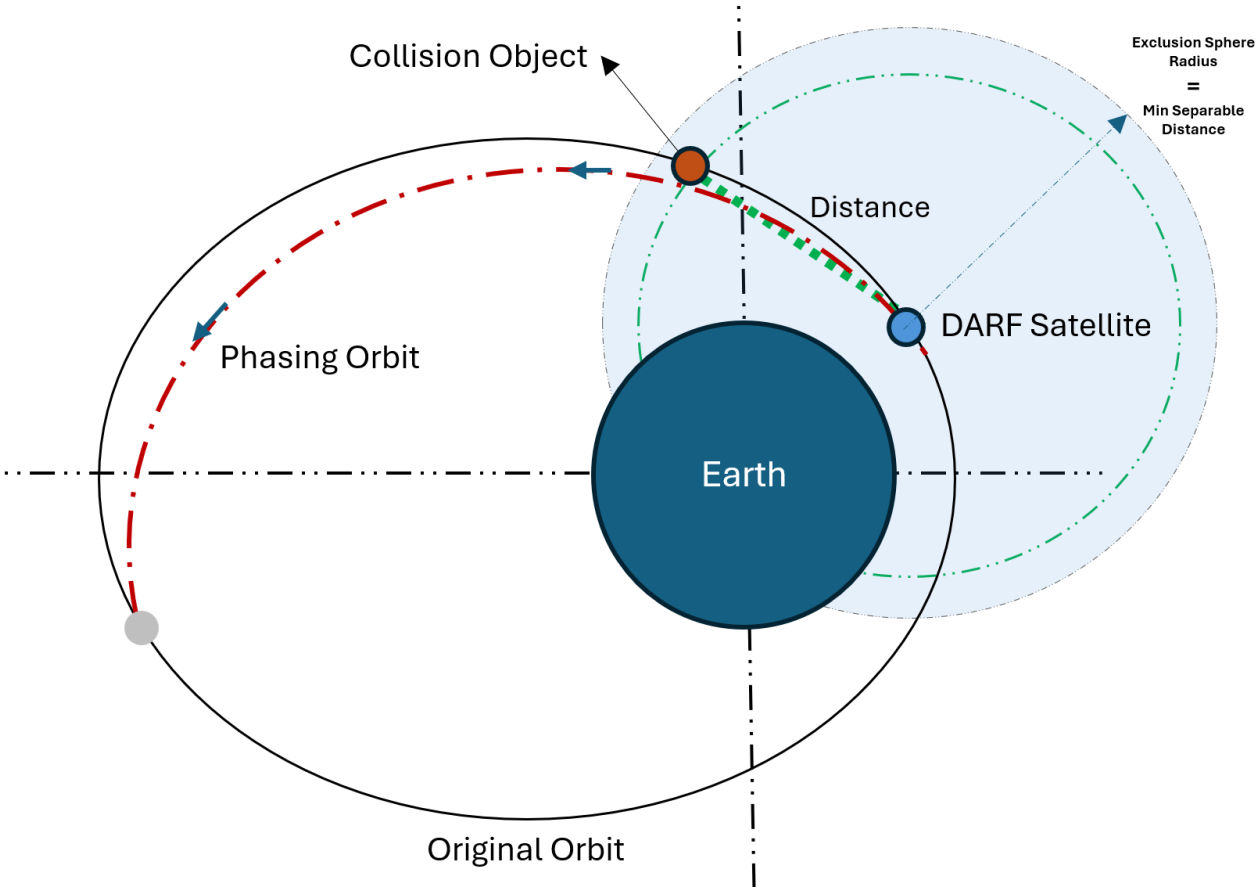

Figure 3.14 Illustration of when satellite (blue) detects the collision object (red) and activates the CAM to perform a phasing maneuver. The exclusion sphere is given in light blue. *Note:* The diagram is NOT according to scale; The exclusion sphere is much smaller compared to the size of the Earth

Phasing Maneuvers

Phasing maneuvers are applied to adjust the orbital period of a satellite subtly, allowing it to 'drift' along its orbit to a safer position. This method is particularly useful for maintaining the operational configuration of the constellation while averting potential collisions. This particular maneuver also adjusts the entry to the original orbit at the original, propagated true anomaly. Using Equation 3.31 and Equation 3.32, DARF computes the time required to return the satellite to its original orbit at the same true anomaly, similar to a rendezvous mission. This data is directly fed into the Astrodynamics Model that leverages STK's differential corrector capabilities to execute the phasing maneuver.

$$T_2 = \frac{2\pi a_2^{3/2}}{\sqrt{\mu}} \tag{3.32}$$

$$T_1 = \frac{2\pi a_1^{3/2}}{\sqrt{\mu}} \tag{3.33}$$

Non-Hohmann and Spline-Based Trajectories

In more complex scenarios, where simple phasing may not suffice, the model calculates non-Hohmann transfers, often resulting in spline-based trajectories. These trajectories are not optimized maneuvers since they do not occur at the periapsis if the parking orbit is not circular, this increases fuel consumption but

ensures rapid and safe satellite repositioning. Again, STK is provided with calculations derived in Section 2.4.8.

3.8.3 Simulation Integration and Visualization

The CAM is integrated with simulation environments, such as STK, to visualize and validate the collision avoidance maneuvers. The model can simulate various scenarios, from simple avoidance to complex reconfiguration of the entire constellation.

STK Astrogator Integration

The CAM utilizes STK's Astrogator module for accurate representation and analysis. This allows for detailed modeling of the satellite's environment, including gravitational forces, atmospheric drag, and solar radiation pressure, which are crucial for precise maneuver planning.

3.9 Reward Function Model

The Reward Function Model quantifies the efficacy of satellite maneuvers within the DARF framework through a composite fitness parameter. This parameter integrates several key aspects of maneuver execution, reflecting the strategic balance between maneuver efficiency and resource utilization.

Table 3.14 Inputs and Outputs of the Reward Function Model

Type	Description	Source/Destination
Input	FOMs (Figures of Merit) from Maneuver Subsystem	Maneuver Subsystem
Input	FOMs from Capability/Availability Subsystems	Reconfiguration Model
Output	Fitness Parameters	Reward Function Subsystem

3.9.1 Rationale and Impact of Figures of Merit *(f)*

f1: Propellant Mass

Rationale: Propellant mass influences the longevity and resources-effectiveness of satellite operations (13). In a decentralized constellation, where each satellite operates semi-autonomously, minimizing propellant usage is vital for maximizing mission duration and reducing logistical constraints.

Impact: By prioritizing maneuvers that require less propellant, we ensure that satellites maintain operational capability for longer periods, enabling more reconfiguration opportunities and enhancing the constellation's resilience to dynamic operational demands.

f2: Time for Maneuver

Rationale: The maneuver time impacts the constellation's ability to quickly adapt to new configurations or respond to collision threats. Swift maneuverability will be crucial in a congested orbital environment where the timing between collision avoidance and potential disaster can differ.

Impact: Shorter maneuver times increase the responsiveness of the constellation to reconfiguration requests and urgent collision avoidance needs, thereby maintaining the integrity and safety of the satellite federation.

f3: Time for Burn

Rationale: The burn time reflects the efficiency of the propulsion system and its impact on the satellite's operational capacity. Burn time, like in the case of electric propulsion, can significantly delay the execution of precise maneuvers, albeit saving fuel more effectively than chemical propulsion.

Impact: Efficient burn times reduce the propellant expenditure for maneuvers, conserving valuable resources and ensuring satellites remain functional for other mission-critical tasks.

f4 and *f5*: Capability and Availability

***Rationale*:** These metrics gauge satellites' readiness and functional status within the constellation. Capability and Availability indicate a satellite's ability to undertake maneuvers and contribute to the constellation's objectives when set to zero. A Penalty, as discussed in *Section 3.7.6* is otherwise levied to make the satellite unsuitable for maneuvering. Available means the satellite is operational and free of schedules to perform the maneuver. Capable means the satellite is equipped with a thruster for maneuvering, or has propellant mass for maneuvering.

Impact: Prioritizing satellites with superior capability and availability for reconfiguration maneuvers ensures that the most reliable assets are utilized, thereby minimizing the risk of maneuver failure and optimizing the operational effectiveness of the constellation.

3.9.2 Fitness Parameter Calculation and Objective

Integrating these considerations, the fitness parameter is formulated as follows:

$$\min \sum \text{Fitness} = A \cdot m_{\text{prop}} + B \cdot t_{\text{maneuver}} + C \cdot t_{\text{burn}} + D \cdot \textit{Capability} + E \cdot \textit{Availability} \tag{3.34}$$

Equation 3.32 strategically weights each FOM according to its anticipated impact on the simulation and operational priorities by normalizing each merit to a double-digit number. The selection of FOMs and their respective weights was meticulously conducted, over various statistical trials to align with the goals of the DARF framework—minimizing resource consumption, ensuring operational flexibility, and safety within a decentralized satellite constellation management approach. The Reward Function Model aims to identify and prioritize satellite maneuvers that achieve the optimal balance of resource utilization, maneuver efficiency, and operational readiness. By doing so, the model is crucial in guiding decision-making processes within the decentralized framework, ensuring that satellite constellations can adapt dynamically to evolving operational requirements and environmental challenges. This comprehensive and logical selection of FOMs and their integration into the Reward Function Model underpins the framework's ability to effectively manage and optimize satellite constellation configurations, paving the way for sustainable and efficient space operations in an increasingly crowded and complex orbital domain.

Selection Criteria

The model seeks the least fitness parameters. *Equation 3.33* identifies maneuvers that offer optimal reconfiguration efficacy. Satellites with the lowest fitness parameters are prioritized for maneuver execution, ensuring efficient use of propulsion resources and operational readiness. Table 3.15 and Table 3.16 detail the chosen Figure of merits and weights in DARF respectively. The rationale for was aimed at normalizing the FOMs so that their impact would be assessed without bias and provide a normalized, fair input in the fitness parameter calculations.

Table 3.15 Weights for Normalizing Fitness Calculation Factors

Figure of Merit	Weight
Propellant Mass (A)	-1000
Time (B)	10×10^{-2}
Burn (C)	10×10^{4}
Capability (D)	1
Availability (E)	1

Table 3.16 Figure of Merits (FOMs) in the DARF Simulation

FOM	FOM Definition
f_1	Propellant Mass
f_2	Time For Maneuver
f_3	Time For Burn
f_4	Capability
f_5	Availability

3.10 DARF's Base Configuration - Walker Delta 54: 25/5/1

This section briefly presents the default setting of the DARF. The Walker Delta constellation, outlined in Table 3.17, signifying an inclination of 54 degrees, with 25 satellites distributed over 5 orbital planes, with a relative spacing of 1. It is the foundational architecture upon which the DARF is validated for scalability.

Table 3.17 Design Variables and Inputs for Base Configuration - Walker Delta 54: 25/5/1

Variable	Value
Configuration	Walker Delta 54: 25/5/1
Satellites	25
Satellites Per Plane	5
Planes	5
Phasing	1
Simulation Time (s)	86400
Inclination (deg)	54
Altitude (km)	550
Step Size (s)	10

3.11 Simulating Scalability

This section outlines the approach to lay the foundational scenario setup to validate the scalability of the DARF from our default configuration model to the test scenarios outlined in Table 3.18. The aim is to test scaling down and scaling up and also test one very large-scale configuration of 50000 satellites. The last case of a very large set of satellites is to push the DARF's computational capacity to accommodate the predicted satellites by 2030 as outlined in Chapter 1. Even though the satellites in that timeline will not be in one formation, like our last scalable test case, the goal is to validate whether the framework can generate and process data for such a large dataset. This section lastly aims to exhibit DARF's robust adaptability and capability to manage extensive satellite constellations while maintaining high operational effectiveness even when scaling up.

Table 3.18 Scalability Test Cases

Test No.	Test Name	Purpose
1	Scaling Down - Walker Delta 54: 15/5/1	Test framework under scaling down
2	Scaling Up - Walker Delta 54: 500/25/1	Test framework under scaling up
3	Scaling Up Largely - Walker Delta 54: 50000/200/1	Test framework's limit.

3.11.1 Scaling Methodology

The scalability assessment is conducted by incrementally increasing the number of satellites in a Walker Delta constellation from the base model of 54:25/5/1 to the proposed test cases. This increment during scaling up, or decrement during scaling down in the number of satellites is linear and a corresponding escalation or de-escalation in the number of orbital planes and relative spacing to maintain the constellation's geometry respectively. The design variables are inputs directly presented to the framework's main code. Upon execution DARF executes the simulation to create, read, and present the performance and resource allocation under the strain of enlarged or reduced constellation parameters. The DARF's framework coding is implemented to take in the number of satellite planes and satellites per plane and other essential design variables as discussed in Section 3.2 and further outlined for each test case in Table **??**. This allows us to leverage STK's to visualize the simulation from DARF's Reconfiguration Model and leaves room for further customized simulations for the scaled version on STK's user interface, like generating further reports, analyses, and its other computational capabilities.

3.11.2 Scaling Down - Walker Delta 54: 15/5/1

While scaling down, we examine a Walker Delta configuration with a 54:15/5/1 layout. This modification reduces the constellation to fifteen satellites, distributed across five planes with a relative phasing 1. This test aims to evaluate the performance of the DARF framework under a significantly minimized constellation size while maintaining the Walker constellation's fundamental geometric and operational properties.

3.11.3 Scaling Up - Walker Delta 54: 500/25/1

The scaling-up test examines the expansion of the constellation to a 54:500/25/1 configuration. This enlargement quintuples the number of satellites from the original model, introducing five hundred satellites distributed over twenty-five planes, each with a relative phasing of 1. This scenario is designed to assess how the DARF framework manages a substantial increase in satellite numbers, scrutinizing its capability to sustain the Walker constellation's design principles and operational efficacy at a larger scale.

Table 3.19 Design Variables and Inputs for Scaling Down Test - Walker Delta 54: 15/5/1

Variable	Value
Configuration	Walker Delta 54: 15/5/1
Satellites	15
Satellites Per Plane	3
Planes	5
Phasing	1
Simulation Time (s)	86400
Inclination (deg)	54
Altitude (km)	550
Step Size (s)	10

Table 3.20 Design Variables and Inputs for Scaling Up Test - Walker Delta 54: 500/25/1

Variable	Value
Configuration	Walker Delta 54: 500/25/1
Satellites	500
Satellites Per Plane	20
Planes	25
Phasing	1
Simulation Time (s)	86400
Inclination (deg)	54
Altitude (km)	550
Step Size (s)	10

3.11.4 Scaling Up Largely - Walker Delta 54: 50000/200/1

This test pushes the scaling boundaries by exploring a 54:50000/200/1 Walker Delta configuration. It represents a hypothetical yet insightful examination into the extremes of constellation expansion, where fifty thousand satellites are organized across two hundred orbital planes, maintaining a relative phasing of 1. The objective is to explore the theoretical limits of the DARF framework's scalability and operational flexibility, highlighting the challenges and potential strategies for managing many satellites while adhering to the Walker constellation design's intrinsic geometric and operational characteristics.

Table 3.21 Design Variables and Inputs for Scaling Up Largely Test - Walker Delta 54: 50000/200/1

Variable	Value
Configuration	Walker Delta 54: 50000/200/1
Satellites	50000
Satellites Per Plane	250
Planes	200
Phasing	1
Simulation Time (s)	86400
Inclination (deg)	54
Altitude (km)	550
Step Size (s)	10

3.12 Simulating Adaptability

This section examines the adaptability of the DARF within various operational scenarios, outlined as test cases in Table 3.22 demonstrate its robustness and flexibility in accommodating changes in satellite constellation configurations. Adaptability tests assess the framework's responsiveness to modifications in altitude, inclination, RAAN configuration adjustments.

Table 3.22 Adaptability Test Cases

No.	Test Name	Purpose
1	Walker Star 54: 25/5/1 - Same Altitude	Verify adaptability without altitude changes.
2	Walker Delta SSPO 98: 25/5/1 - Altitude + Inclination	Examine adaptability of i, h and Ω.
3	Walker Delta SSPO 98: 25/5/1 - Inclination Change	Test adaptability to inclination modifications.

3.12.1 Adaptability Methodology

Adaptability is gauged through implementing different operational scenarios on our base configuration model of 54:25/5/1 to three distinctive test cases, each designed to challenge and evaluate the DARF's dynamic reconfiguration capabilities. These scenarios include maintaining the same altitude, altering the satellite's altitude, and modifying the constellation's inclination. Each test case's inputs, such as satellite numbers, orbital planes, inclination, and altitude, are directly provided to DARF's main code. Upon execution, DARF simulates these adaptations, showcasing its ability to effectively manage constellation reconfigurations, taken as reconfiguration requests under varied operational demands.

3.12.2 Test 1 - Walker Star 54: 25/5/1 - Same Altitude

This test evaluates the adaptability of the DARF to manage the operational dynamics of the Walker Star configuration, maintaining the same altitude and exploring the effects of changes within the same orbital parameters from our base walker delta configuration.

Table 3.23 Design Variables and Inputs for Test 1 - Walker Star 54: 25/5/1 - Same Altitude

Variable	Value
Configuration	Walker Star 54: 25/5/1
Satellites	25
Satellites Per Plane	5
Planes	5
Phasing	1
Simulation Time (s)	86400
Initial Inclination (deg)	54
Final Inclination (deg)	54
Initial Altitude (km)	550
Final Altitude (km)	550
Step Size (s)	10

3.12.3 Test 2 - Walker Delta 98: 25/5/1 - Inclination + Altitude Change

This test probes the framework's capability to seamlessly navigate altitude adjustments from 550 km to 950 km, showcasing the DARF's adaptability to significant orbital environmental changes.

Table 3.24 Design Variables and Inputs for Test 2 - Walker Delta 54: 25/5/1 - Altitude Change

Variable	Value
Configuration	Walker Delta 54: 25/5/1
Satellites	25
Satellites Per Plane	5
Planes	5
Phasing	1
Simulation Time (s)	86400
Initial Inclination (deg)	54
Final Inclination (deg)	98
Initial Altitude (km)	550
Final Altitude (km)	950
Step Size (s)	10

3.12.4 Test 3 - Walker Delta SSPO 98: 25/5/1 - Inclination Change, Same Altitude SSPO

The third test assesses the DARF's ability to adapt to inclination changes while maintaining the same altitude. It further stresses operational flexibility under varying spatial dynamics and simulates coverage-focused reconfiguration requests to take advantage of the SSPO.

Table 3.25 Design Variables and Inputs for Test 3 - Walker Delta 98: 25/5/1 - Inclination Change, Same Altitude

Variable	Value
Configuration	Walker Delta 98: 25/5/1
Satellites	25
Satellite Per Plane	5
Planes	5
Phasing	1
Simulation Time (s)	86400
Initial Inclination (deg)	54
Final Inclination (deg)	98
Initial Altitude (km)	550
Final Altitude (km)	950
Altitude (km)	550
Step Size (s)	10

3.13 Simulating a Use-case: Walker to Pendulum Formation

This section delves into DARF's capacity to handle real-world applications, particularly its adaptability and efficiency in resource optimization during constellation reconfigurations. The use-case presented involves transitioning five satellites from our base Walker constellation model to occupy designated positions in a Pendulum (Delta RAAN) formation. This scenario is intended to validate the DARF's decision-making process under two distinct assessment criteria outlined in Table 3.26, individually and collectively. It is important to note that the framework accesses fitness parameters and assigns a ranking, with the least of the fitness parameters being the best individually and collectively. The model paths are computed and displayed on the command window of MATLAB. But only the chosen method preselected as the method will be executed and simulated.

Table 3.26 Use-case Scenarios for DARF's Transitioning Strategy

No.	Use-case Type	Description
1	Individual Assessment	Optimal Positioning based on individual satellite fitness parameters.
2	Collective Assessment	Collective optimization to achieve minimal cumulative fitness parameters.

3.13.1 Case 1 - Individual Satellite Assessment for Optimal Positioning

In this case study, we evaluate each of the five satellites individually, aiming to determine the best fit for each available position in the Pendulum formation. The satellites are assessed based on performance metrics and sorted from the optimal candidate to the fifth. This highlights DARF's capability to identify and sequence satellites based on their suitability for a given specific maneuver. Allocating satellites from slots 1 to 5 is based only on the ranking, at the first timestep it receives the reconfiguration request and preselected path, i.e., in this case, individual. DARF selects the best satellite from the pool of twenty-five satellites evaluated for slot 1, i.e., a RAAN of 10 degrees. Simultaneously, the framework computes the best Satellites for slots 2, 3, 4, and 5, for the same timestep with RAAN values of 20, 30, 40, and 50 degrees. These slots are filled based on the least fitness parameter for that particular slot parameter.

Table 3.27 Design Variables and Inputs for Individual Satellite Assessment

Variable	Value
Assessment Criterion	Individual Satellite Performance
Number of Satellites	5 from the base model (25)
Target Formation	Pendulum (Delta RAAN = 10 degrees)
Evaluation Metric	Fitness Parameters (Individual)
Decision Strategy	Optimal to 5th Best Fit

3.13.2 Case 2 - Collective Assessment for Overall Optimization

The second case study focuses on collective performance over a defined period, aiming to achieve the lowest cumulative fitness parameters for a group of five satellites. This approach examines the synergistic effects of satellite operations, where a satellite not individually ranked among the top five could be selected based on its contribution to the collective efficiency of the maneuver. Allocating satellites from slots 1 to 5 is based on selecting the sum of the 5 least fitness parameters in the ranking. Upon receiving the reconfiguration request and preselected path, i.e., in this case collective, DARF selects the five best satellites from the pool of twenty-five satellites by evaluating combinations of five. The framework assigns the slots when the least of the sets is determined.

Table 3.28 Design Variables and Inputs for Collective Assessment

Variable	Value
Assessment Criterion	Collective Satellite Performance
Number of Satellites	5 from the base model (25)
Target Formation	Pendulum (Delta RAAN = 10 degrees)
Evaluation Metric	Cumulative Fitness Parameters
Decision Strategy	Least Collective Fitness

3.13.3 Key Simulation Parameters for Use-Case Evaluation

This use-case simulation incorporates specific design considerations to accurately assess DARF's adaptability and decision-making efficacy in reallocating satellites to a new formation. Key parameters and their impact on the simulation outcomes are outlined below:

- **Propulsion System Variability:** In each simulation iteration, DARF dynamically assigns propulsion types (chemical or electric) to satellites within the initial formation. This adds uniqueness to every run, affecting maneuver times and thruster burn durations due to the inherent performance differences between propulsion systems.
- **Satellite Availability and Capability:** Given that all satellites in the base configuration are deemed fully operational and capable, these variables remain constant across simulations. This assumption simplifies the analysis by focusing on propulsion dynamics and their influence on maneuver strategies, without the need to account for variable satellite conditions.
- **Maneuver Time Representation:** To facilitate a more intuitive comparison between propulsion systems, maneuver times for satellites equipped with Chemical Thrusters are represented with positive values, whereas those with Electric Thrusters are depicted with negative values. This visual distinction aids in quickly identifying propulsion types within graphical outputs. It's important to note that absolute values of maneuver times are used to compute the Fitness Parameter, ensuring that the propulsion system's impact is accurately reflected without biasing the results.

3.13.4 Satellite Index Allotment

we present two tables that map out the positions of satellites within a 5x5 matrix, corresponding to their assignments within a satellite constellation. This visualization aids in understanding how the Dynamic Adaptive Reconfiguration Framework (DARF) simulation, conducted in MATLAB, and the satellite toolkit (STK) representation correlate regarding satellite identification and placement. Table 3.29 uses a straightforward numerical sequence (1 to 25) to allocate satellite indices across five planes, each comprising five satellites. This cell serves as a base reference, demonstrating the logical arrangement used within DARF's MATLAB simulation to identify and manage each satellite's position within the constellation. Table 3.30 shifts from a simple numerical sequence to a more detailed naming convention, employing DARF-PN format. In this nomenclature, "P" represents the plane number, and "N" indicates the satellite index within that plane. This convention facilitates an intuitive understanding of each satellite's specific location and role within the constellation, translating the MATLAB simulation data into STK's more descriptive and operational context.

Table 3.29 DARF's MATLAB Simulation Satellite Allotment

	S	**S**	**S**	**S**	**S**
P	1	2	3	4	5
P	6	7	8	9	10
P	11	12	13	14	15
P	16	17	18	19	20
P	21	22	23	24	25

Table 3.30 STL's Naming Convention for DARF Satellites

	N1	**N2**	**N3**	**N4**	**N5**
P1	DARF11	DARF12	DARF13	DARF14	DARF15
P2	DARF21	DARF22	DARF23	DARF24	DARF25
P3	DARF31	DARF32	DARF33	DARF34	DARF35
P4	DARF41	DARF42	DARF43	DARF44	DARF45
P5	DARF51	DARF52	DARF53	DARF54	DARF55

4 Results

This Chapter presents the research findings. of our setup and

4.1 Scalability Results

This section validates the thesis objectives TO-7 outlined in *Table 1.1*, the third research question RQ-3 outlined in Section 1.7, summarized in *Table 4.7*. This section presents the findings from the scalability simulations in Chapter 3 to test the scaling capacity of the DARF framework. We compare the base model, which employs the Walker Delta 54: 25/5/1 constellation, to the scaled-down model with a Walker Delta 54: 15/5/1, a scaled-up model of Walker Delta 54: 500/25/1 constellation and a largely scaled-up model of Walker Delta 54: 50000/200/1 Constellation. The first setup result is the successful running of the entire DARF's default setting, with no reconfiguration requests in this setting, only the base configuration was propagated as seen in Figure 4.1 and visualize its goundtrack in Figure 4.2.

Table 4.1 Adaptability Goals

ID	Objective
TO-7	Assess and validate the framework's working and scalability by evaluating performance under configuration size changes.
ID	**Thesis Research Question**
RQ-3	How does the developed optimization algorithm demonstrate **scalability** and adaptability?

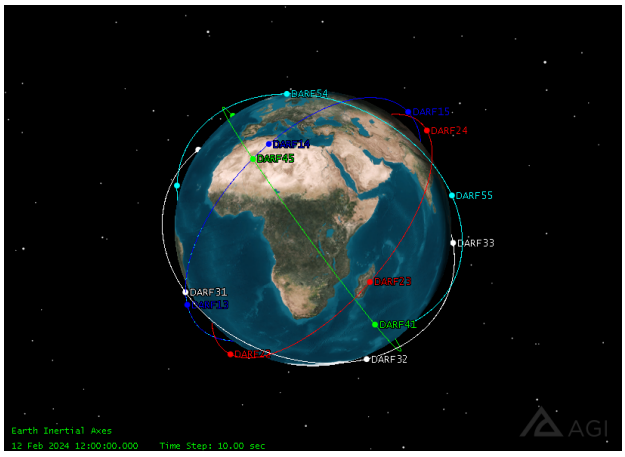

Figure 4.1 DARF's Base Configuration showing the Walker Delta 54: 25/5/1 on STK

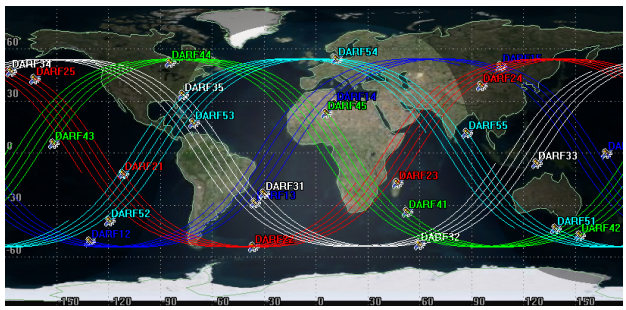

Figure 4.2 DARF's Base Configuration Grountrack of the Walker Delta 54: 25/5/1 on STK

4.1.1 Scalability Test Case 1 Scaling Down - Walker Delta 54: 15/3/1

The first test involved scaling down the constellation to a 54:15/3/1 configuration. The DARF framework successfully managed the reduced constellation size, demonstrating efficient resource allocation and collision avoidance in a minimized satellite environment. The operational integrity of the framework was maintained, indicating its flexibility and robustness in handling smaller constellations effectively when scaled down. Table 4.3 informs that for a step size of 1 second, DARF requires a cell size of 12,96,000 x 8 each for both reports, which amounts to the framework accessing 20.7 million data points involving keplerian elements and positional data over each timestep for one day. There were no noticeable lags during the entire simulation for all timesteps. The performance metrics are visualized in Figure 4.3.

Table 4.3 Performance Metrics for Scaling down to 54: 15/3/1 Constellation

Step Size (seconds)	Report Gen. Time (s) Orbital Elems	Report Gen. Time (s) Positional Data	Exec. Time (s)	Total File Size (MB) Orbit + Pos	Total Time Steps	Cell Size	Data Read Time (s)
1	698.47	703.43	102.5	273.00	86 400	1296000 X 8	23.44
10	203.43	213.55	20.89	27.30	8640	129600 X 8	16.23
30	124.23	132.42	13.27	8.23	2880	43200 X 8	9.34
60	96.24	102.34	12.44	3.60	1440	21600 X 8	1.67
120	58.34	68.45	8.56	1.37	720	5400 X 8	0.98
240	25.56	32.48	5.67	1.02	360	2700 X 8	0.56

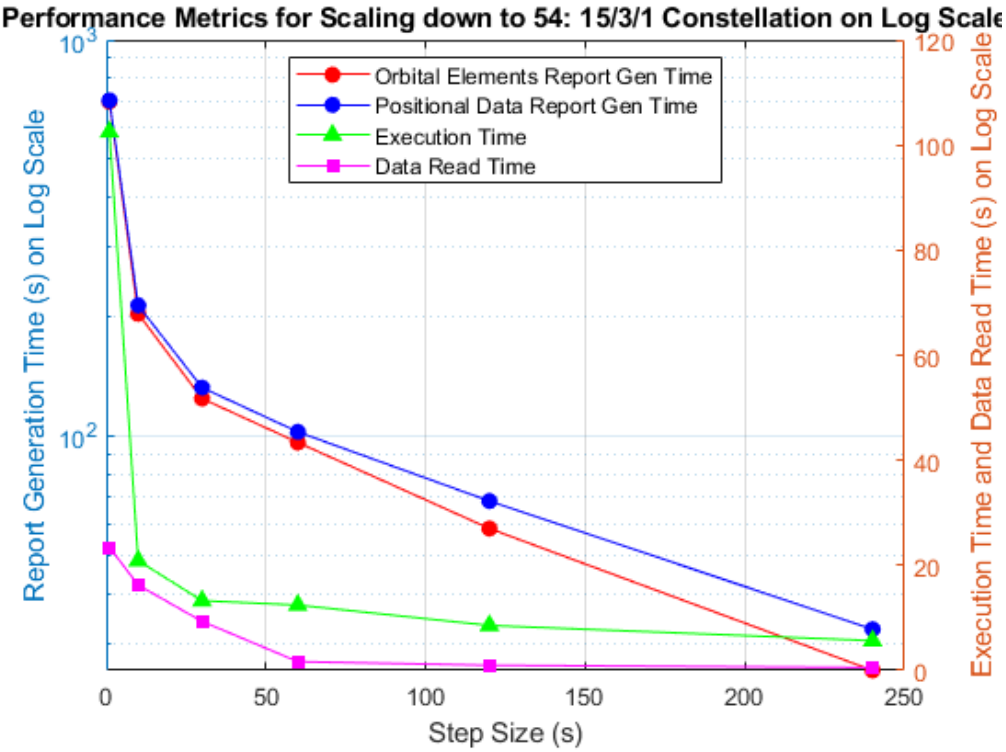

Figure 4.3 Performance plot for various stepsizes for Scalability Test Case 1 Scaling Down - Walker Delta 54: 15/3/1

4.1.2 Scalability Test Case 2 Scaling up - Walker Delta 54: 500/20/1

The second test involved scaling the constellation to a 54:500/20/1 configuration. The DARF framework successfully enlarged the constellation size, demonstrating efficient resource allocation and collision avoid-

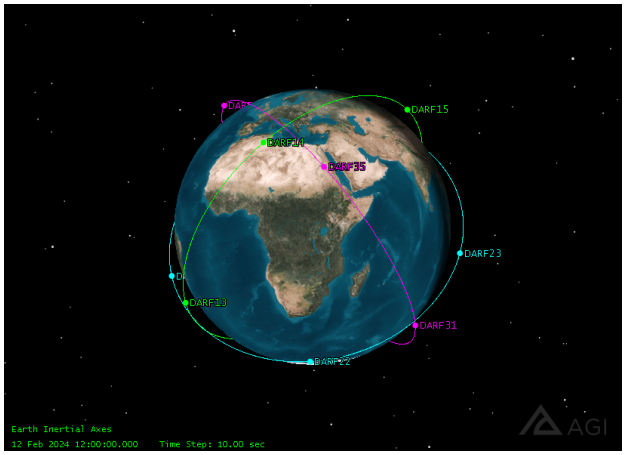

Figure 4.4 DARF's Scaled-down showing the Walker Delta 54: 15/3/1 on STK

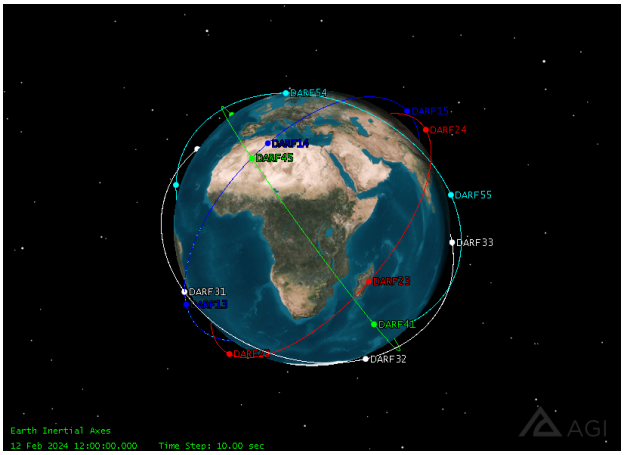

Figure 4.5 DARF's Base Configuration showing the Walker Delta 54: 25/5/1 on STK

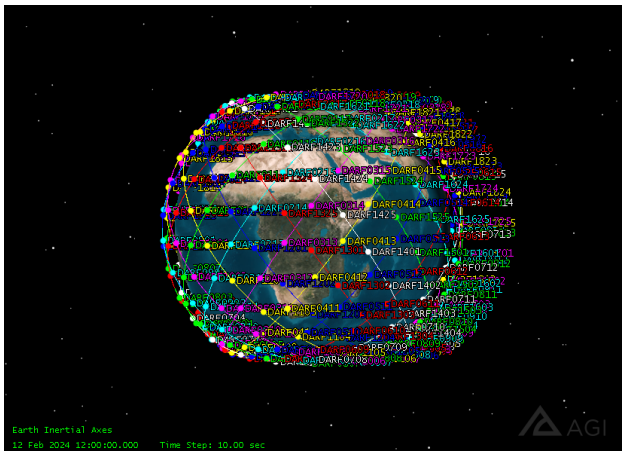

Figure 4.6 DARF's Scaled Configuration showing the Walker Delta 54: 500/20/1 on STK

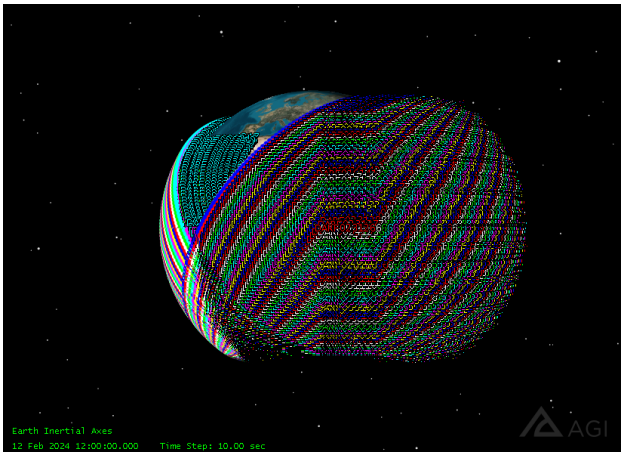

Figure 4.7 DARF's Large Scale Configuration showing the Walker Delta 54: 50000/200/1 on STK

ance in a minimized satellite environment. The operational integrity of the framework was maintained, continuing to indicate its flexibility and robustness in handling larger constellations effectively when scaled up. *Table 4.4* informs that for a step size of 1 second, DARF requires a cell size of 43,200,000 x 8 for both reports each, which amounts to the framework accessing 691.2 million data points for one day of simulation time. As depicted in Figure 4.6 and 4.10, the DARF successfully scale itself up to the required 500 Satellites. The plots show a sinusoidal pattern for each satellite traced across one day. Upon scaling the constellation to 500 satellites, the simulations reveal insights into the extended capabilities of the DARF framework and the increased complexity in maneuver coordination and resource allocation and showcase the augmented constellation coverage and the heightened challenges in maintaining system integrity over a larger fleet of satellites, discussed in detail in Chapter 5. The scaling-up test challenged the DARF framework with a significantly larger constellation comprising 500 satellites across 20 planes. Despite the increase in the number of satellites, the framework exhibited remarkable adaptability, managing the expanded constellation without compromising on operational efficiency or collision avoidance capabilities. This test underscored the framework's scalability and potential to support the growth of satellite constellations in line with future space traffic trends. The performance metrics are visualized in Figure 4.12

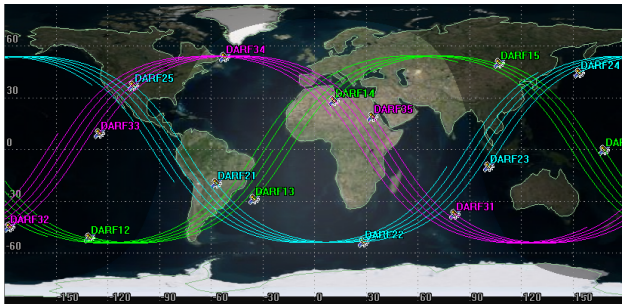

Figure 4.8 DARF's Scaled-Down GroundTrack of Walker Delta 54: 15/3/1 on STK

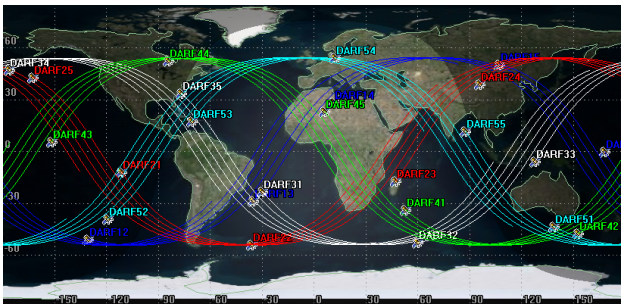

Figure 4.9 DARF's Base Configuration GroundTrack of Walker Delta 54: 25/5/1 on STK

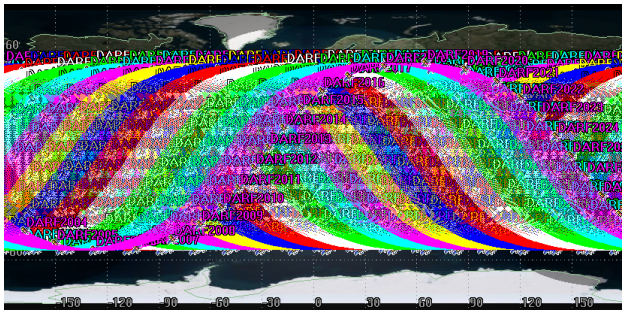

Figure 4.10 DARF's Scaled Configuration GroundTrack of Delta 54: 500/20/1 on STK

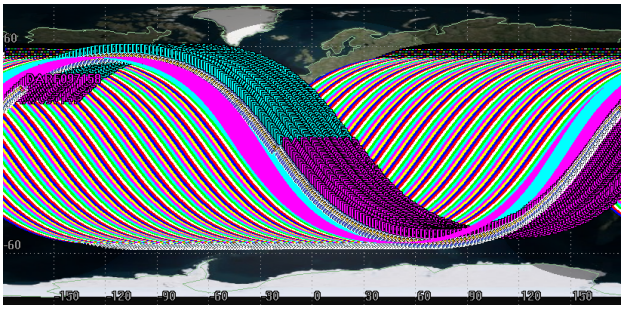

Figure 4.11 DARF's Large Scale Configuration GroundTrack of Walker Delta 54: 50000/200/1 on STK

Table 4.4 Performance Metrics for Scaling up to 54: 500/20/1 Constellation

Step Size (seconds)	Report Gen. Time (s) Orbital Elems	Report Gen. Time (s) Positional Data	Exec. Time (s)	File Size (MB) Orbit + Pos	Total Time Steps	Cell Size	Data Read Time (s)
1	12 845.34	12 787.45	12 354.04	2100.00	86 400	43200000 X 8	254.34
10	3080.18	302.14	305.37	210.00	8640	4320000 X 8	140.34
30	1415.70	279.51	279.28	112.00	2880	1440000 X 8	67.89
60	334.60	268.65	245.23	56.40	1440	720500 X 8	14.80
120	347.60	221.76	222.33	28.20	720	360000 X 8	12.98
240	190.84	176.65	153.45	14.10	360	180000 X 8	11.23

4.1.3 Scalability Test Case 3 Large Scaling up - Walker Delta 54: 50000/200/1

The final test pushed the DARF framework to its theoretical limits by simulating a 54:50000/200/1 constellation configuration. While this large-scale test presented a substantial challenge, the framework demonstrated its ability to process and manage many satellites, albeit with increased computational demands. This test provided valuable insights into the framework's scalability limits and identified areas for optimization to enhance its performance in managing extremely large constellations.

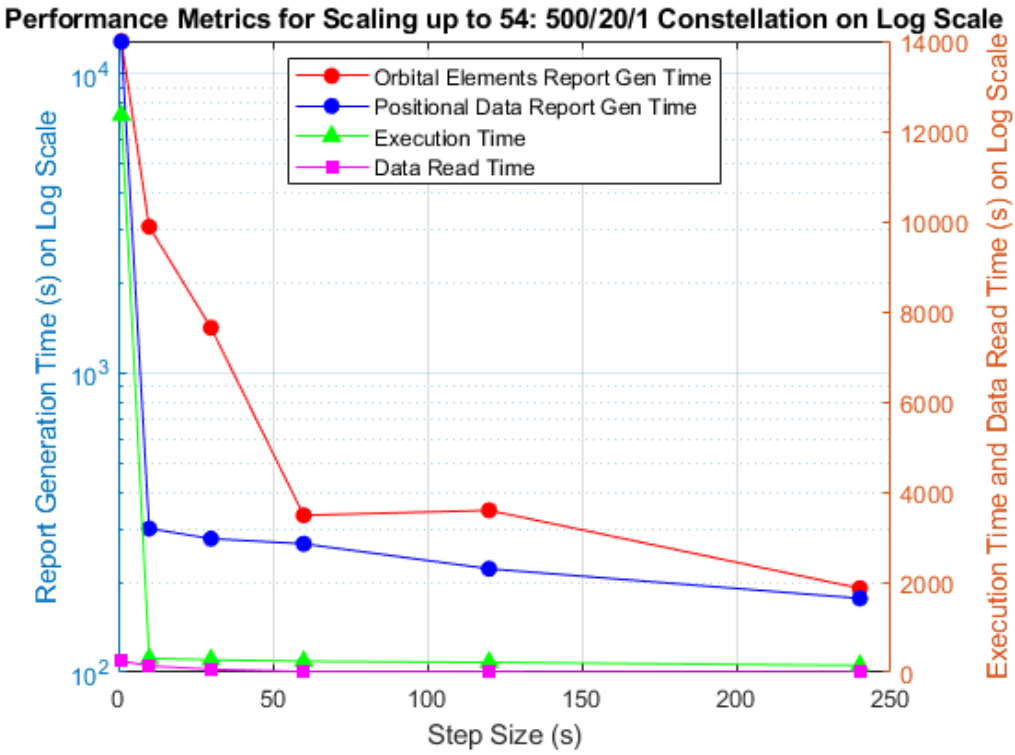

Figure 4.12 Performance plot for various stepsizes for Scalability Test Case 2 Scaling Up - Walker Delta 54: 500/20/1

4.2 Adaptability Results

This section validates the thesis objectives TO-8 outlined in *Table 1.1*, the third research question RQ-3 outlined in Section 1.7 for adaptability, summarized in *Table 4.5*. This section presents the findings from the adaptability simulations outlined in Chapter 3 to test the adaptive nature of the DARF framework. This section presents the adaptability outcomes from the test scenarios detailed in Chapter 3. These results showcase DARF's ability to dynamically reconfigure satellite constellations in response to changes in altitude, inclination, and RAAN adjustments, demonstrating its flexibility and robust adaptability.

Table 4.5 Adaptability Goals

ID	Objective
TO-8	Validate the adaptability of the framework through simulations involving multiple operational scenarios and configurations.

ID	Thesis Research Question
RQ-3	How does the developed optimization algorithm demonstrate scalability and **adaptability?**

4.2.1 Test 1 - Adapt to Walker Star 54: 25/5/1 - Same Altitude Adaptability

In the first test case scenario, DARF successfully reconfigured from the base configuration upon receiving a reconfiguration request for Walker Star 54: 25/5/1, and maintained the same altitude of 550 km and an inclination of 54 degrees. The operation within the same inclination ensured performance and resource utilization stability, illustrating DARF's effective handling of operational dynamics without altitude variations. Figure 4.14 illustrates the successful simulation of the reconfiguration

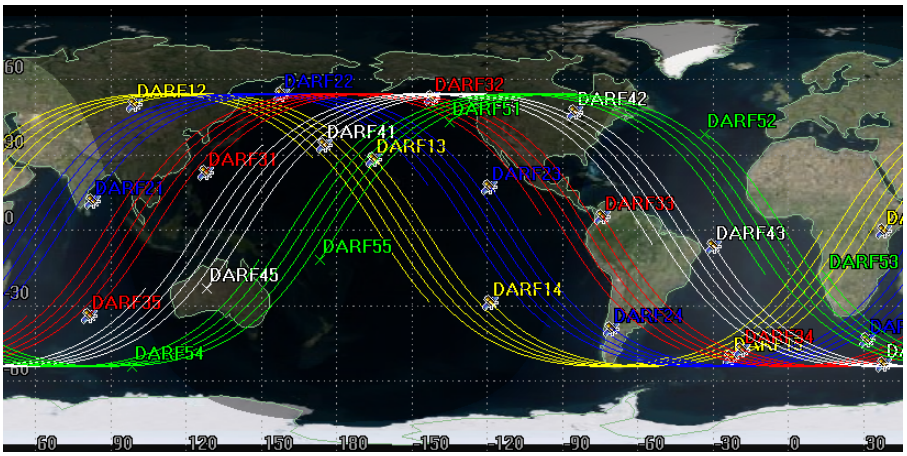

Figure 4.13 Groundtrack of Walker Star 54: 25/5/1 - Same Altitude Adaptability on STK

4.2.2 Test 2 - Walker Delta 98: 25/5/1 - Inclination + Altitude Change Adaptability

The second adaptability test DARF successfully reconfigured from the base configuration upon receiving a reconfiguration request for Walker Delta 54: 25/5/1 and demonstrated DARF's capability to smoothly transition the base configuration from an altitude of 550 km to 950 km and change in inclination. The

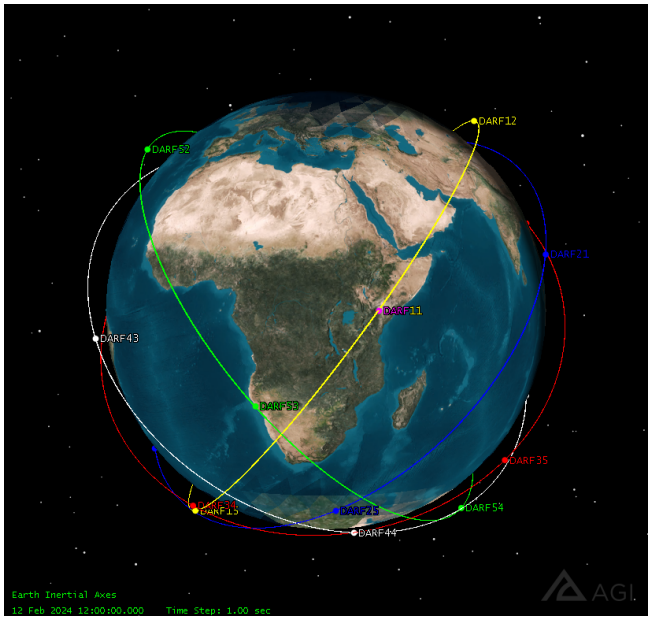

Figure 4.14 Walker Star 54: 25/5/1 - Same Altitude Adaptability on STK

framework's responsiveness to this significant environmental change was evidenced by successfully reconfiguring the satellite constellation, ensuring optimal operation despite a significant altitude adjustment. This adaptability test underlined the framework's potential in managing large-scale altitude shifts within satellite constellations.

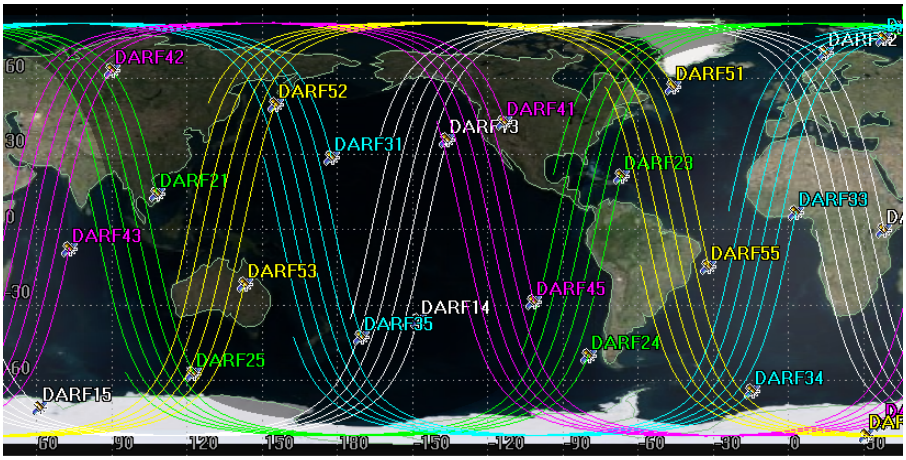

Figure 4.15 Groundtrack of Walker Delta 54: 25/5/1 - Altitude Change - Same Altitude Adaptability on STK

4.2.3 Test 3 - Walker Delta SSPO 98: 25/5/1 - Inclination Change, Same Altitude Adaptability

For the third test case, DARF successfully reconfigured from the base configuration upon receiving a reconfiguration request for Walker Delta SSPO 98: 25/5/1, altering the constellation's inclination while maintaining the same altitude presented an opportunity to use the Manuever Model to its full potential. The DARF framework adeptly navigated this scenario, adjusting the constellation's spatial dynamics to benefit from the SSPO orbit's coverage advantages. This inclination change, from 54 to 98 degrees, showcases DARF's operational flexibility and capability to handle complex reconfiguration demands, affirming its adaptability to inclination modifications while ensuring mission objectives are met. This test also conducted a simulation run to the original base configuration, keeping Walker Delta SSPO 98: 25/5/1 as the

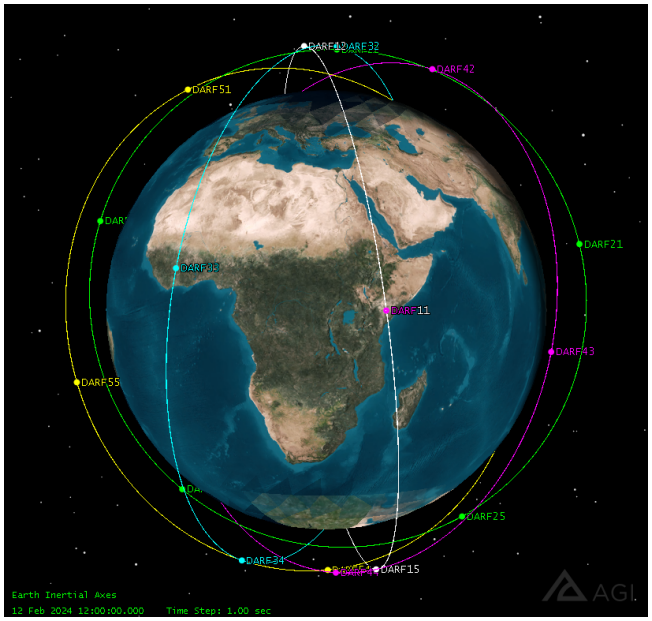

Figure 4.16 Walker Delta 54: 25/5/1 - Altitude Change Adaptability on STK

new base configuration. The results of DeltaV consumption in both cases will be discussed in detail in Chapter 5.

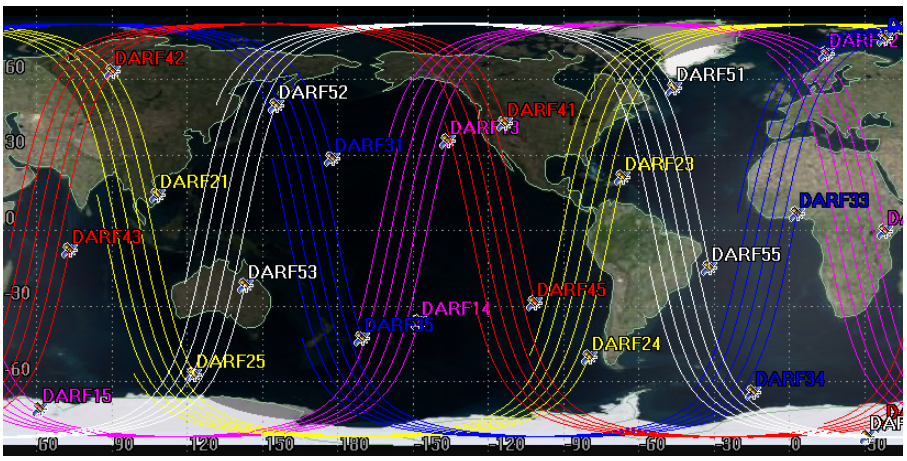

Figure 4.17 Groundtrack of Test 3 - Walker Delta SSPO 98: 25/5/1 - Inclination Change Adaptability on STK

4.2.4 Discussion

The adaptability tests underscore DARF's robust framework capable of efficiently responding to various operational scenario changes. Whether maintaining stability in uniform conditions, adapting to significant altitude adjustments, or navigating complex inclination changes, DARF demonstrates its versatility and dynamic reconfiguration capability. These results affirm the framework's suitability for future satellite constellations, emphasizing its potential to enhance operational flexibility and ensure the sustainability of space activities in increasingly crowded and complex orbital environments.

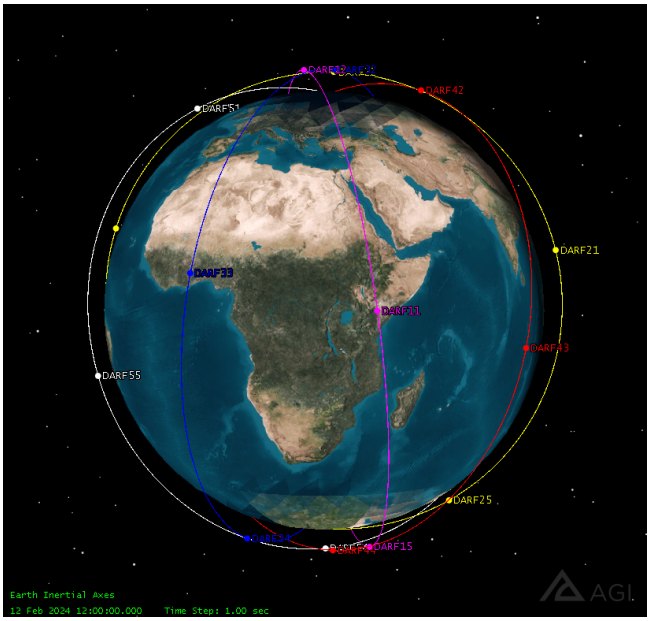

Figure 4.18 Test 3 - Walker Delta SSPO 98: 25/5/1 - Inclination Change Adaptability on STK

4.3 Use-case Results: Transition to Pendulum Formation

This section presents the results of our primary thesis objectives. It focuses on evaluating the choice of the figure of merits and optimization strategy laid out in Chapter 3 for DARF's core objective: To minimize the resource expenditure for n number of satellites in federation with each other. This section also helps validate the thesis objectives TO-9 and T-10 outlined in *Table 1.1*, the first research question RQ-1 outlined in Section 1.7 for , summarized in *Table 4.5*. This section presents the practical application of the DARF framework through a specific use-case scenario, demonstrating its adaptability, scalability, and optimization capability in real-world constellation reconfiguration tasks. Under two distinct evaluation scenarios, the focus was on transitioning five satellites from DARF's all capable and available satellites in the base configuration to the designated positions in a Pendulum (Delta RAAN) formation. Two test cases were outlined in Chapter 3 for this use-case simulation study, which differentiated themselves within the Reward Function Model since we aimed to access individual and collective optimization strategies for this particular test case. It is to be noted that Case 1 was modeled to maneuver by the individual assessment and not the collective route, which is the path set for Case 2.

Table 4.7 Optimization Goals

ID	Objective
TO-9	Simulate one use case scenario to provide practical implications for the framework.
TO-10	Validate the created decentralized decision-making algorithms to enable autonomous satellite responses within the framework.

4.3.1 Case 1 - Individual Satellite Assessment for Optimal Positioning

The individual assessment involved DARF meticulously evaluating each satellite's fitness metrics to ascertain the most suitable candidate for each available spot in the Pendulum formation. This process underscored DARF's precision in ranking satellites based on their fitness parameters, affirming its effectiveness in identifying optimal reconfiguration strategies for each satellite individually. The simulation, conducted at a finer time step of 1 second, revealed the distinct fitness parameters of the evaluated satellites.

Table 4.9 DARF's MATLAB Simulation Satellite Allotment

	S1	S2	S3	S4	S5
P1	1	2	3	4	5
P2	6	7	8	9	10
P3	11	12	13	14	15
P4	16	17	18	19	20
P5	21	22	23	24	25

The selected five satellites emerged as the best fit for the transition through MATLAB's computational window, as illustrated in Figure A.1 validated through visualization as outlined in Section 4.3.4. Table 4.9 shows the results of the 5 satellites chosen by DARF's optimization algorithm to carry out the maneuvers in sequence for achieving the required pendulum formation. Table 4.10 represents the same for STK's side of the simulator. It is to be noted that color grading is not important, and they are assigned randomly by the simulator. Table 4.14 and Figure 4.19 state the best five chosen by the simulator, ranked best from left to right. It is observed that the collective assessment includes Satellite 21 (DARF51) as one

Table 4.10 STK's Naming Convention for DARF Satellites

	N1	N2	N3	N4	N5
P1	DARF11	DARF12	DARF13	DARF14	DARF15
P2	DARF21	DARF22	DARF23	DARF24	DARF25
P3	DARF31	DARF32	DARF33	DARF34	DARF35
P4	DARF41	DARF42	DARF43	DARF44	DARF45
P5	DARF51	DARF52	DARF53	DARF54	DARF55

of the chosen satellites instead of Satellite 16 (DARF41), which came fifth in the individual individual assessments. Satellite 1 is unavailable since it detected the collision object placed 50 km away from it strategically during the start of the simulation, details of which will be presented in Section 4.4 and Subsection 4.3.3.

Table 4.11 Colours for DARF's best 5 satellites for Case 1, ranked highest in fitness parameter from left to right.

DARF22	DARF32	DARF42	DARF21	DARF41
7	12	17	6	16

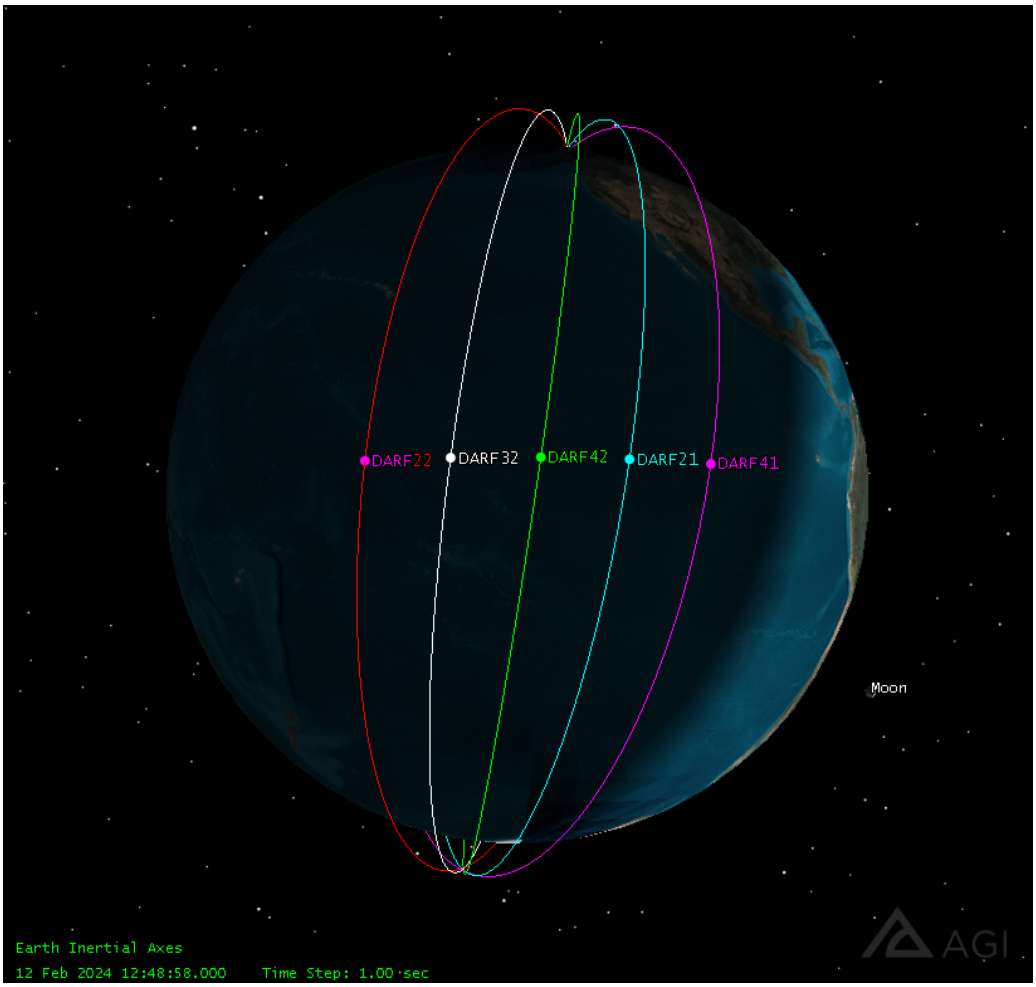

Figure 4.19 Case 1 - Pendulum Formation with ΔRAAN $= 10^{\circ}$

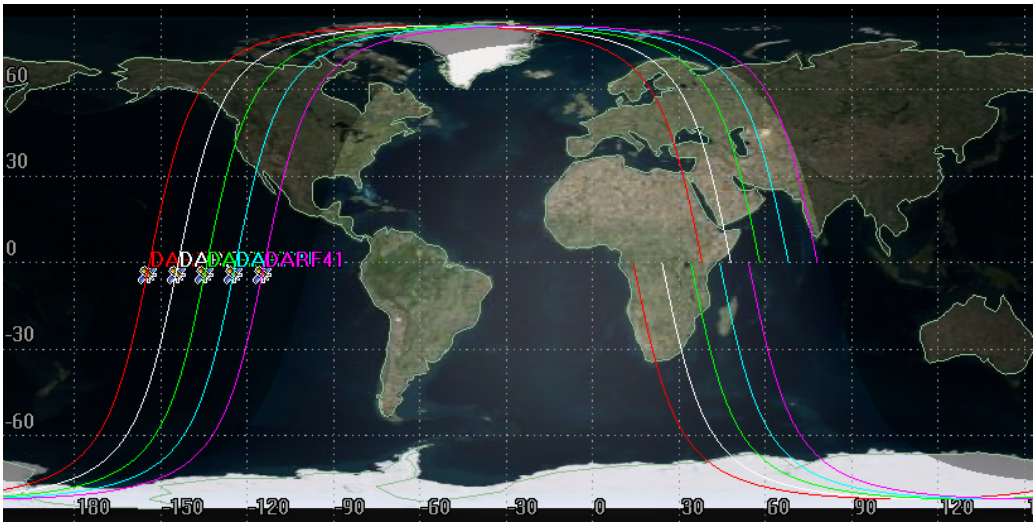

Figure 4.20 Case 1 - Groundtrack of Pendulum Formation with ΔRAAN $= 10°$. Left to Right: DARF22, DARF32, DARF42, DARF21, DARF41

4.3.2 Case 2 - Collective Assessment for Overall Optimization

In the collective assessment scenario, the focus shifted to evaluating groups of five satellites, aiming to achieve the lowest cumulative fitness parameters of the group itself. This approach highlighted DARF's capability to consider collective performance over time, leading to the selection of a group of satellites that, while not individually the top performers, collectively offered the most efficient configuration for the Pendulum formation. The simulation, conducted at a finer time step of 1 second, revealed the distinct fitness parameters of the evaluated satellites. The selected five satellites emerged as the best fit for the transition through MATLAB's computational window, as illustrated in Figure A.1 validated through visualization as outlined in Section 4.3.4. Table 4.9 shows the results of the 5 satellites chosen by DARF's optimization algorithm to carry out the maneuvers in sequence for achieving the required pendulum formation. Table 4.10 represents the same for STK's side of the simulator. It is to be noted that color grading is not important, and they are assigned randomly by the simulator. Table 4.14 and Figure 4.19 state the best five chosen by the simulator, ranked best from left to right. It is observed that the collective assessment includes Satellite 21 (DARF51) as one of the chosen satellites instead of Satellite 16 (DARF41), which came fifth in the individual individual assessments. Satellite 1 is unavailable since it detected the collision object placed 50 km away from it strategically during the start of the simulation, details of which will be presented in Section 4.4 and Sub-section 4.3.3.

Table 4.12 Case 2 - MATLAB Simulation Satellite Allotment

	S1	S2	S3	S4	S5
P1	1	2	3	4	5
P2	6	7	8	9	10
P3	11	12	13	14	15
P4	16	17	18	19	20
P5	21	22	23	24	25

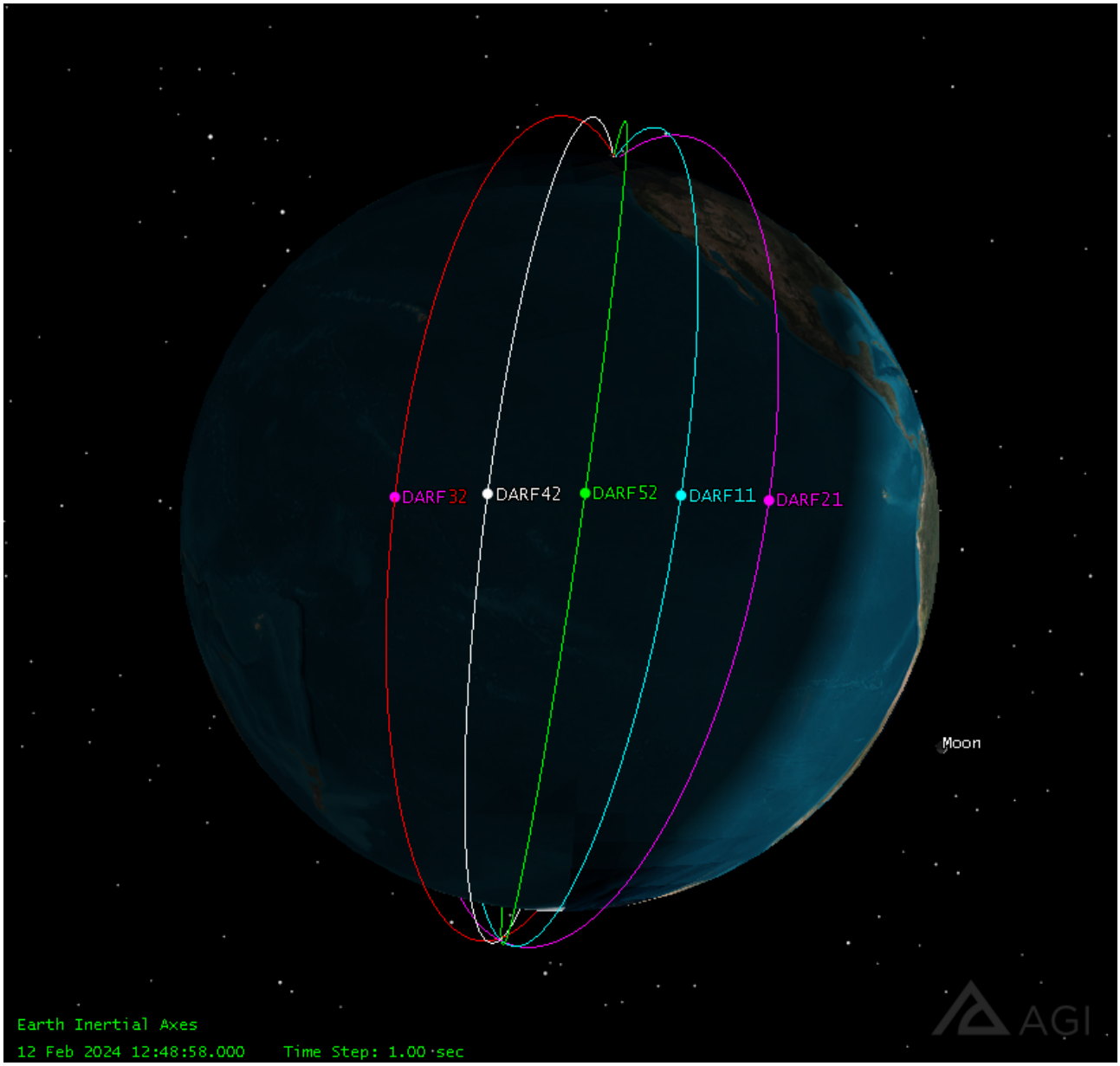

Figure 4.21 Case 2 - Pendulum Formation with ΔRAAN $= 10°$

Table 4.13 Case 2 - STK's Naming Convention for DARF Satellites

	N1	N2	N3	N4	N5
P1	**DARF11**	DARF12	DARF13	DARF14	DARF15
P2	**DARF21**	DARF22	DARF23	DARF24	DARF25
P3	DARF31	**DARF32**	DARF33	DARF34	DARF35
P4	DARF41	**DARF42**	DARF43	DARF44	DARF45
P5	DARF51	**DARF52**	DARF53	DARF54	DARF55

4.3.3 Use Case Detection and Collision Avoidance Validation

This section will be further discussed in detail in Section 4.4.

Table 4.14 Colours for DARF's best 5 satellites for Case 1, ranked highest in fitness parameter from left to right.

DARF32	DARF42	DARF52	DARF11	DARF21
12	17	22	1	6

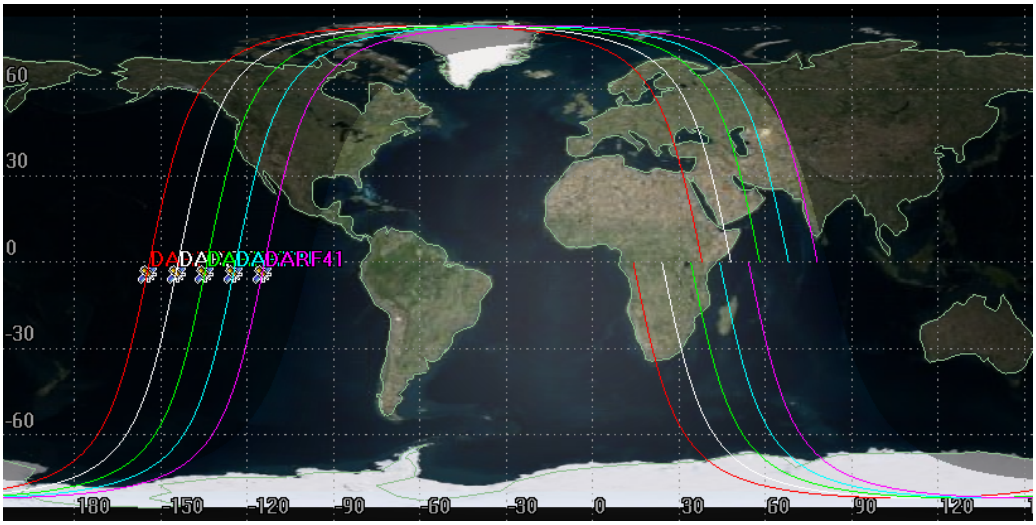

Figure 4.22 Case 1 - Groundtrack of Pendulum Formation with ΔRAAN $= 10°$. Left to Right: DARF22, DARF32, DARF42, DARF21, DARF41

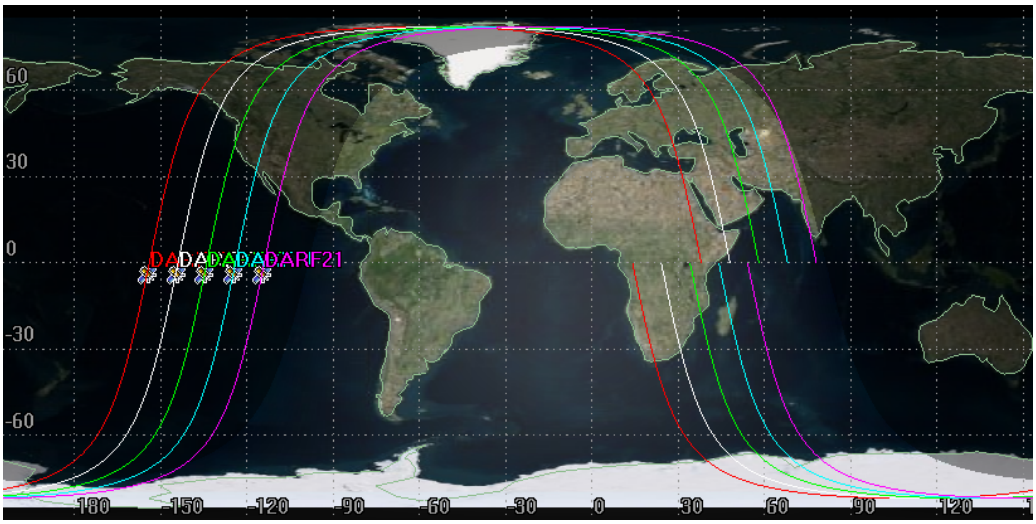

Figure 4.23 Case 2 - Groundtrack of Pendulum Formation with ΔRAAN $= 10°$. Left to Right: DARF32, DARF42, DARF52, DARF11, DARF21

The simulation's validation was further supported by STK's 3D and 2D visualizations, demonstrating the successful detection of a potential collision object and the execution of a collision avoidance maneuver for the first satellite, which reported a GSD of 0.984 m during one of the simulation timesteps. This scenario vividly illustrates DARF's adaptability and proactive measures to ensure mission safety and efficiency. STK's simulation tools played a pivotal role in visualizing the transition process and validating the effectiveness of DARF's decision-making algorithm.

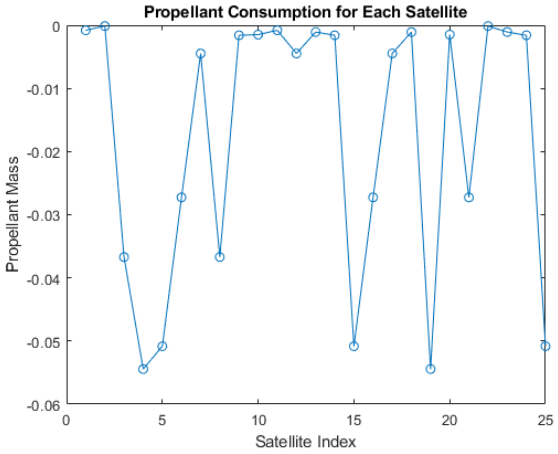

Figure 4.24 Case 1- Figure of Merit 1: Propellant Mass with Time of each Satellite

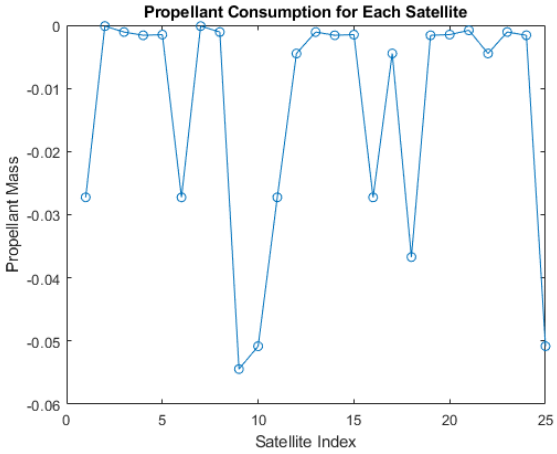

Figure 4.25 Case 2 - Figure of Merit 1: Propellant Mass with Time of each Satellite

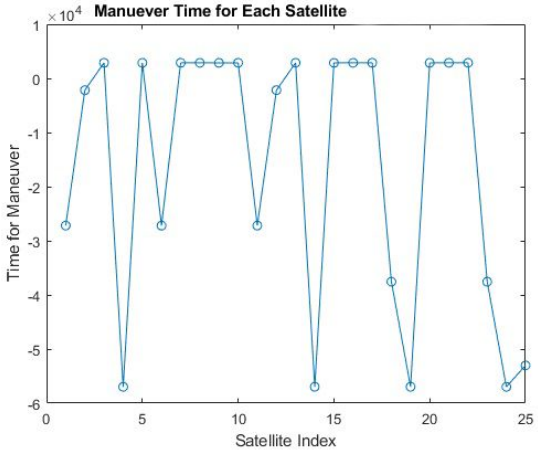

Figure 4.26 Case 1 - Figure of Merit 2: Maneuver Time with Time of each Satellite. Positive Index for Chemical, Negative for Electric

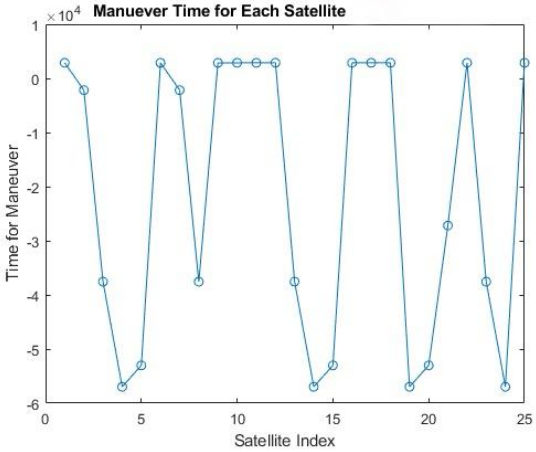

Figure 4.27 Case 2 - Figure of Merit 2: Maneuver Time with Time of each Satellite. Positive Index for Chemical, Negative for Electric

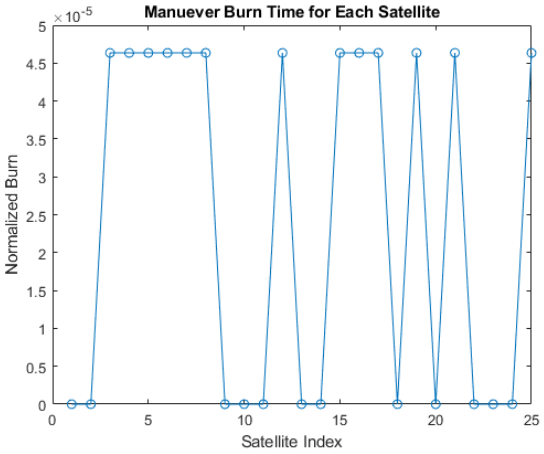

Figure 4.28 Case 1 - Figure of Merit 3: Burn Time with Time of each Satellite

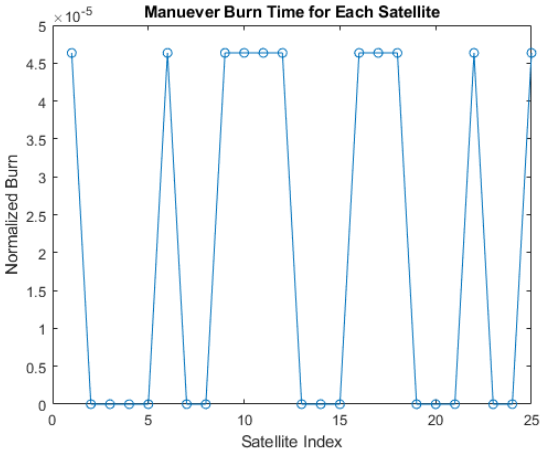

Figure 4.29 Case 2 - Figure of Merit 3: Burn Time with Time of each Satellite

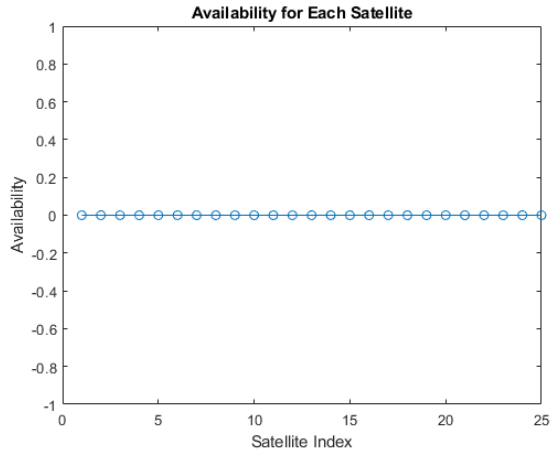

Figure 4.30 Case 1 - Figure of Merit 5: Availability of each Satellite. "0" is Available

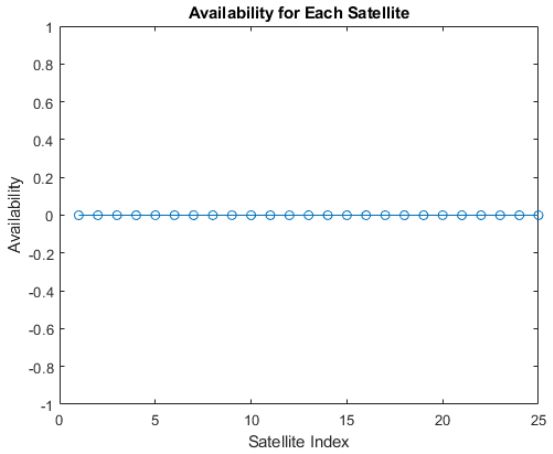

Figure 4.31 Case 2 - Figure of Merit 5: Availability of each Satellite. "0" is Available

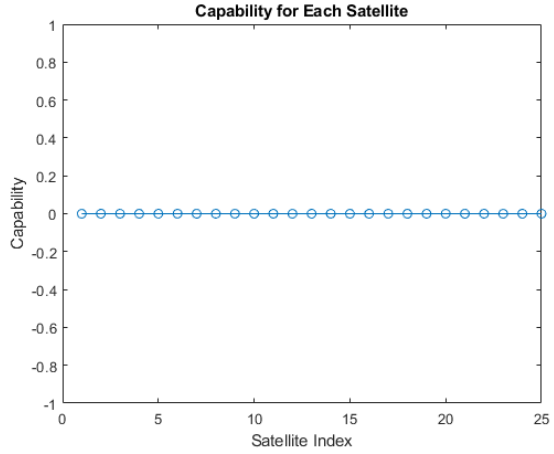

Figure 4.32 Case 1 - Figure of Merit 4: Capability of each Satellite. "0" is Capable

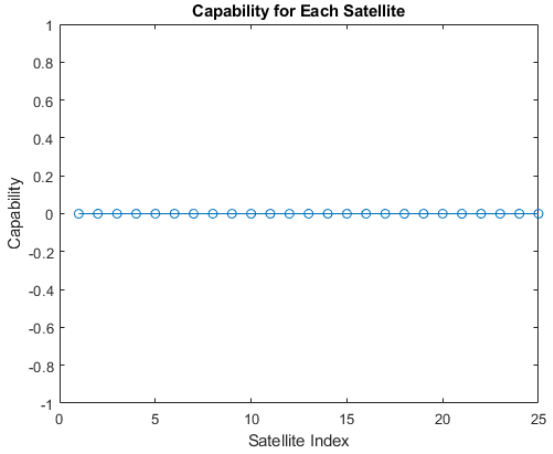

Figure 4.33 Case 2 - Figure of Merit 4: Capability of each Satellite. "0" is Capable

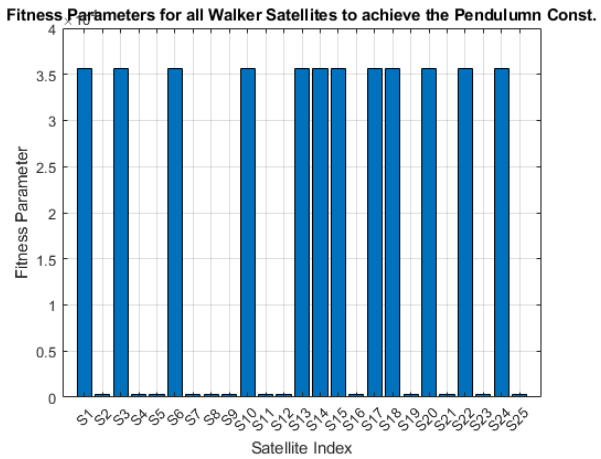

Figure 4.34 Case 1 - Overall Fitness Parameter of each Satellite

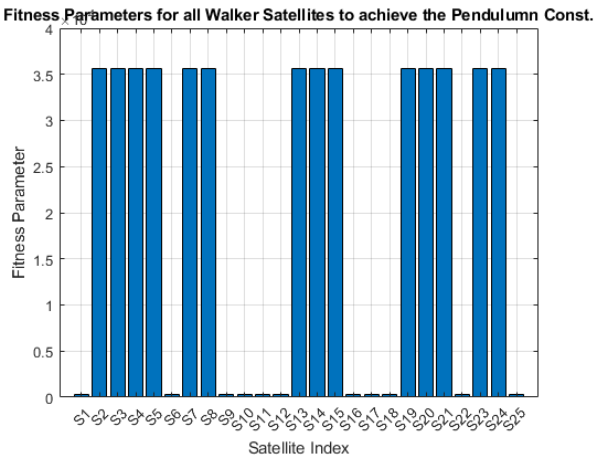

Figure 4.35 Case 2 - Overall Fitness Parameter of each Satellite

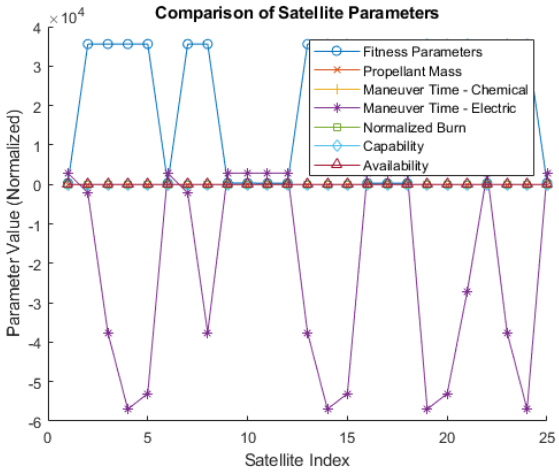

Figure 4.36 Case 2 - Figure of Merit vs Satellite Index

4.3.4 Use Cases Result Validation

The 3D graphics vividly portrayed the satellites' repositioning into the Pendulum formation, while the 2D graphics represented the ground track and ensured the satellites were propagated to maintain operational integrity. Figures 4.4 through 4.7 illustrate these aspects in detail. In Figure 4.24 and Figure 4.25, a varying distribution of propellant mass values is reported in both cases. We also note that the two cases are largely different different from one another. This is suspected to be because of the random distribution of propulsion types to these formations. It is further noticed that when comparing the propellant mass figure of merit, the highest value, observed at Satellite Index 19 for Case 1 and Satellite Index 9 for Case 2 corresponds to the burn time in Figure 4.28 and Figure 4.29 where Satellite 19 of Case 1 and Satellite 9 from Case 2 depicts a burn time of about 4.6e5 seconds. This puts a hypothesis that these two satellites are assigned as electric class. The dominating factor for such a presumption is the burn times. If we were to go along this hypothesis, then if we compare burn times to Figure 4.26 and Figure 4.27, we observe that Satellite 19 has noticeably the largest maneuver time in case 1 whereas Satellite 9 from case 2 has noticeably the second lowest maneuver time. Satellite 9 from Case 2 also has a very low fitness parameter, as does Satellite 19 from Case 1. This indicates that they are in the generally good cases of the fitness regime, even though both these satellites were not selected in the best 5 categories with the two outlined cases.

For the best satellite from Case 1, Satellite 7 exhibits a very low propellant mass consumption and maneuver time, with a noticeable low fitness parameter. For the best satellite from case 2, Satellite 12 exhibits a propellant usage in the moderate range relative to the data set and a very low maneuver time. It is suspected that the discrepancy found when comparing the maneuver time with the fitness parameter values, the effect of normalization, and the inclusion of very large time values in the case of electric class propulsion. In Figure 4.36, a combined graph of all the merits figures is traced along each case's fitness parameter. Although not clearly accurate the exact point of the fitness parameter value for Satellite 12 from Case 2, which is the best one to perform the maneuver, can be seen on the x-axis, indicating a very low fitness parameter. Suppose we do not rely on the visualization of the graphs and look at the data from MATLAB. In that case, it reports a fitness parameter of 297.1693824, compared to the highest value, the worst one to perform the maneuver, with a fitness parameter of 35585.26805. For the adaptability and Scalability, no effect was observed in either case, as seen in Figure 4.30, Figure 4.31, Figure 4.32 and Figure 4.33, displaying null values, which as outlined before means they are fully capable and available.

4.4 Collision Avoidance Validation

This section presents the comprehensive results of implementing the collision avoidance model within the DARF simulation framework. It includes the model's detection validation, maneuver simulation, the impact on GSD, and STK Astrogator for validation. The MATLAB's COM window is outlined in Annexture A1. illustrates the DARF's execution sequence, and activation of all models when the object was detected with a reported GSD of 0.984 m. This can also be visualized in Figure 4.39 where Satellite 1 in plane 1 detects the test collision object placed 40 km away from it during the start of the simulation. The purpose of displaying the seven timesteps with an increment of one second is to visualize the detection. Figure 4.40 shows the sam plot style representing the GSDs of all satellites for 86400 seconds.

Table 4.15 Collision Avoidance Goals

ID	Objective
TO-10	Validate the created decentralized decision-making algorithms to enable autonomous satellite responses within the framework.
TO-11	Validate coordination protocols within the framework to prevent conflicts during maneuver execution.

4.4.1 STK Astrogator Simulation for Collision Avoidance

Following the detection of potential collision threats through GSD flagging, the DARF collision avoidance model triggers a sequence of maneuvers designed to mitigate the risk. To validate these maneuvers and assess their impact on mission objectives, simulations were conducted using STK Astrogator. A specific scenario was chosen where a close approach with another object was identified, necessitating a phasing maneuver to adjust the satellite's orbit. The maneuver aims to change the timing of the satellite's orbit, allowing it to occupy a different position along its path that is safe from collision threats.

Simulation Results

The STK Astrogator simulation confirmed the effectiveness of the phasing maneuver in avoiding the potential collision. Figure 4.37 illustrates the satellite's orbital path before and after the maneuver, highlighting the successful alteration of the orbit to prevent the close approach.

4.5 Simulating Collision Avoidance

The simulation process within the STK Astrogator involved several steps:

- Scenario Setup: A new scenario was created in STK, with the initial conditions set based on the current orbit of the satellite and the predicted close approach data.
- Maneuver Definition: A phasing maneuver was defined using Astrogator's maneuver planning tools. This maneuver was designed to adjust the satellite's velocity vector, changing its orbital period slightly to avoid a potential collision.
- Simulation Execution: The maneuver was executed within the simulation, with the Astrogator calculating the satellite's new trajectory and orbit post-maneuver.

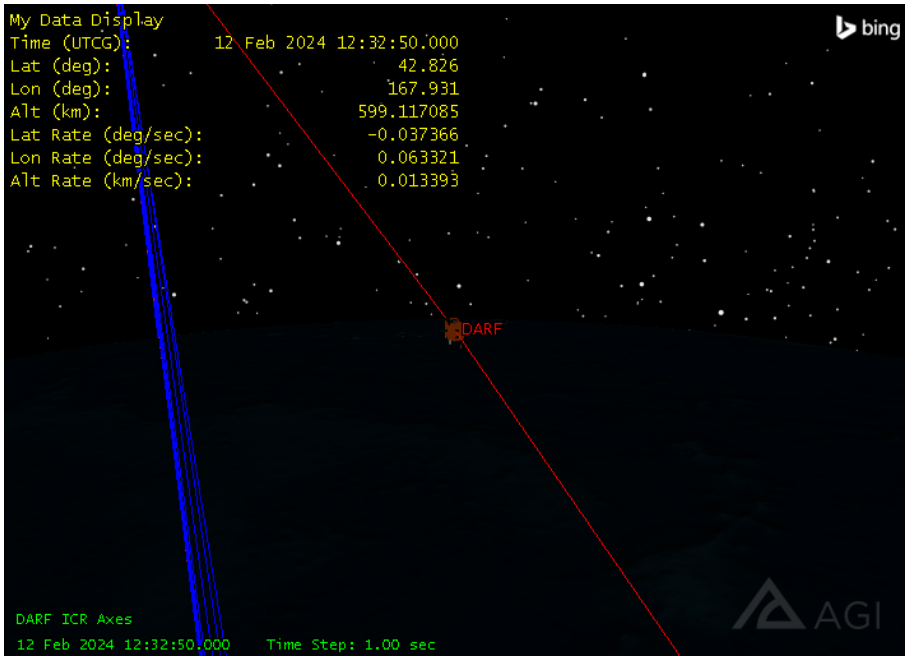

Figure 4.37 3D Zoomed-in View of DARF's Collision Avoidance Model flagging Satellite 1 from Plane 5 in 54: 25,5,1 Walker base constellation and performing a Phasing Maneuver, as auto-simulated by STK's Astrogator engine. Blue represents the original path and Red represents the altered trajectory

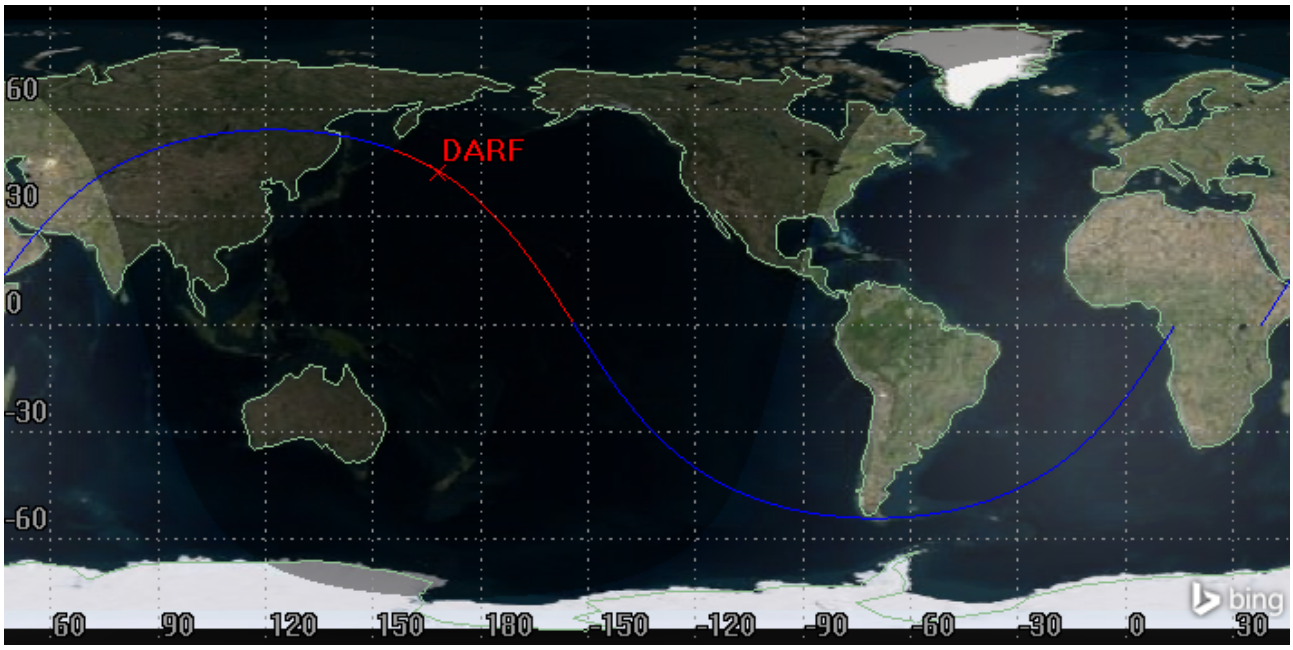

Figure 4.38 Groundtrack of DARF's Collision Avoidance Model flagging Satellite 1 from Plane 5 in 54: 25,5,1 Walker base constellation and performing a Phasing Maneuver, as auto-simulated by STK's Astrogator engine

- Results Analysis: The post-maneuver orbit was analyzed to ensure the collision threat was successfully mitigated. Additionally, the impact of the maneuver on mission objectives, such as imaging schedules and GSD, was assessed.

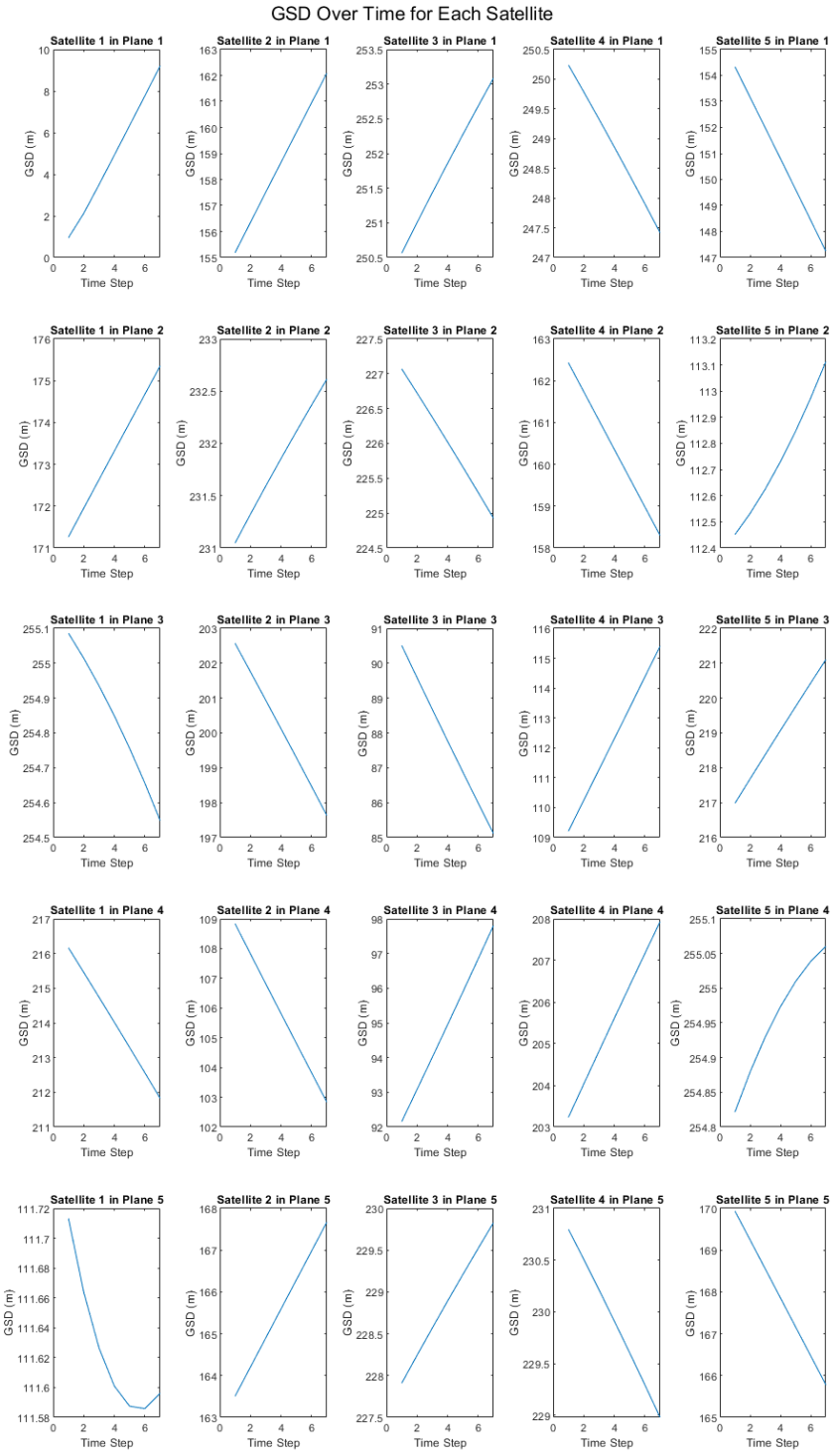

Figure 4.39 DARF'S's Optics Model flagging Satellite 1 from Plane 1 in 54: 25,5,1 Walker base constellation with a GSD of 0.984m

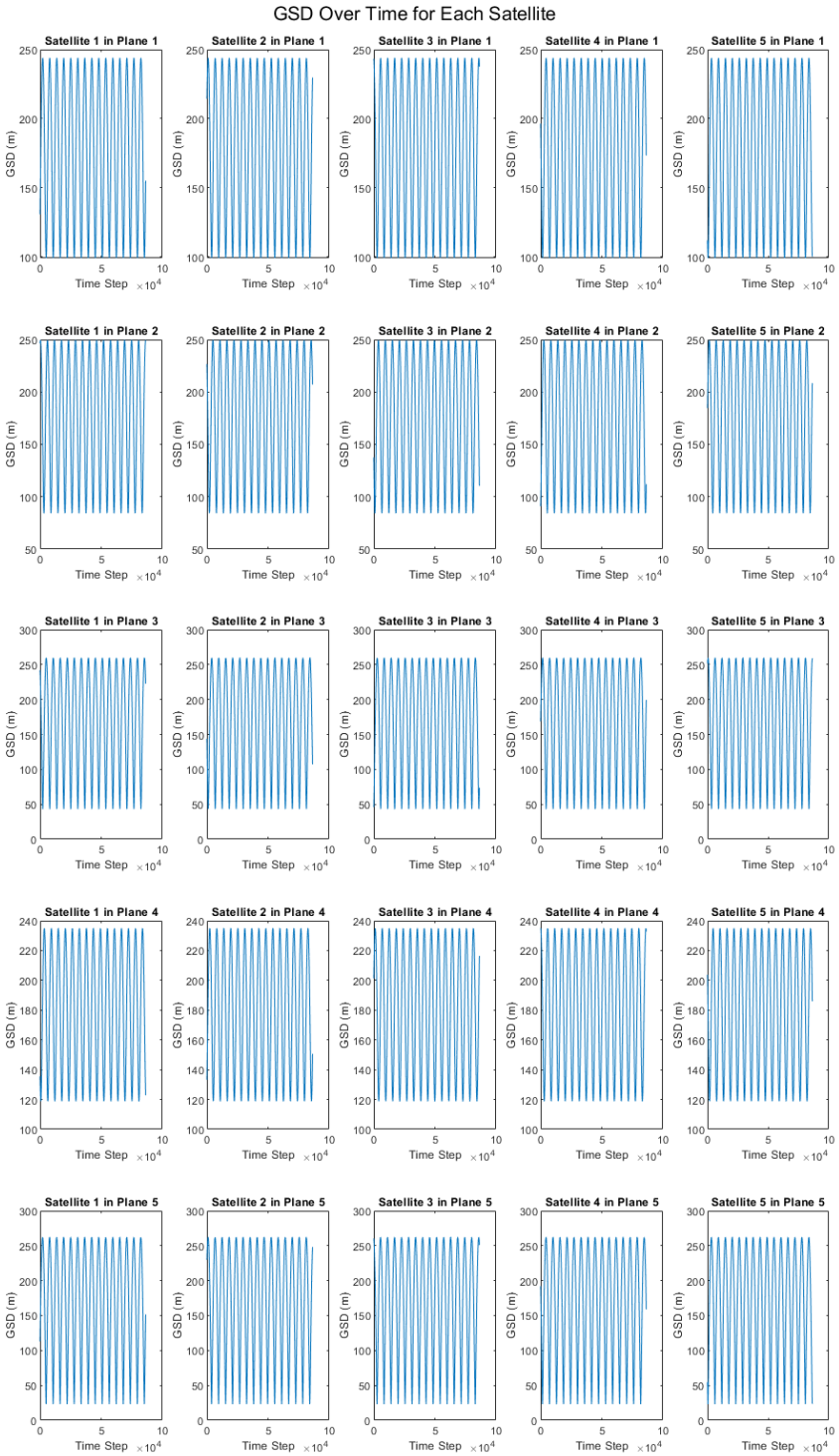

Figure 4.40 DARF'S's GSD with time for all Satellites in Case 1 of Use Case with

5 Discussions

Table 5.1 Chapter 5 Objective

ID	Objective
TO-12	Analyze and discuss the simulation results to validate the framework's effectiveness in optimizing satellite formation configurations.

The exploration and development of a dynamic framework capable of reconfiguring satellite constellations, as detailed in this thesis, embarked upon a path filled with substantial achievements, intricate challenges, and profound insights into the optimization complexities inherent in decentralized satellite management systems. This work, which rigorously tested and successfully implemented the proposed framework under various scenarios, showcases our approach's robustness and underscores its potential applicability in satellite operations.

However, integrating the Satellite Tool Kit (STK) with MATLAB presented unexpected complexities, primarily due to limited software support and a dearth of resources. This challenge highlighted significant gaps in existing documentation and user support for such advanced tasks. Despite these obstacles, the choice of STK over the General Mission Analysis Tool (GMAT) libraries was justified by STK's superior reliability and comprehensive simulation capabilities, particularly its proficiency in conducting detailed maneuver simulations and generating reliable data crucial for our analyses. One notable limitation encountered was the dynamic simulation capabilities of STK, constrained by the nature of STK's COM and Connect interfaces, as well as the limitations inherent in commercially available orbit propagators. Although a workaround involving multiple instances of STK for parallel computations was devised, this method did not achieve the level of dynamic adaptability envisaged. This was particularly evident in our attempts to conduct real-time complex maneuvers and constellation reconfigurations, highlighting the necessity for advancements in simulation technologies to better support such sophisticated endeavors.

During the computation of the reward function, an intriguing anomaly was observed—a discrepancy between the collective assessment of five satellites and their evaluations. In Case 1, when satellites were assessed individually, they were ranked as 7, 12, 17, 6, and 16 for optimal slots. However, a collective assessment yielded a slightly different order: 6, 7, 12, 17, 21, diverging from the individual assessments. This discrepancy suggests that collective optimization does not merely replicate the sum of individual optimizations but introduces a dynamic that alters the selection process. Case 2 further validated this observation, where the collective selection of satellites—12, 17, 22, 1, and 6—mirrored the best individuals, albeit with a different prioritization for the individual assessment, being 1, 6, 12, 17, and 22. This phenomenon indicates that a satellite deemed not the most optimal in individual assessments could become crucial in a collective context, emphasizing the unique contribution of each satellite to the overall system's efficiency. It underscores the complex interplay between individual capabilities and collective system performance, suggesting that integrating individual parameters into a collective optimization framework can reveal synergies not apparent in isolated assessments. This approach encourages a more nuanced consideration of satellite attributes in maneuver planning, allowing for strategically allocating resources and tasks within a

satellite constellation based on collective system optimization rather than individual satellite performance alone.

The intricate task of selecting and fine-tuning fitness parameters for satellite maneuvers and federation reconfigurations within this thesis underscores the complexity and sophistication required in the optimization processes. This complexity was compounded by the incorporation of electric propulsion systems, which introduced a new dimension of challenge in our optimization efforts due to their characteristically long-duration maneuvers. The endeavor to balance maneuver efficiency with resource optimization and maintain operational readiness throughout demanded a deep dive into multi-objective optimization's nuanced intricacies, especially within a decentralized satellite management framework. This necessitated a profound understanding of the satellite operational environment, pushing us to meticulously consider how each fitness parameter—propellant mass, maneuver time, or satellite capability and availability—impacts the overall mission success. The task was not merely about achieving operational efficiency but also about ensuring the longevity and sustainability of satellite operations in the face of finite resources and ever-evolving mission objectives. The complexity of this balance was further highlighted by the need to normalize and appropriately weigh these parameters, a task made challenging by the diverse nature of satellite missions and the varying capabilities of propulsion systems. Electric propulsion systems posed a particular challenge with their slow yet efficient thrust capabilities. They necessitated a reevaluation of traditional optimization metrics, pushing us to consider not just the immediate impact of a maneuver but its long-term implications on mission architecture and resource utilization. This reevaluation was critical in ensuring that our framework could adapt to a wide range of propulsion technologies, thereby broadening its applicability and relevance in the rapidly evolving space industry.

Moreover, the process illuminated the inherent trade-offs in satellite constellation management, where decisions to optimize one mission aspect could inadvertently compromise another. For instance, optimizing for minimal propellant use might extend a satellite's lifespan. Still, it could also result in longer maneuver times that might not be viable in scenarios requiring rapid reconfiguration in response to collision threats or mission parameter changes. The choice between chemical and electric propulsion affects maneuver times and propellant usage and has broader implications for mission planning and satellite design. The challenges encountered in this optimization process also underscored the limitations of existing models and the need for innovative approaches to satellite constellation optimization. Traditional methods often simplify assumptions that may not hold in space operations' complex, dynamic environment. Our exploration of these challenges highlights the importance of developing more adaptive, nuanced models to accommodate the diverse needs of satellite constellations, from small cubesats to large, multifunctional satellites in federation.

In striving to configure an optimal set of fitness parameters, we ventured into an area where every choice had profound implications for overall system performance. The task was not merely a mathematical exercise but a strategic endeavor to harmonize the conflicting demands of maneuver efficiency, satellite longevity, and mission effectiveness. The quest for an optimal balance led to a deep dive into the methodologies of multi-objective optimization, where the objective was not simply to find a singular solution but to navigate the complex trade-off landscape to identify a suite of viable solutions. Each potential solution has implications for the constellation's ability to respond to dynamic operational requirements, manage resource constraints, and maintain a readiness posture for unforeseen challenges. The optimization process thus became a critical component of our framework's design, demanding a level of precision and insight that could only be achieved through rigorous analysis and a willingness to engage with the complexity of satellite constellation management holistically.

The results indicate that the DARF framework scales effectively to manage larger constellations. However, scaling up the number of satellites necessitates more sophisticated resource allocation and collision avoidance algorithms. The slight reduction in system uptime could be attributed to the increased probability of collision events and the resultant complex avoidance maneuvers that temporarily take satellites

offline. Further optimizations in the maneuver planning algorithms could potentially mitigate these impacts. It demonstrates an impressive capacity to adjust to constellations of varying sizes with a commendable degree of efficiency. The scalability tests we conducted were a clear testament to the framework's robust architecture and ability to adapt to the expanding needs of satellite constellation management. However, these tests also highlighted the non-linear growth in computational demands as the constellation size increased. This phenomenon presented a stark trade-off: the pursuit of detailed simulation fidelity against the imperative of maintaining processing efficiency. The challenge was not simply computational but conceptual, prompting us to rethink the parameters of simulation granularity and its impact on the framework's performance and utility. Furthermore, the adaptability tests conducted in this research provided valuable insights into the framework's dynamic reconfiguration capabilities. These tests validated the framework's proficiency in managing transitions between diverse constellation configurations, from routine operational adjustments to comprehensive overhauls in response to evolving mission objectives. The ability to adapt fluidly across a spectrum of operational scenarios highlights the framework's versatility. It underscores its potential to be a foundational tool in the next generation of satellite constellation management.

Analysis of the internal variables revealed that the most significant demand for delta-V arose from adjustments to the Right Ascension of the Ascending Node (RAAN), succeeded by changes in inclination and altitude. The simulation, visualized through STK, notably showed that satellites closer to the equator were more frequently selected for maneuvers than their counterparts near the poles or in higher orbits. This observation underscores the impact of a satellite's initial position on its maneuver requirements within a constellation. A notable challenge encountered in this research was the scarcity of comprehensive literature concerning the time required for maneuvers related to changes in range and inclination. a generalized formula was developed to bridge this gap, leveraging the calculated delta-V from the Dynamic and Autonomous Reconfiguration Framework (DARF) and the satellite's thrust-to-weight ratio. This novel approach enabled a differentiated assessment of maneuver times for changes in inclination, altitude, and RAAN, offering a unique perspective on maneuver planning despite the inherent inaccuracies stemming from the limited literature.

The results also illuminated the significantly higher maneuver requirements for electric propulsion systems, with delta-V values being an order of magnitude of 10e4 greater than those for chemical propulsion. This distinction highlights the different capabilities and limitations of propulsion technologies. It emphasizes the necessity for tailored maneuver strategies to accommodate the specific needs of electrically-propelled satellites within a constellation. The endeavor to simulate and plan maneuvers within the scope of our research brought to light the variable nature of delta-V requirements, a fundamental aspect governed by the intricate dance of orbital dynamics. This variability underscores the importance and inherent complexity of crafting precise and efficient maneuvers within the unforgiving confines of space. The challenge of planning these maneuvers is magnified by the diverse orbital parameters that dictate the trajectory and behavior of satellites, each parameter weaving its layer of complexity into the fabric of satellite operations. In the face of limited comprehensive literature and existing guidelines on maneuver planning, particularly for emerging propulsion technologies and novel operational scenarios, our research embarked on an ambitious path. We aimed to derive and generalize equations that provide a foundation for estimating maneuver times across satellite operations. This pursuit, though fraught with the challenges of potential inaccuracies and assumptions, signifies a bold step forward in satellite constellation management. It embodies the pioneering spirit that characterizes this research, a spirit driven by the quest for innovation and advancement in the face of uncertainty and incomplete information. Developing these generalized equations for maneuver planning was not merely an academic exercise but a practical tool to enhance the decision-making process for satellite operators. By providing a framework for estimating maneuver times, our research contributes to the broader goal of optimizing satellite operations, ensuring that each maneuver is strategically planned and resource-efficient. This contribution is particularly pertinent in an era where the sustainability of space operations has become a pressing concern, given the increasing congestion in popular orbital regions.

Moreover, our efforts to navigate the complexities of maneuver planning and optimization highlight a broader theme of adaptability and resilience in space operations. The ability to plan and execute maneuvers efficiently is a cornerstone of maintaining the operational integrity and longevity of satellite constellations, especially in an environment that is continually evolving. The insights gained from these simulations and the development of generalized maneuver planning equations pave the way for future research and development efforts. They set the stage for a deeper exploration of how emerging technologies, such as electric propulsion and advanced maneuver planning algorithms, can be harnessed to further enhance the efficiency and sustainability of satellite constellations.

A notable limitation was STK's inability to dynamically loop variables during a propagation in progress when controlled programmatically through MATLAB. This restriction hindered our framework's ability to simulate more than two constellations simultaneously and impacted the real-time visualization of dynamic adaptations. Although our framework could generate multiple instances of STK for parallel computations, the inability to update parameters dynamically within STK limited the real-time applicability of our simulations. Further exploration of the framework's capabilities revealed that while STK can simulate complex maneuvers for collision avoidance, such simulations are restricted to visualizing maneuvers for a single satellite at a time. This limitation was particularly impactful in our use case, where the real-time visualization of constellation reconfiguration was crucial. Additionally, the exclusion sphere's radius presented challenges in detection modeling, necessitating careful calibration to avoid false negatives in collision path detection.

To Summarize the findings of this thesis

- Integrating STK with MATLAB presented significant challenges, underscoring a gap in existing documentation for complex integrations required particularly for satellite formation or batch reconfigurations.
- A discrepancy was observed in the reward function computation, suggesting collective optimization dynamically alters the selection process, diverging from individual assessments in about half of the test runs.
- Electric propulsion's long-duration maneuvers introduced challenges in optimization, requiring a reevaluation of the chosen metrics for a strategic balance in maneuver planning.
- Maneuver planning faced limitations due to a lack of comprehensive literature, prompting the development of generalized equations to estimate maneuver times across diverse orbital parameters.
- A successful demonstration of the collision avoidance model was implemented and visualized on STK generated by DARF.
- RAAN change requires the highest deltaV's followed by a change in inclination and altitude.
- DeltaV's were higher when moving from a lower orbit to a higher orbit and transitioning from equatorial plane to polar.
- Scalability tests revealed DARF's robust architecture yet highlighted a non-linear growth in computational demands with increased constellation sizes, presenting a trade-off between simulation detail and efficiency.
- Adaptability tests revealed DARF's flexible and adaptive reconfigurable nature but lacked the visualization of maneuvers for all satellites in a federation in a single visualization window.

6 Conclusions & Future Work

With a developed dynamic framework for reconfiguring satellites in a federation, a variety of scenarios and simulations could be undertaken for satellites in a federation as well as satellites traditional satellite architecture setups, contributing to enhancing the sustainability and safety of space operations amidst the increasingly congested orbital environment of the future and present. The developed framework, DARF identifies the fitness parameters for every satellite from a scalable number of satellites in a formation. The research explored a comprehensive exploration of integrating the STK with MATLAB to demonstrate its capability to adaptively respond to operational demands through various simulations under varying conditions, showcasing its value in future satellite operations. Despite the challenges encountered, notably the challenge of testing a collision object, DARF successfully triggered the flagged satellite for a collision avoidance maneuver whilst presenting the optimal solution set for the group of 5 satellites for reconfiguration in our use case test simulation.

The scalability and adaptability tests have underscored the framework's robustness in handling different sizes and configurations constellations. The performance metrics highlight that collision detection improves for smaller steps but with an increased computation time. These tests have highlighted the trade-offs between simulation detail and processing efficiency, contributing valuable insights into managing and optimizing large satellite constellations. The results also illuminated the significantly higher maneuver requirements for electric propulsion systems, with delta-V values being higher in several orders greater than those for chemical propulsion. Analysis of the internal variables revealed that the most significant demand for delta-V arose from adjustments to the RAAN, succeeded by changes in inclination and altitude. The simulation, visualized through STK, notably showed that satellites closer to the equator were more frequently selected for maneuvers than their counterparts near the poles or in higher orbits. This observation underscores the impact of a satellite's initial position on its maneuver requirements within a constellation. Moreover, a successful collision avoidance strategy was implemented, tested an visualized.

The meticulous selection and optimization of fitness parameters illuminated the intricate trade-offs involved in maneuver planning and constellation management. Our efforts to balance maneuver efficiency, resource optimization, and operational readiness within a decentralized management system have laid some groundwork for future advancements in the field. The successful simulation of maneuvers, particularly those involving electric propulsion, and maneuver time for inclination and RAAN change, though challenged by a lack of comprehensive literature, reflects the pioneering spirit of this research. Despite facing inherent inaccuracies as seen within the results section about collective and individual assessments of the best satellite to perform the maneuver, our efforts to generalize equations for maneuver times pave the way for more informed decision-making in satellite operations, marking a significant step forward in the quest for efficient and sustainable space traffic management.

Building upon the foundational work presented in this thesis, future research endeavors can delve into several promising areas to enhance the capabilities of satellite constellation management frameworks. Key directions include refining integration techniques between simulation tools and programming environments, advancing real-time dynamic simulation capabilities, and developing more accurate models for electric propulsion maneuvers. Further exploration into sophisticated multi-objective optimization strategies, decentralized decision-making algorithms, and the scalability and adaptability of such frameworks holds the potential to significantly improve the efficiency and effectiveness of satellite operations. Collaborative validation efforts with space industry stakeholders and integration with space traffic management initiatives could offer invaluable insights into these advancements' practical applicability and impact. Pur-

suing these avenues will build on the existing body of knowledge and contribute to the sustainable and safe expansion of space activities in an increasingly crowded orbital environment.

Key Conclusion Points

DARF Scales well and Adapts well

Larger constellations spike computational demands. The tradeoff between step sizes and computational time is required. Balancing step size with computational load is crucial: finer steps for collision prevention, coarser for non-urgent reconfigurations.

DARF handles specific reconfiguration requests with best-optimized satellites

Collective optimization diverges from individual assessment in some cases. This reveals that a satellite, although optimal in an individual evaluation for a particular reconfiguration, may not hold its ranking when assessed collectively; even a satellite previously ranked second could ascend to the top, bringing into play another satellite that was not initially among the top five contenders.

The collision avoidance capability was successfully validated in DARF

Electric propulsion falls short for urgent reconfigurations and collision avoidance, due to its slower maneuverability.

Key Points for Future Work

- Fine-tuning of the Reward Functions.
- Consider parameters of Real Satellites.
- Consider Partial Illumination of Objects for Detection.
- Introduce an Urgent FOM, stating a time limit on reconfiguration.

To conclude, this thesis contributes a novel framework for satellite constellation reconfiguration and opens avenues for future research in decentralized satellite management systems. It calls for simulation technology advancements to fully realize constellations' dynamic adaptability and underscores the need for a deeper exploration of multi-objective optimization strategies. As we stand on the brink of a new era in space operations, the insights and methodologies developed through this research offer a foundational step toward ensuring our orbital environment's long-term sustainability and safety.

A Appendix

A.1 MATLAB COM Window

```
Timestep 5: Satellite 25 did not detect the object. GSD is 167.16811 m.
Timestep 6: Satellite 25 did not detect the object. GSD is 166.47466 m.
Timestep 7: Satellite 25 did not detect the object. GSD is 165.78082 m.
Subscribing to DARF Collision Avoidance Model...
Collision objects found within this propagation. Proceeding...
Triggering DARF Collsion Avoidance Phasing Manuever Sub-Model...
Initiating DARF Propulsion Sub-Model...
Type: Collison Avoidance Manuevers...
Simulating Collison Avoidance Manuever on STK...
Elapsed time is 29.466030 seconds.
Checking Reconfiguration Requests...
Triggering DARF Reconfiguration Model...
Initiating DARF Propulsion Sub-Model...
Initiating DARF Manuever Sub-Model...
Subscribing to DARF Reward Functions Model...
Computing Fitness Parameters...
Computation Successful...
Plotting Data...
Plotting Successful. Terminating Execution of DARF
>>
```

Figure A.1 Execution of DARF Simulation displaying MATLAB's Command Window highlighting the CAM was activated and subsequently flagging collision avoidance maneuver strategies

```
Initiating DARF Manuever Sub-Model...
Subscribing to DARF Reward Functions Model...
Computing Fitness Parameters...
Computation Successful...
Satellites with the lowest fitness parameters:
Satellite Index: 7
Satellite Index: 12
Satellite Index: 17
Satellite Index: 6
Satellite Index: 16
Combination of 5 satellites with the lowest sum of fitness parameters:
Satellite Indices: 6   7  12  17  21
```

Figure A.2 MATLAB's command window for Case 2

```
Timestep 86400: Satellite 25 did not detect the object. GSD is 23.59412 m.
Timestep 86401: Satellite 25 did not detect the object. GSD is 23.56546 m.
Subscribing to DARF Collision Avoidance Model...
No collision objects within this propagation.
Checking for Reconfiguration Requests...
No Applicable Simulation to show Collsion Avoidance Manuever, skipping...
Checking Reconfiguration Requests...
Found a Reconfiguration Request...
Triggering DARF Reconfiguration Model...
Initiating DARF Propulsion Sub-Model...
Initiating DARF Manuever Sub-Model...
Subscribing to DARF Reward Functions Model...
Computing Fitness Parameters...
Computation Successful...
Satellites with the lowest fitness parameters:
Satellite Index: 12
Satellite Index: 17
Satellite Index: 22
Satellite Index: 1
Satellite Index: 6
Combination of 5 satellites with the lowest sum of fitness parameters:
Satellite Indices: 1   6  12  17  22
Plotting Data...
Elapsed time is 144.025669 seconds.
Plotting Successful. Terminating Execution of DARF
>>
```

Figure A.3 MATLAB's command window for Case 1

A.2 Graphs generated from DARF and compared with STK

Figure A.4 DARF's Satellite Position over time plot

Figure A.5 STK's Satellite Position over time plot

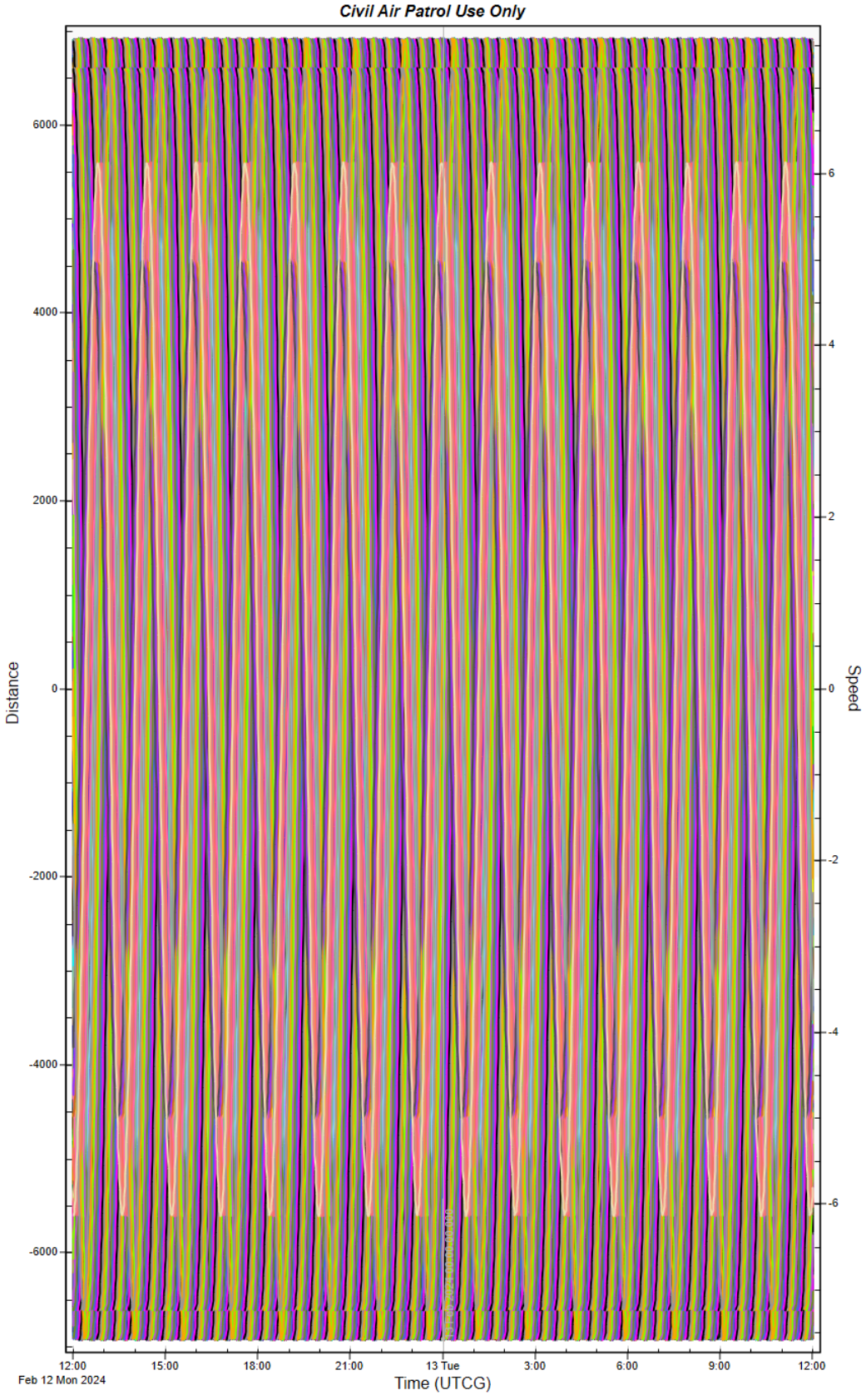

Figure A.6 GSD over time for 500 satellites, Too large data set for one page

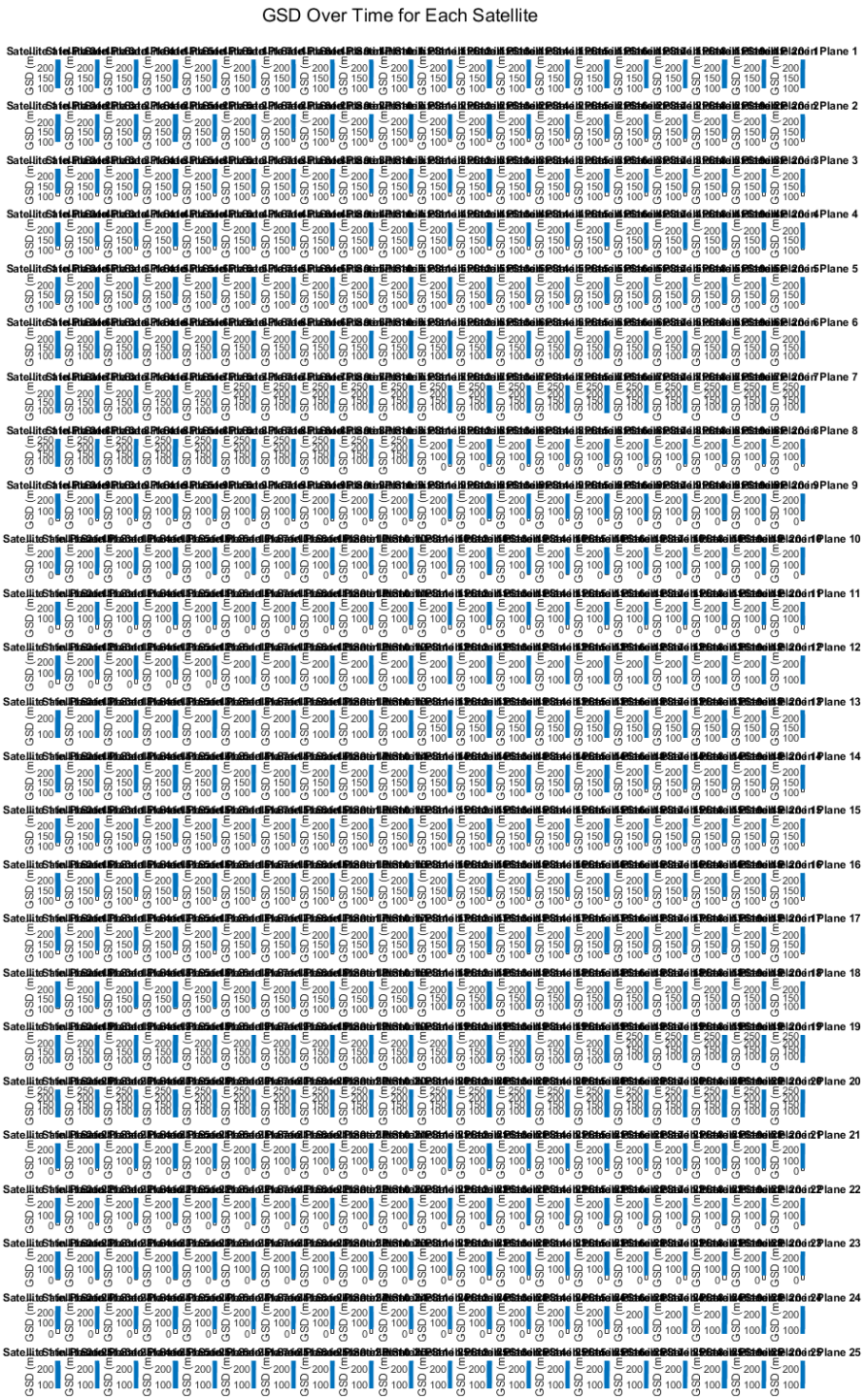

Bibliography

[1] D. Mosher, “Analytical graphics, inc.,” 2023.

[2] S. Kumar, “Chapter 3 - global navigation satellite systems and their applications in remote sensing of atmosphere,” in *Atmospheric Remote Sensing* (A. Kumar Singh and S. Tiwari, eds.), Earth Observation, pp. 39–62, Elsevier, 2023.

[3] D. Oltrogge, “57,000 planned satellites swarm earth within 9 years,” tech. rep., Analytical Graphics Inc., 2020.

[4] U. S. G. A. Office, “Technology assessment large constellations of satellites,” tech. rep., GAO-22-105166, 2022.

[5] S. Koshova, “Prospects for space-based earth observation systems in ukraine,” *Publishing House “Baltija Publishing”*, 2023.

[6] U. of Concerned Scientists, “Ucs satellite database,” 2023.

[7] Nanoavionics, “How many satellites are in space?,” 2023.

[8] O. Junge, J. E. Marsden, and S. Ober-Blobaum, “Optimal reconfiguration of formation flying spacecraft —a decentralized approach,” in *Proceedings of the 45th IEEE Conference on Decision and Control*, pp. 5210–5215, 2006.

[9] S. Alfano, D. Oltrogge, H. Krag, K. Merz, and R. Hall, “Risk assessment of recent high-interest conjunctions,” *Acta Astronautica*, vol. 184, pp. 241–250, 2021.

[10] Z. Yang, H. Wang, Y. Liu, M. Zhang, and J. Wu, “Satellite trajectory planning for space debris collision avoidance,” in *Proceedings of 2022 International Conference on Autonomous Unmanned Systems (ICAUS 2022)* (W. Fu, M. Gu, and Y. Niu, eds.), (Singapore), pp. 2789–2798, Springer Nature Singapore, 2023.

[11] M. R. Kabir, T. I. Faysal, M. S. Hossain, J. N. Shorno, and S. Siddique, “A satellite collision avoidance system based on general regression neural network,” in *2020 IEEE/ACM International Conference on Big Data Computing, Applications and Technologies (BDCAT)*, pp. 154–160, 2020.

[12] V. Kuznetsov, V. Sinelnikov, and S. Alpert, “Sputnik 1 and the first satellite ionospheric experiment,” 08 2014.

[13] “Extending satellite longevity and life-cycle effectiveness through dynamically reconfigurable communications systems,” 2009.

[14] J. McDowell, “Starlink launch statistics,” tech. rep., Jonathan’s Space Pages., 01 2024.

[15] S. Alfano, D. L. Oltrogge, , and R. Shepperd, “Leo constellation encounter and collision rate estimation: An update,” in *2nd IAA Conference on Space Situational Awareness (ICSSA)*, vol. IAA-ICSSA-20-0021, 2020.

[16] A. Poghosyan, I. Lluch, H. Matevosyan, A. Lamb, C. Moreno, C. Taylor, A. Golkar, J. Cote, S. Mathieu, S. Pierotti, J. Grave, J. Narkiewicz, S. Topczewski, M. Sochacki, E. Lancheros, H. Park, A. Camps, and A. Ru, “Unified classification for distributed satellite systems,” 10 2018.

[17] R. Preston, *Distributed Satellite Constellations Offer Advantages Over Monolithic Systems*. Santa Monica, CA: RAND Corporation, 2004.

[18] J. Underwood, "Distributed satellite communications system design: first-order interactions between system and network architectures," 03 2006.

[19] M. Daniels and M. Elisabeth Pate-Cornell, "Risk aversion and optimal satellite systems," in *2015 IEEE Aerospace Conference*, pp. 1–20, 2015.

[20] A. G. Vincenzo Messina, "Initial formulation of a time varying dynamic graph decentralized optimization framework for scaled satellite network infrastructure operations," in *IAC 2023 Congress Proceedings, 74th International Astronautical Congress*, Oct 2023.

[21] P. J. Lin and T. J. Kostas, "Flexible satellite systems," pp. 1–7, IEEE, 2007.

[22] G. Dubos and J. Saleh, "Comparative cost and utility analysis of monolith and fractionated spacecraft using failure and replacement markov models," *Acta Astronautica - ACTA ASTRONAUT*, vol. 68, pp. 172–184, 02 2011.

[23] A. Golkar and I. L. i Cruz, "The federated satellite systems paradigm: Concept and business case evaluation," *Acta Astronautica*, vol. 111, pp. 230–248, 2015.

[24] E. A. Carlos, R. Pinard, and M. Hassani, "Over-the-air federated learning in satellite systems," 2023.

[25] H. Hellström, V. Fodor, and C. Fischione, "Federated learning over-the-air by retransmissions," *IEEE Transactions on Wireless Communications*, vol. 22, no. 12, pp. 9143–9156, 2023.

[26] A. Camps, J. Munoz-Martin, J. Ruiz-de Azua, L. Fernandez, A. Pérez Portero, D. Llaveria, C. Herbert, M. Pablos, A. Golkar, A. Gutierrez, C. Antonio, J. Bandeiras, J. Andrade, D. Cordeiro, S. Briatore, N. Garzaniti, F. Nichele, R. Mozzillo, A. Piumatti, and A. Reagan, "Fsscat: The federated satellite systems 3 cat mission: Demonstrating the capabilities of cubesats to monitor essential climate variables of the water cycle," *IEEE Geoscience and Remote Sensing Magazine*, vol. PP, pp. 2–11, 11 2022.

[27] A. Camps, J. F. Munoz-Martin, J. A. Ruiz-de Azua, L. Fernandez, A. Perez-Portero, D. Llavería, C. Herbert, M. Pablos, A. Golkar, A. Gutiérrez, C. António, J. Bandeiras, J. Andrade, D. Cordeiro, S. Briatore, N. Garzaniti, F. Nichele, R. Mozzillo, A. Piumatti, M. Cardi, M. Esposito, C. van Dijk, N. Vercruyssen, J. Barbosa, J. Hefele, R. Koeleman, B. C. Dominguez, M. Pastena, G. Filippazzo, and A. Reagan, "Fsscat: The federated satellite systems 3cat mission: Demonstrating the capabilities of cubesats to monitor essential climate variables of the water cycle [instruments and missions]," *IEEE Geoscience and Remote Sensing Magazine*, vol. 10, no. 4, pp. 260–269, 2022.

[28] J. L. Stern and P. T. Grogan, "Federated space systems' trade-space exploration for strategic robustness," *Journal of Spacecraft and Rockets*, vol. 59, no. 4, pp. 1240–1254, 2022.

[29] J. C. Dong-Hyun Jung, Joon-Gyu Ryu, "Satellite clusters flying in formation: Orbital configuration-dependent performance analyses," 05 2023.

[30] K. T. Alfriend, S. R. Vadali, P. Gurfil, J. P. How, and L. Breger, *Spacecraft Formation Flying: Dynamics, Control and Navigation*. 2009.

[31] H. Ferraz and J. P. Hespanha, "Iterative algorithms for distributed leader-follower model predictive control," in *2019 IEEE 58th Conference on Decision and Control (CDC)*, pp. 3533–3539, 2019.

[32] A. Alzubairi, B. Kada, and A. Tameem, "Decentralized cooperation control for formation flying spacecraft," in *2022 IEEE IAS Global Conference on Emerging Technologies (GlobConET)*, pp. 187–190, 2022.

[33] R. Apa, M. B. Quadrelli, and R. M. Beauchamp, “Dynamics and control of helical arrays in low earth orbit,” in *2022 IEEE Aerospace Conference (AERO)*, pp. 1–20, 2022.

[34] D. Fan, W. Cai, L. Yang, and R. Zhang, “Sequential convex optimization based spacecraft formation reconfiguration with collision avoidance,” in *2022 China Automation Congress (CAC)*, pp. 6821–6825, 2022.

[35] D. Menegatti, A. Giuseppi, and A. Pietrabissa, “Model predictive control for collision-free spacecraft formation with artificial potential functions,” in *2022 30th Mediterranean Conference on Control and Automation (MED)*, pp. 564–570, 2022.

[36] S. Mazouffre, “Electric propulsion for satellites and spacecraft: Established technologies and novel approaches,” *Plasma Sources Science and Technology*, vol. 25, p. 033002, 04 2016.

[37] J. G. Walker, “Satellite Constellations,” *Journal of the British Interplanetary Society*, vol. 37, p. 559, Dec. 1984.

[38] R. R. B. D. D. M. J. E. White, *Fundamentals of Astrodynamics*. DOVER PUBLICATIONS, INC., 1971.

[39] “Electric propulsion for satellites and spacecraft: established technologies and novel approaches,” 2016.

[40] U. Walter, *Astronautics: The Physics of Space Flight*. Springer Cham, 2019.

[41] O. B. George P. Sutton, *Rocket Propulsion Elements*. John Wiley Sons, 2001.

[42] B. Weber, “Orbital mechanics astrodynamics,” 2024.

[43] “Development and test of a cost-efficient gridded ion thruster propulsion system for small satellites – ionjet,” 2022.

[44] NASA, “Spacecraft, planet, instrument, camera-matrix, events.”

[45] A. AGI, “Ansys stk software for digital mission engineering and systems analysis.”

[46] J. L. C. Rodríguez, “poliastro - astrodynamics in python.”

[47] A. G. Jaspar Sindermann, “Distributed hardware-in-the-loop satellite simulation architecture for creating “digital shadows” of satellite constellations,” in *IAC 2023 Congress Proceedings, 74th International Astronautical Congress*, Oct 2023.

[48] A. V. S. A. Laboratory, “Basilisk: an astrodynamics simulation framework.”

[49] MathWorks, “Systems tool kit (stk).”

[50] H. P. Langtangen, ed., *Numerical Computing in Python*, pp. 131–188. Berlin, Heidelberg: Springer Berlin Heidelberg, 2008.

[51] M. Mahooti and S. Mousavi, “Sgp4 (python code),” 02 2022.

[52] MathWorks, “Simulink - model and simulate cubesats.”

[53] A. Alcantarilla Romera, “Spacex opens busy second half of 2022 with starlink launch". retrieved 7 july 2022.,” 07 2022.

[54] J. C. Pizzicaroli, “Launching and building the iridium® constellation,” in *Mission Design & Implementation of Satellite Constellations: Proceedings of an International Workshop, held in Toulouse, France, November 1997*, pp. 113–121, Springer, 1998.

[55] Á. Mozo-García, E. Herráiz-Monseco, A. B. Martín-Peiró, and M. M. Romay-Merino, “Galileo constellation design,” *GPS Solutions*, vol. 4, pp. 9–15, 2001.

[56] M. Turnock, “Deep space propulsion with electromagnetic tethers - a literature study,” 02 2020.